



20<sup>th</sup> International Visual Field  
and Imaging **Symposium**  
Trinity College, The University of  
Melbourne, Victoria, Australia  
22-25 JANUARY 2012

# Program and Abstract Handbook

[www.ivfis.com](http://www.ivfis.com)

GOLD SPONSORS



SILVER SPONSORS



BRONZE SPONSORS



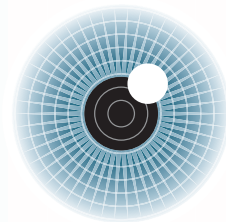


## TABLE OF CONTENTS

Speakers	3
Social Program	6
General Information	8
Venue	10
Day 1 - Monday 23 January 2012	
Oral Presentation Program	11
Oral Presentations: Abstracts	13
Day 2 - Tuesday 24 January 2012	
Oral Presentation Program	23
Oral Presentations: Abstracts	25
Day 3 - Wednesday 25 January 2012	
Oral Presentation Program	31
Oral Presentations: Abstracts	33
Posters	39
Presenter Index	56
Exhibition	57

## THANK YOU

We would like to thank the following organisations for their generous support of the 20th International Visual Field and Imaging Symposium:

### SPONSORS

#### Gold Sponsors



#### Silver Sponsors



#### Bronze Sponsors



## DISCLAIMER

The organisers have made every attempt to ensure that all information in this program/abstract book is correct. Some information printed has been provided by external sources. The organisers take no responsibility for changes to the program or any loss that may occur as a result of changes to the program.

## CONFERENCE ORGANISERS

**thinkbusiness**events

*passionate about conferences*

Suite 6, 19-23 Hoddle Street, Richmond VIC 3121

Phone: +61 3 9417 1350

Fax: +61 3 8610 2170

Email: [enquires@thinkbusinessevents.com.au](mailto:enquires@thinkbusinessevents.com.au)

## LOCAL ORGANISING COMMITTEE

**Dr Andrew Anderson**  
The University of Melbourne

**Professor Stuart Graham**  
Macquarie University

**Professor Ted Maddess**  
The Australian National University

**Dr Allison McKendrick**  
The University of Melbourne

**Associate Professor Andrew Turpin**  
The University of Melbourne

**Professor Algis Vingrys**  
The University of Melbourne

## SPEAKERS

### KEYNOTE SPEAKERS



#### **Professor Balwantray C. Chauhan**

##### *Presenting The IPS Lecture*

Balwantray Chauhan is Professor and Research Director of Ophthalmology and Visual Sciences, and Professor of Physiology and Biophysics at Dalhousie University. He is also the holder of first endowed Chair in Vision Research at Dalhousie. He obtained his PhD at the University of Wales, Cardiff and his postdoctoral training at the University of British Columbia under the supervision of Dr. Stephen Drance.

Prof. Chauhan's clinical research interests are in the diagnosis of early changes in the visual field and optic disc in glaucoma. He has devised new strategies for detecting glaucomatous progression and conducted additional research leading to their translation to clinical practice. A key contribution in this area is the Topographical Change Analysis (TCA), a widely used technique for identifying changes in optic disc topography with modern imaging techniques such as scanning laser tomography. Prof. Chauhan is the principal investigator of the Canadian Glaucoma Study, a multicentre study and the largest of its kind, investigating the risk factors for the progression of open-angle glaucoma. His research is shedding new information on the nature and mode of glaucomatous progression.

His research interests also include experimental models of optic nerve damage. This work complements his clinical research and address research questions to provide new clues about the aetiology of glaucoma and possible new avenues of therapy. Recent areas of activity include studies of neuron-glia the retina and optic nerve, in vivo imaging of retinal neurons and neuroprotection. He conducts his basic science research in the Retina and Optic Nerve Research Laboratory, a multidisciplinary facility he was instrumental in establishing. This laboratory of 6 principal investigators from 4 departments in the Dalhousie Medical Faculty, and over 25 students, fellows and technicians, is unique in the country and provides an excellent opportunity for discovery and training.

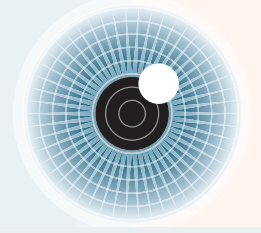
Prof. Chauhan holds research grants for both his clinical (since 1991) and basic science (since 1997) research from the Canadian Institutes of Health Research (CIHR), Atlantic Innovation Fund, and other public and private sector agencies. He is a member of the CIHR Group in Retina of 4 scientists at Dalhousie involved in collaborative basic science research.



#### **Professor Joanne Wood BSc(Hons) PhD Aston, MCOptom, FAAO**

##### *Presenting the Aulhorn Lecture*

Joanne Wood is a Professor in the School of Optometry and the Institute of Health and Biomedical Innovation at Queensland University of Technology (QUT), and has research expertise spanning a number of key areas. Joanne received her PhD in visual science from the University of Aston, Birmingham, U.K., which included a series of studies on static automated perimetry in normal and abnormal eyes. Her PhD was followed by a post doctoral fellowship in clinical psychophysics at Oxford University. She then joined the School of Optometry at Queensland University of Technology (QUT) in Brisbane, Australia in 1989 as a Post Doctoral Fellow and currently holds the position of Professor and Director of Research in the School. Joanne has an international reputation for her investigations of the relationship between vision, ageing and driving performance and has made a significant contribution to understanding how visual impairment affects driving performance, identifying risk factors for unsafe older drivers and on the factors affecting pedestrian visibility at night-time. This research approach has led to the development of a wide research network overseas, attracting visiting scholars from around the world to participate in collaborative research projects. Joanne's research has resulted in the publication of 155 articles in national and international refereed journals, and presentation of 150 research papers at major international conferences.



## SPEAKERS

### INVITED SPEAKERS



**Professor Nathan Efron**  
School of Optometry, Queensland University of Technology

Nathan Efron completed his BScOptom and PhD at the University of Melbourne in 1981, and after two years of post-doctoral studies in Berkeley, USA and Sydney, he returned to Melbourne as lecturer then senior lecturer responsible for contact lens education. In 1990 he took up the foundation Chair of Clinical Optometry at the University of Manchester, England, and established a contact lens research and consultancy unit known as Eurolens Research. In Manchester, he served as Head of Department from 1992-97 and Dean of Research for the university from 2001-2004, and was admitted to the degree of Doctor of Science in 1995. Professor Efron returned to Australia in 2006 and joined the Institute of Health and Biomedical Innovation in the School of Optometry at the Queensland University of Technology (QUT), as Research Professor. At QUT he established the Anterior Eye Laboratory and is currently exploring a range of novel ophthalmic markers of diabetic neuropathy. He lectures extensively world-wide and has published over 700 scientific papers, abstracts and textbook chapters, and has written/edited 12 books.



**Clinical Associate Professor Paul Healey**  
Director of Glaucoma Research, University of Sydney

Completing a B(Med)Sc in Cell Biology at the Garvan Institute in 1988, Prof. Healey went on to graduate with Honours from the Medical School of the University of New South Wales in 1991. He subsequently completed his MMed in Clinical Epidemiology and PhD in Medicine from Sydney University. After a glaucoma fellowship at Moorfields Eye Hospital he was appointed to Westmead Hospital where he directs the Glaucoma Service. He is also Director of Glaucoma Research at the Centre for Vision Research and chief glaucoma investigator for the Blue Mountains Eye Study. Paul's worldwide appointments include the South East Asia Glaucoma Interest Group, Asia-Oceanic Glaucoma Society, Asia-Pacific Academy of Ophthalmology, and World Glaucoma Association. He has interests in postgraduate education most recently as Director of Training for Sydney Eye Hospital. In 2005, he was honoured with the International Young Clinician-Scientist Award from the Association of International Glaucoma Societies. He has made over 180 scientific presentations at meetings throughout the world. He is an editorial board member of number of journals, and has published over 100 articles based on original research.



**Associate Professor Andrew Metha**  
Department of Optometry & Vision Sciences, The University of Melbourne

Andrew Metha is currently an Associate Professor in the Department of Optometry and Vision Sciences at the University of Melbourne, where he has taught at all levels in the Bachelor and now new Postgraduate Optometry Degree courses. His first degree was a Bachelor of Science (Physics and Mathematics) from Monash University, before undertaking his Optometry undergraduate degree from the University of Melbourne where he also obtained his PhD. He is an eclectic vision scientist, first gaining expertise in psychophysical methods of understanding visual processes during his PhD, then branching into single and multi-cell electrophysiological recordings in the visual cortex to investigate adaptation and brain plasticity, and most recently uses adaptive optics to directly image single cells and other microstructure in living eyes. He joined the University of Melbourne department in 2000 after serving postdoctoral positions in Montreal (McGill Vision Research Unit), the University of Rochester's Centre for Visual Science and the Psychobiology Laboratory in Canberra's Australian National University.



**Professor William Morgan**  
Lions Eye Institute, University of Western Australia

Prof. William Morgan is a glaucoma subspecialist in Perth, Western Australia. He completed a PhD measuring the tissue and vascular pressures across the optic disk, exploring their relationships to IOP and CSF pressure. His studies have extended in to the association of retinal vein properties with glaucoma severity and progression. His more basic work includes studies of axonal cytoskeleton and astrocytes within the optic nerve. He is interested in clinical measures of glaucoma progression.



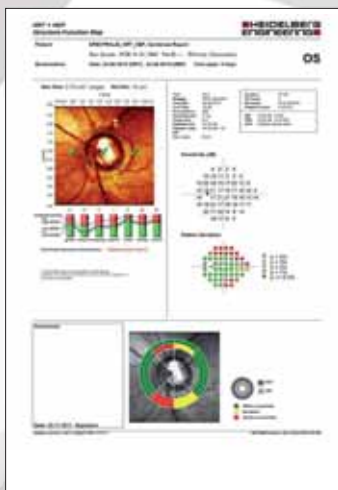
Don't be Puzzled by Glaucoma –  
The Comprehensive Solution for Your Practice

**HRT · HEP · SPECTRALIS**

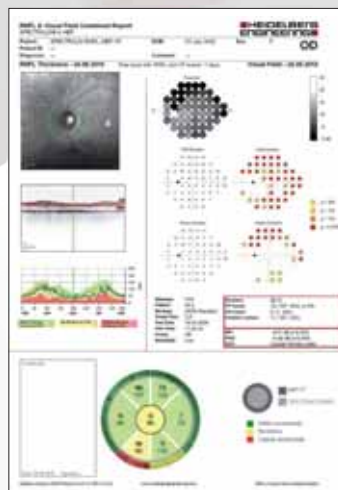
93326-003.ERI © Heidelberg Engineering GmbH. All rights reserved.



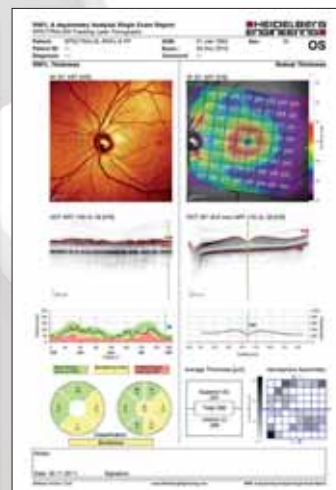
The detection and monitoring of glaucoma requires a targeted combination of clinical expertise and reliable, reproducible examination results. The complete picture of glaucoma develops only if the diagnostic information fits together like the pieces of a puzzle.



HRT & HEP Visual Field



RNFL & HEP Visual Field

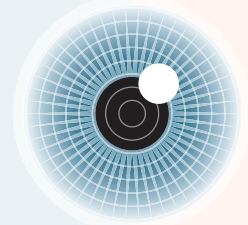


RNFL & Asymmetry Analysis

Structural and functional information is conjointly displayed in unique combined reports of the **Heidelberg Retina Tomograph (HRT)**, the **Heidelberg Edge Perimeter (HEP)** and the **SPECTRALIS OCT**.

**Lunch Symposium**  
Monday, January 23<sup>rd</sup>:  
**Use of Diagnostic Testing for  
the Detection and Follow-up  
of Glaucoma**

**HEIDELBERG  
ENGINEERING**



## SOCIAL PROGRAM

### WELCOME RECEPTION

*(This function is included in the Full Conference registration)*

<b>Date:</b>	Sunday 22nd January 2012
<b>Time:</b>	6.00pm - 8.00pm
<b>Location:</b>	Garden House, Royal Botanical Gardens
<b>Cost:</b>	Inclusive for full delegates
<b>Inclusions:</b>	Drinks and canapés
<b>Additional Tickets:</b>	\$75

**Buses will depart at 8pm back to the Conference hotels with a stop off in the city.**

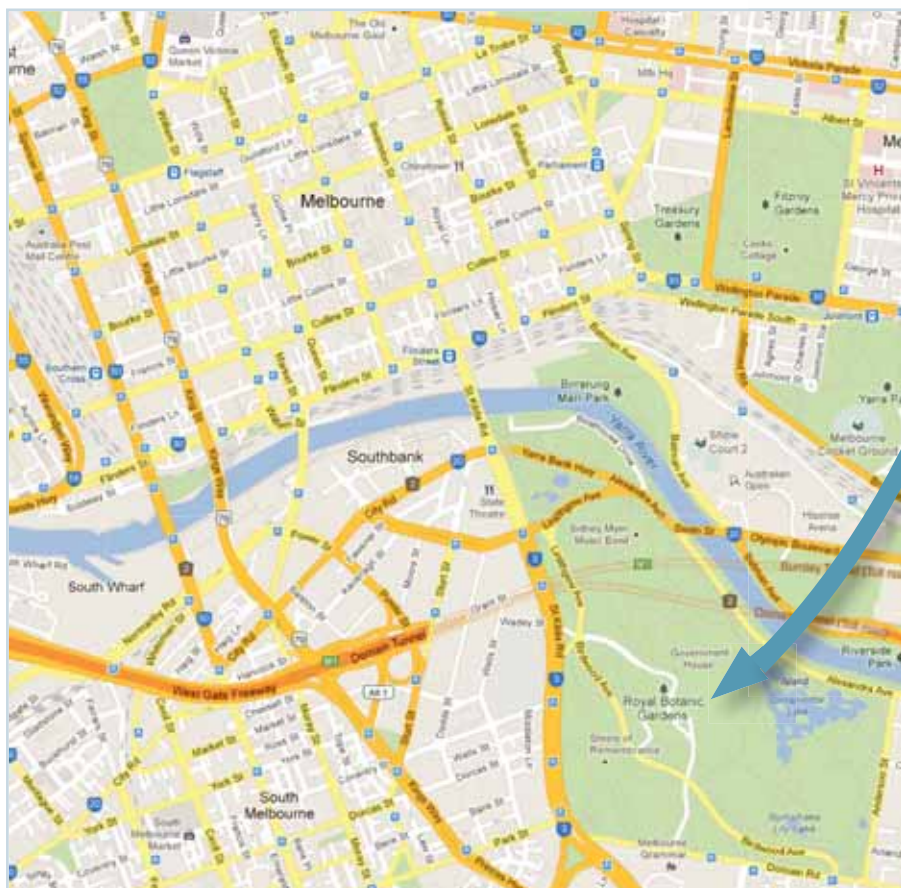
Not catching the bus into the city or back to your hotel. Want to catch a tram back into the City?

From Gardens house walk back to Gate O then walk down the hill towards the Shrine of Remembrance. On St Kilda Road, from stop number 20, Domain Road Interchange catch trams 3, 5, 8, 16, 64, or 67 north along St Kilda Road towards the central business district. Trams only accept coins on board for tickets.



#### **Garden House, Royal Botanical Gardens**

Established in 1846 beside the Yarra River, Melbourne's Royal Botanic Gardens offers an expansive garden haven adjacent to the bustle of city, and is one of the key reasons why Victoria is known as "The Garden State". The opening reception will take place in the elegant "Garden House" - a two-storey Georgian mansion with original fittings, nestled in the gardens amongst acres of green.







## FIELD TRIP

Visit to Hanging Rock Reserve, and Kyneton Ridge Winery  
(This function is included in the Full Symposium registration)

<b>Date:</b>	Tuesday 24th January 2012
<b>Time:</b>	1.00pm - 6.00pm
<b>Location:</b>	Hanging Rock
<b>Cost:</b>	Inclusive for full delegates
<b>Additional Tickets:</b>	\$75
<b>Inclusions:</b>	Deluxe coach transport, entry to Hanging Rock Reserve, afternoon tea, guide.



### Visit to Hanging Rock, and Kyneton Ridge Winery

Created over 6 million years ago, Hanging Rock is an impressive geological formation of volcanic origin rising over 100 metres above the surrounding plains of

Central Victoria. Originally a site of ceremonial initiation for aboriginal men of the Wurundjeri people, the rock was also famously the inspiration for the novel "Picnic at Hanging Rock" immortalised in the iconic and haunting Australian film by director Peter Weir ([www.imdb.com/title/tt0073540](http://www.imdb.com/title/tt0073540)).

Victoria is also world-famous for its wine making, and a short trip from the rock is the stunning Macedon Ranges, being Australia's coolest grape growing region.

## SYMPOSIUM DINNER

(This function is included in the Full Symposium registration)

<b>Date:</b>	Wednesday 25th January 2012
<b>Time:</b>	7.00pm - 11.00pm
<b>Location:</b>	Ormond College 49 College Crescent Parkville VIC 3052
<b>Cost:</b>	Inclusive for full delegates
<b>Additional Tickets:</b>	\$120
<b>Inclusions:</b>	Dinner, drinks and entertainment



### Ormond College

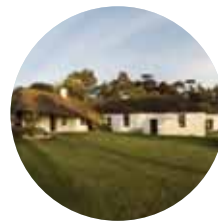
Established in 1881 and set amongst extensive gardens, Ormond College is the largest residential college for the University of Melbourne. The Dining Hall is one of the finest Neo-Gothic buildings in Australia, and its historic

wood panelled interior, stained glass windows and vaulted ceilings make it an unforgettable location for our concluding conference dinner.

## OPTIONAL DINNER

(This function is **not** included in Full Symposium registration)

<b>Date:</b>	Monday 23rd January 2012
<b>Time:</b>	6.30pm - 10.30pm
<b>Location:</b>	Emu Bottom Homestead
<b>Cost:</b>	\$170.00 per person
<b>Inclusions:</b>	Bus transfers to and from Melbourne University and Emu Bottom Homestead, Dinner, drinks and entertainment.

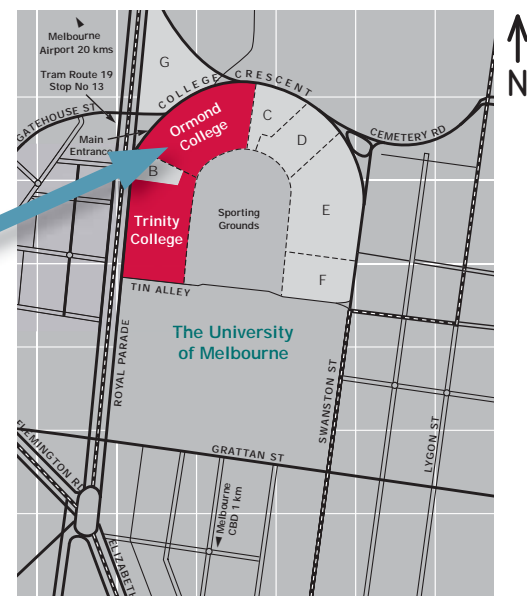


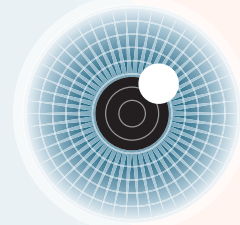
### Emu Bottom Homestead

The story of Emu Bottom Homestead begins on August 30 1835, when the schooner Enterprize sailed up Port Phillip Bay. On board was the first party of settlers who built the huts of the banks of the Yarra from which the City of Melbourne then grew.

Among that group was George Evans, who after exploring the area, chose to settle 40kms from the city, in a picturesque valley. It was here, in 1836, that he built the handsome stone building now known as Emu Bottom Homestead. George Evans named his homestead 'Emu Bottom' because he had settled in the low-lying ground of the valley well frequented by large flocks of emus.

Nestled amid verdant countryside and surrounded by fertile valley pastures, Emu Bottom Homestead captures the magical spirit of Australia's pioneer past. The windows of the homestead look out upon unspoilt landscape and enchanting garden views. It's hard to believe that this secluded spot is just a short drive from the heart of bustling Melbourne.





## GENERAL INFORMATION

### REGISTRATION AND INFORMATION DESK

The Registration & Information Desk will be centrally located onsite at the Welcome Reception and at the Symposium venue. On arrival at the Symposium, please collect your badge and other materials at the registration desk.

#### Opening hours:

Sunday 22 January 2012	18:00 – 20:00
Monday 23 January 2012	08:00 – 17:00
Tuesday 24 January 2012	08:00 – 13:00
Wednesday 25 January 2012	08:00 – 17:00

### NAME BADGES

Each delegate registered for the Symposium will receive a name badge at the Registration Desk. This badge will be your official pass and must be worn to obtain entry to all sessions, Welcome Reception and Conference Dinner and should be worn during the conference.

### CATERING

Catering breaks including muffins and coffee on arrival, morning and afternoon teas will be served in the Drama Room and Room 1 in the Evan Burge Building, Trinity College. If you have indicated special dietary needs and are unable to select appropriate food during the catering breaks, please notify the catering staff. They will have a special meal available for you.

Lunch will be served in the dining marquee..

### EXHIBITION

You can visit the exhibitors who have supported the 20<sup>th</sup> International Visual Field and Imaging Symposium in the Drama Room and Room 1 in the Evan Burge Building, Trinity College. All morning and afternoon teas will be served in the exhibition areas during the conference.

### POSTERS

There has been time allocated for official Poster Presentations at the conference.

Posters will be divided into two sessions – either 10:00am – 11:00am on Monday 23<sup>rd</sup> January 2012 or 10:00am – 11:00am on Wednesday 25<sup>th</sup> January 2012. During this time, authors will be present at their poster to answer questions and discuss their work with delegates.

### PARKING

#### University Square Car Park [no. 107]

<b>Entry:</b>	Berkeley St (near corner of Grattan St)
<b>Hours:</b>	Weekdays – 6:30am to 10:00pm Weekends – 7:00am to 7:00pm
<b>Availability:</b>	During semester (weekdays) the car park fills and closes to public parking, normally around 9:00am – 9:30am.

#### Eastern Precinct Underground Car Park

<b>Entry:</b>	375 Cardigan St, Carlton (near the corner of Elgin St)
<b>Hours:</b>	Weekdays – 7:00am to 7:00pm Weekends – press intercom for access (Staff and Students can request access on their ID card.)
<b>Availability:</b>	Staff and Student Casual parking. Parking for visitors attending University functions or events.

### PUBLIC TRANSPORT

The closest public transport to the conference venue is the tram network. The nearest stop is number 13 on Royal Parade. From the Melbourne central business district catch tram number 19 heading North on Elizabeth Street. Alternatively, trams to Melbourne University can be caught heading North on Swanston Street, after which a short (10 minute) walk across campus to reach Trinity College is required. For information on transport routes and timetables, please visit [www.metlinkmelbourne.com.au](http://www.metlinkmelbourne.com.au)

### TAXI

Taxi ranks are situated throughout the city, or can be flagged on the street.

Melbourne's major taxi companies include:

<b>Arrow</b>	13 2211
<b>Black Cabs Combined</b>	13 2227
<b>Silver Top Taxis</b>	13 1008
<b>wheelchair accessible taxis</b>	1300 364 050

### INTERNET FACILITIES AT VENUE

Delegates can purchase wireless internet from the Main Reception in Leeper Building during office hours. The cost will be \$10 for the duration of the conference.





## INSURANCE

Insurance of any kind is NOT included in the registration fees – it is advised that delegates take out appropriate health and travel insurances prior to travelling. The 20th International Visual Field and Imaging Symposium Organising Committee and the Conference Office do not take any responsibility for delegates failing to insure.

## CONFERENCE PHOTOGRAPHY DISCLAIMER

There will be a photographer present over the course of the conference to capture images. Any images will be retained and used by Melbourne University and Think Business Events for their purposes (for example, on website and publications). If you object to your photograph being taken, please contact the Registration Desk.

## DRESS CODE

Neat casual attire is appropriate for attendance at symposium and social functions. Weather in Melbourne in January can be variable, with hot days up to 40°C (typically only one or two in a row, but sometimes accompanied by a strong, unpleasant north wind) along with cooler days below 20°C (occurring about once a week). Humidity is rarely high, and although it is not uncommon for there to be no rain for a fortnight it is also possible for heavy rain to occur occasionally. Delegates are advised to dress appropriately for the forecast temperature for the day, with the option of adding layers to accommodate air-conditioned indoor temperatures or an abrupt cool change in the weather.

Ultraviolet (UV) radiation is also extreme in Australia during summer, and so delegates are advised to use appropriate sunscreen, clothing and eye-protection when outdoors. Further advice can be obtained from the SunSmart website ([www.sunsmart.com.au](http://www.sunsmart.com.au)).

## MOBILE PHONES

Please respect the presenter and other delegates by ensuring that your mobile phone is switched off or on silent while you are in sessions.

## SMOKING POLICY

The 20th International Visual Field and Imaging Symposium is a non-smoking Symposium. The University of Melbourne is a non-smoking venue.

## MESSAGES AND PROGRAM CHANGES

Messages and program changes will be placed on a notice board near the Registration Desk. Delegates are advised to check the message board at regular intervals.

## ACCOMMODATION

### Rydges on Swanston

701 Swanston Street, Carlton VIC 3053  
Phone: +61 3 9347 7811  
[www.rydges.com](http://www.rydges.com)

### Quest Carlton Clocktower

255 Drummond Street, Carlton VIC 3053  
Phone: +61 3 9349 9700  
[www.questapartments.com.au](http://www.questapartments.com.au)


### Vibe Hotel Carlton


441 Royal Parade, Parkville VIC 3052  
Phone: +61 3 9380 9222  
[www.vibehotels.com.au](http://www.vibehotels.com.au)

### Trinity College

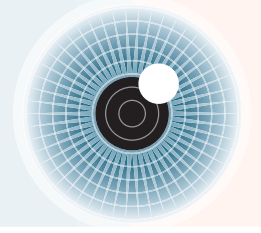
Royal Parade, Parkville VIC 3052  
Phone: +61 3 9348 7100

Allergan is proud  
to participate in the  
20th International  
Visual Field and  
Imaging Symposium



 **ALLERGAN**  
Our pursuit. Life's potential.®

[www.allergan.com](http://www.allergan.com)

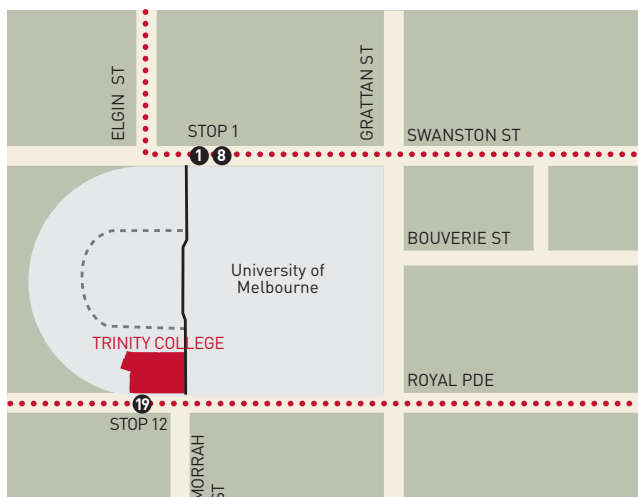
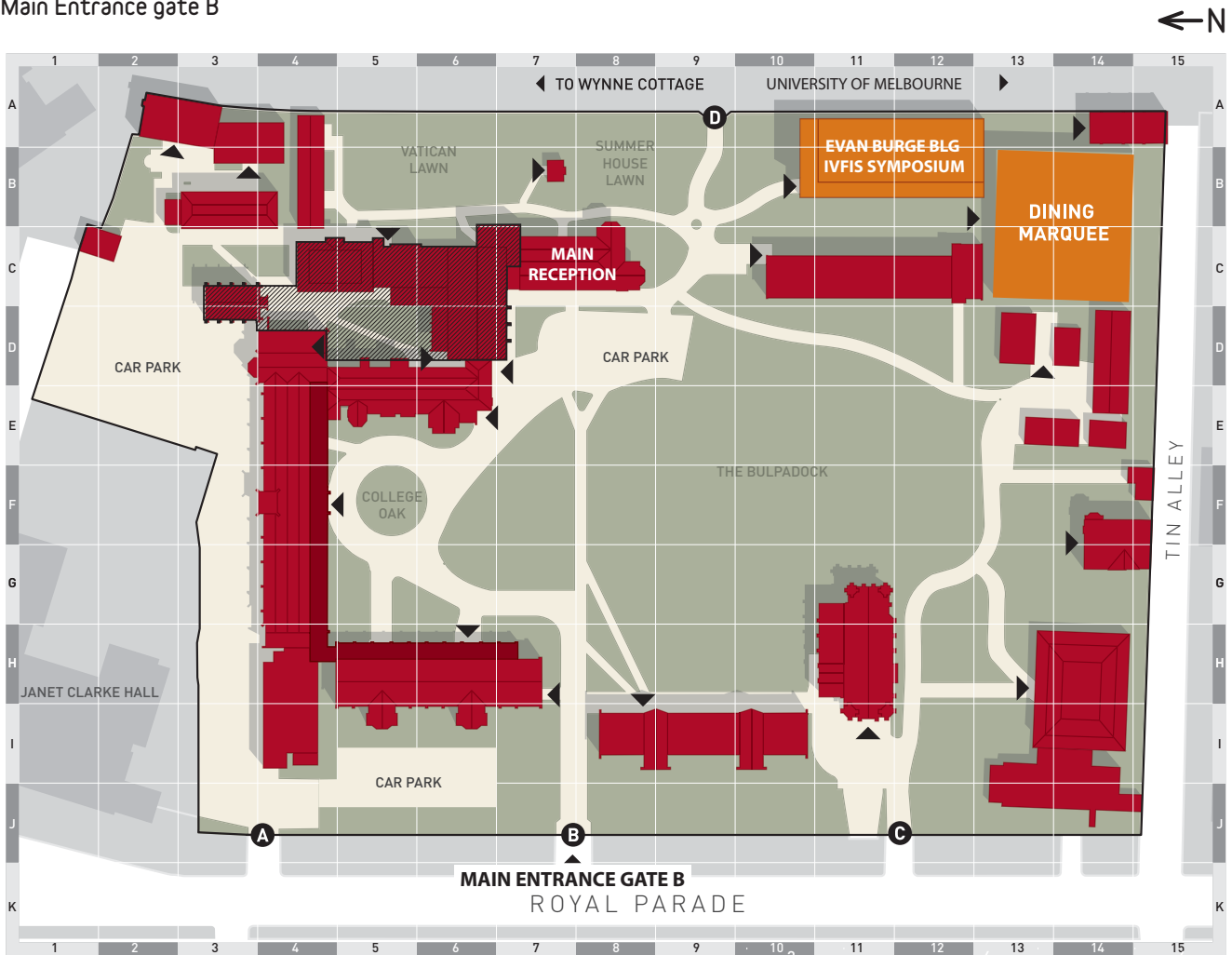


## GENERAL INFORMATION

### VENUE

Evan Burge Building,  
Trinity College, The University of Melbourne,  
Royal Parade, Parkville VIC 3052

Main Entrance gate B

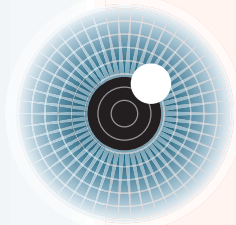


**MONDAY 23 JANUARY 2012**

8:00	<b>Registration opens</b>
8:45	<b>Opening Session</b>
9:00	<p><b>SE-01</b>  <b>Macular Structure and Function</b>  <b>Chairs: David Henson and Algis Vingrys</b></p>
	<p>Examining cone photoreceptor structure-function relationships in retinitis pigmentosa with adaptive optics scanning laser ophthalmoscope-based microperimetry  <b>William Tuten</b></p> <p>Macular function and structure in differing patterns of glaucomatous perimetric defects  <b>Sandeep Parwal</b></p> <p>Relationship between selective visual field testing and macular ganglion cell layer thickness in glaucoma  <b>Mariko Eura</b></p> <p>Structure-function relationships in the macula of glaucoma patients  <b>Chris Johnson</b></p>
10:00	<p><b>Poster Session A</b>  <b>Chair: Andrew Anderson</b></p>
11:00	<b>Morning Tea</b>
11:30	<p><b>SE-02</b>  <b>Perimetry I</b>  <b>Chairs: Chota Matsumoto and Paul Artes</b></p>
	<p>A Bayesian thresholding procedure for perimetry that models both spatial relations and sensitivity  <b>Andrew Turpin</b></p> <p>A new multi stimulus self-check visual field screener, CLOCK CHART®  <b>Chota Matsumoto</b></p> <p>Characteristics of spikes-shaped isopters in automated kinetic perimetry  <b>Shigeki Hashimoto</b></p> <p>Normal variability for two forms of perimetry using anatomically inspired test locations  <b>Mitchell Dul</b></p> <p>Relationship of the threshold values between the kinetic target and static target in normal subjects  <b>Tomoyasu Kayazawa</b></p> <p>The relative performance of visual field tests using subsets of the 24-2 test pattern at detecting glaucomatous field loss  <b>Yanfang Wang</b></p>
13:00	<b>LUNCH</b>
	<p><b>Luncheon Presentation:</b>  <b>Use of Diagnostic Testing for the Detection and Follow-up of Glaucoma</b>  <b>Sponsored by Heidelberg Engineering</b></p> <p><b>Balwantray C. Chauhan</b>, Professor of Ophthalmology, Halifax, Canada  <b>Fritz Dannheim</b>, Professor of Ophthalmology, Hamburg, Germany  <b>Paul Healey</b>, Professor of Ophthalmology, Sydney, Australia</p>







MONDAY 23 JANUARY 2012	
14:15	<p><b>SE-03</b>  <b>Ageing and Quality of Life</b>  <b>Chairs: Chris Johnson and Joanne Wood</b></p>
	<p>Evaluation and comparison to functional performance of the California Central Visual Field Test (CCVFT)  <b>Ronald Schuchard</b></p> <p>Flicker perimetry can be used to monitor progression in age-related macular degeneration  <b>Algis Vingrys</b></p> <p>Investigating perceptual learning effects in standard automated perimetry in ageing and in central and peripheral vision  <b>Josephine Battista</b></p> <p>Mobility limitations in patients with glaucoma  <b>Sharon Bentley</b></p> <p>Relationship between attentional visual fields and integrated visual field sensitivity among older adults with glaucoma  <b>Alex Black</b></p>
15:30	<b>AFTERNOON TEA</b>
16:00	<p><b>SE-04</b>  <b>Change</b>  <b>Chairs: Linda Zangwill and Bal Chauhan</b></p>
	<p>Peripapillary Retinal Nerve Fiber Layer (RNFL) – Thickness compared with RNFL retardance and electroretinographic changes at the onset of optic nerve head surface topography change in experimental glaucoma  <b>Brad Fortune</b></p> <p>Rates of Matrix and standard automated perimetry change in glaucoma and high-risk ocular hypertension  <b>Deborah Goren</b></p> <p>Relationship of central corneal thickness to visual field progression in eyes with glaucoma  <b>Deepa Viswanathan</b></p> <p>Sensitivity and specificity of a series of glaucoma change probability criteria  <b>Gideon Zamba</b></p> <p>Visual field progression in glaucoma: estimating the overall significance of deterioration with permutation analyses of point-wise linear regression  <b>Paul Artes</b></p>
17:15	<b>Sessions Finish</b>
18:30 - 22:30	<p><b>Optional Dinner</b>  <b>Emu Bottom Homestead</b></p>

## SE-01, Macular Structure and Function 9:00 am – 10:00 am

### Examining cone photoreceptor structure-function relationships in retinitis pigmentosa with adaptive optics scanning laser ophthalmoscope-based microperimetry

William Tuten<sup>1</sup>, Pavan Tiruveedhula<sup>2</sup>, Jacque Duncan<sup>3</sup>, Austin Roorda<sup>1,2</sup>

<sup>1</sup>Vision Science Graduate Group, University of California, Berkeley, Berkeley, CA, USA, <sup>2</sup>School of Optometry, University of California, Berkeley, Berkeley, CA, USA, <sup>3</sup>Department of Ophthalmology, University of California, San Francisco, San Francisco, CA, USA

**Purpose:** To evaluate the relationship between cone photoreceptor structure and function in a patient with autosomal dominant retinitis pigmentosa (ADRP) using adaptive optics scanning laser ophthalmoscope-based microperimetry (AOSLO-MP).

**Method:** An AOSLO was used to conduct simultaneous high-resolution retinal imaging and visual function testing in a 39 year-old female with ADRP. Three measures of visual sensitivity were collected at each of four retinal eccentricities between 0.75° and 5.0°. A high-speed eye tracking algorithm enabled the delivery of aberration-corrected Goldmann I-sized stimuli (diameter = 6.5 arcmin;  $\lambda$  = 680nm) to targeted retinal loci. Increment thresholds were obtained using a 4-2dB staircase procedure and compared to results from a group of five normal subjects. Images of the photoreceptor mosaic were generated and cone spacing at each test location was assessed using custom software.

**Results:** Visual thresholds increased linearly with eccentricity ( $R^2 = 0.9203$ ), with a rate of change significantly greater than in normal subjects ( $P < 0.001$ ). Relative to normal subjects, the threshold elevation in the patient with ADRP ranged from 3.04 to 5.22 logTrolands (at 0.75° and 5.0°, respectively). The increase in cone spacing ranged from 33% to 57%, with each test location falling outside the 95% confidence interval for normal subjects.

**Conclusions:** The increase in visual threshold cannot be entirely attributed to a decrease in the number of cone photoreceptors sampling the perimetric stimulus, suggesting cone photoreceptor dysfunction. AOSLO-MP shows promise for establishing the functional correlates of photoreceptor mosaic structure on a microscopic scale in patients with retinal disease.

### Macular function and structure in differing patterns of glaucomatous perimetric defects

Ramanjit Sihota, Sandeep Parwal, Viney Gupta, Tanuj dada, Swati Phuljelhe

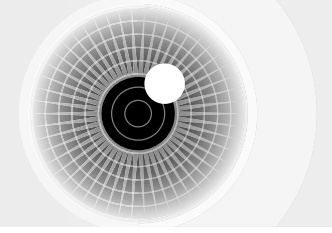
Dr. R.P. Centre for Ophthalmic sciences, All India Institute of Medical Sciences, delhi, India

**Purpose:** Evaluation of functional and morphologic changes of macula using Microperimetry (MP-1) and Optical Coherence Tomography (OCT) in differing pattern of Glaucomatous Perimetric Defects.

**Method:** Cross sectional, case control study recruited 80 adult glaucoma patients and 20 controls at a tertiary eye care centre after written consent. Macular threshold was evaluated with MP-1, 20°, 10dB with 4-2 strategy. Morphological evaluation of macula was performed with OCT stratus. Results from each eye were divided into four quadrants for analysis. Normal and abnormal quadrants by HFA were compared with the corresponding normal and abnormal quadrants by MP-1 and OCT. Correlation analysis was used to correlate the mean values of MP-1, HFA and OCT in each quadrant.

**Results:** There was a significant correlation between MP-1 and HFA results in all quadrants (Spearman correlation 0.83,  $p < 0.001$ ). All abnormal HFA quadrants had a corresponding abnormal MP-1 quadrant, however the normal HFA quadrants had abnormalities on microperimetry. Mean sensitivity on microperimetry showed a greater correlation (Spearman correlation coefficient = 0.59) with total macular thickness on OCT, compare to standard automatic perimetry (Spearman correlation coefficient = 0.49) in differing pattern of glaucomatous field defects.

**Conclusions:** Defects on MP-1 were more extensive and closer to fixation than HFA, suggesting that subtle functional defects may be picked up earlier with MP-1.



## Relationship between selective visual field testing and macular ganglion cell layer thickness in glaucoma

Mariko Eura<sup>1</sup>, Chota Matsumoto<sup>1</sup>, Sachiko Okuyama<sup>1</sup>, Sonoko Takada<sup>1</sup>, Eiko Arimura<sup>2</sup>, Shigeki Hashimoto<sup>1</sup>, Hiroki Nomoto<sup>1</sup>, Fumi Tanabe<sup>1</sup>, Tomoyasu Kayazawa<sup>1</sup>, Yoshikazu Shimomura<sup>1</sup>

<sup>1</sup>Department of Ophthalmology, Kinki University Faculty of Medicine, Osaka-Sayama, Osaka, Japan, <sup>2</sup>Department of Ophthalmology, Kinki University Faculty of Medicine, Sakai Hospital, Osaka-Sayama, Osaka, Japan

**Purpose:** To evaluate the relationship between function-selective visual field (VF) testing and the macular ganglion cell layer (GCL) thickness in glaucoma.

**Method:** Subjects were 34 eyes of 34 glaucoma patients (17 with preperimetric, 17 with early-stage) and 20 eyes of 20 normal subjects (52.07 ± 14.8 years). Besides Standard Automated Perimetry (SAP) using the Humphrey Field Analyzer, function-selective VF testing including Short Wavelength Automated Perimetry (SWAP), flicker perimetry on the Octopus 311, Frequency Doubling Technology (FDT) on the Humphrey Matrix, and Heidelberg Edge Perimeter (HEP) were performed. Structurally, the GCL (total, superior and inferior) and inner plexiform layer (IPL) thickness was measured using Fourier Domain Optical Coherence Tomography with a macular 6 mm×6 mm cube scan (Topcon, Inc). First, using the number of abnormal points in 52 test points, the areas under the receiver operating characteristic curves (AUCs) for the VF testing were calculated for glaucoma detection. Second, the correspondence between the number of abnormal points within the range of the macular cube scan (8 points each for the superior and inferior VFs) and the GCL+IPL thickness was evaluated separately for the superior and inferior VFs. A VF with more than two abnormal points and the GCL+IPL thickness with a half VF corresponding to sensitivity worse than the normal 5% probability level for an age-similar group were defined as abnormal.

**Results:** The AUCs of the total deviation for SWAP, Flicker, FDT and HEP were 0.66, 0.76, 0.70 and 0.69, respectively. When the GCL+IPL thickness was abnormal, the respective percentages of abnormality were 75.0%, 46.7%, 37.5% and 87.5% (superior), and 72.7%, 50.0%, 45.5% and 90.9% (inferior). When the GCL+IPL thickness was normal, the respective percentages of abnormality were 50.0%, 15.8%, 16.7% and 61.1% (superior), and 43.5%, 20.0%, 34.8% and 56.5% (inferior).

**Conclusions:** The function-selective VF testing could detect the corresponding abnormality in the GCC thickness. However, SWAP and HEP indicated abnormality when the GCC thickness appeared normal.

## Structure-function relationships in the macula of glaucoma patients

Chris Johnson<sup>1</sup>, Jameson Guthmiller<sup>1</sup>, Mona Garvin<sup>2</sup>, Pavlina Kemp<sup>1</sup>

<sup>1</sup>University of Iowa Department of Ophthalmology and Visual Sciences, Iowa City, Iowa, USA, <sup>2</sup>University of Iowa Department of Electrical and Computer Engineering, Iowa City, Iowa, USA

**Purpose:** Traditionally, structural and functional damage in the macular region has been reported to occur with advanced stages of glaucoma. However, several recent studies have demonstrated that there are structural and functional losses that occur in the macular region of glaucoma patients, and that in many instances, these deficits have the appearance of nerve fiber bundle defects. The purpose of this study was to evaluate structural and functional losses in the macula of glaucoma patients who have asymmetric visual field loss in the arcuate nerve fiber bundle regions.

**Method:** Fourteen glaucoma patients with mean deviation (MD) values ranging from 1.78 to -16.04 and an MD asymmetry of 3 or more dB between eyes (range = 3.82 to 16.72) for SITA Standard 24-2 testing were evaluated with Cirrus Optical Coherence Tomography (OCT) and Rarebit automated perimetry of the macular region in both eyes. SITA Standard 10-2 measurements and central 30 degree Rarebit perimetry tests were also performed. The inner and outer sectors of the Cirrus retinal thickness measurements were obtained for the macula along with Rarebit perimetry hit and miss rates for corresponding visual field locations. Asymmetry of these measures between eyes was also determined.

**Results:** Higher miss rates and thinner retinal layers were obtained for the asymmetry measures for 11 out of 14 to 13.5 out of 14 cases for each of the eight sectors evaluated, indicating a strong relationship between structural and functional glaucomatous damage in the macula.

**Conclusions:** There is a strong structure-function relationship in the macular region that reflects glaucomatous damage at relatively early and moderate stages of glaucoma, with the primary areas of loss occurring in the superior and inferior sectors of the macula. In this view, Rarebit perimetry and Optical Coherence Tomography (OCT) appear to be informative, useful clinical tools for quantitative assessment of glaucomatous damage in the macular region of glaucomatous eyes. Subsequent segmentation of the OCT images to specifically identify retinal ganglion cell layer thickness was also performed.



## SE-02, Perimetry I 11:30 am – 1:00 pm

### A Bayesian thresholding procedure for perimetry that models both spatial relations and sensitivity

Andrew Turpin, Luke Chong, Allison McKendrick  
University of Melbourne, Parkville, Australia

**Purpose:** To explore the utility of a new Bayesian perimetric thresholding algorithm that exploits relationships between neighbouring locations.

**Method:** BUSS is a Bayesian algorithm where a probability distribution (pdf) is maintained across all possible pairs of sensitivities for two locations: in this example, (9,9) and (15,15). The prior distribution has pairs where (15,15) is 3dB higher than (9,9) (the eccentricity correction used in the Full Threshold (FT) algorithm) weighted 50 times that of others. The likelihood function is based on a Cumulative Gaussian distribution with standard deviation of 1 dB, and asymptotes of 3%. Stimuli are chosen to minimise the expected entropy of the posterior distributions with a lookahead of one step. The procedure terminates when entropy of the pdf falls below 4, and returns the expected sensitivity at each location.

Using computer simulation, we compare BUSS to FT. We investigate the bias, precision and number of presentations required to estimate all possible thresholds at each location (range 0..40dB) assuming two false positive (FP) rates (3% or 15%), false negatives of 3% and a variability based on Russell et al [ARVO 2011]. Further, a pair of locations from each quadrant of 163 glaucomatous visual fields were tested.

**Results:** When the first presentation of FT is close to threshold, it is faster than BUSS, on average (FP=3%, up to 2.5 presentations per location; fp=15%, 1.5). Otherwise, BUSS is faster than FT (eg. if one location has reduced sensitivity). About 90% of the 652 pairs of real visual field locations were more accurately determined using BUSS, and 20% were both more accurate and faster. FT was faster and more accurate than BUSS in fewer than 10% of real pairs, with the mean loss in accuracy less than 1dB in all cases.

**Conclusions:** When the assumptions underlying the "growth pattern" in FT and SITA are violated (eg: at the borders of scotomas or not matching normative database values), BUSS returns more accurate estimates in fewer presentations. The price BUSS pays for improved performance is 1-2 extra presentations per location for pairs that match FT's assumptions.

In future work we will extend BUSS to more than two locations, and explore its utility as a retest algorithm.

### A new multi stimulus self-check visual field screener, CLOCK CHART®

Chota Matsumoto<sup>1</sup>, Mariko Eura<sup>1</sup>, Sachiko Okuyama<sup>1</sup>, Sonoko Takada<sup>1</sup>, Eiko Arimura<sup>1,2</sup>, Shigeki Hashimoto<sup>1</sup>, Fumi Tanabe<sup>1</sup>, Yoshikazu Shimomura<sup>1</sup>

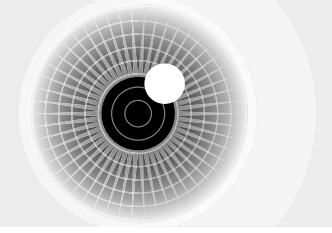
<sup>1</sup>Department of Ophthalmology, Kinki University Faculty of Medicine, Osaka-Sayama, Japan, <sup>2</sup>Department of Ophthalmology, Kinki University Faculty of Medicine, Sakai Hospital, Sakai, Japan

**Purpose:** CLOCK CHART® is a multi stimulus type self-check visual field screening sheet developed by us. The test chart is rotated during the examination and the visual field abnormalities are pointed out by patients themselves. In this study we evaluate the clinical usefulness of this chart with hospital patients with glaucoma and the population screening.

**Method:** 122 eyes of 122 glaucoma patients ( the average age 60.4±10.9 years old ) and 35 eyes of 35 normal subjects (the average age 42.6±15.4 years old) were tested using CLOCK CHART®. The static visual fields were obtained by using a Humphrey Field Analyzer with program 24-2 or 30-2 or Octopus 101 G2 program and were classified using the Aulhorn's classification modified by Graves. The sensitivity and the specificity of the CLOCK CHART® for detecting visual field abnormalities were evaluated in whole 30 degrees and at each 5, 10, 15, 20, and 25 degrees eccentricity zone. Between October 18, 2009 and November 15, 2009, 62,455,367 copies of CLOCK CHART® were released in newspapers for the population screening and panel research on the internet was performed.

**Results:** The sensitivity of CLOCK CHART® was 85% (Stage I) , 93% (Stage II) and 100% (Stage III to VI) in glaucoma. The agreement of the visual field defect area in CLOCK CHART® with the static fields were 93% (Stage I to VI) and 100% (Stage II to VI). The specificity of CLOCK CHART® was 90%. In the population screening, 350,783 (5%) subsequently consulted a doctor and 31,076 (16.4%) of them were diagnosed with glaucoma. Of those diagnosed, 9,342 (48.4%) received medical treatment.

**Conclusions:** CLOCK CHART® is a simple and highly reliable self-check screening chart for detecting visual field abnormalities in patients with glaucoma.



## Characteristics of spikes-shaped isopters in automated kinetic perimetry

Shigeki Hashimoto<sup>1</sup>, Chota Matsumoto<sup>1</sup>, Sachiko Okuyama<sup>1</sup>, Sonoko Takada<sup>1</sup>, Eiko Arimura<sup>2</sup>, Hiroki Nomoto<sup>1</sup>, Fumi Tanabe<sup>1</sup>, Tomoyasu Kayazawa<sup>1</sup>, Mariko Eura<sup>1</sup>, Yoshikazu Shimomura<sup>1</sup>

<sup>1</sup>Department of Ophthalmology, Kinki University Faculty of Medicine, Osaka-sayama, Osaka, Japan, <sup>2</sup>Department of Ophthalmology, Kinki University Faculty of Medicine, Sakai Hospital, Sakai, Osaka, Japan

**Purpose:** To eliminate spikes-shaped isopters due to response variability in false-positive (FP)/false-negative (FN) rates, frequency-of-seeing (FOS) curve, and reaction time (RT) in automated kinetic perimetry, we developed a new algorithm and evaluated its effectiveness in virtual patients using our fully automated kinetic perimetry, Program K.

**Method:** Subjects were 120 eyes of 120 patients (average age,  $61.8 \pm 12.8$  years; 76 eyes with glaucoma, 29 eyes with neuro-ophthalmological diseases, and 15 eyes with retinitis pigmentosa) who were classified into two groups according to the characteristic of their visual field changes: Group I with flat changes and Group II with steep changes. All the subjects underwent Goldmann manual kinetic perimetry (MKP) and their isopters were digitized in K-Train (an Octopus kinetic perimetry training software developed by Tübingen University) to be used on 120 virtual patients. Using target sizes of V/4e, III/4e, I/4e, I/3e, I/2e, and I/1e at a speed of 3 degrees/sec, we assessed the visual field loss of the 120 virtual patients by Program K. With K-Train, we could adjust the virtual patients' FP and FN rates, scatter in the FOS curve, and scatter of RT. By evaluating these factors, the number of vectors and test duration, we compared the results of Program K and the Goldmann MKP.

**Results:** If the FP and FN rates were both lower than 20%, the results by both methods were comparable. If the FP and FN rates were equal to or higher than 20%, and the number of vectors and test duration also increased significantly, spikes were observed in some of the Program K isopters. However, if the scattering in the FOS curves in K-Train for Group I and II was less than 0.7 and 0.9, respectively; and the scatter of reaction times was less than 0.4, the results by both methods were comparable. This showed that the new algorithm for Program K could effectively eliminate the spikes in the isopters and yield results comparable to those by the Goldmann MKP.

**Conclusions:** The new algorithm in Program K appeared to be able to effectively reduce the occurrence of spikes in the isopters and optimize the use of Program K.

## Normal variability for two forms of perimetry using anatomically inspired test locations

Mitchell Du<sup>1</sup>, William Swanson<sup>2</sup>, Irene Tran<sup>1</sup>

<sup>1</sup>State University of New York, State College of Optometry, New York, New York, USA, <sup>2</sup>Indiana University School of Optometry, Bloomington, Indiana, USA

**Purpose:** To assess normal variability at test locations inspired by optic nerve and nerve fiber layer maps, using size III perimetry and Contrast Sensitivity Perimetry (CSP).

**Method:** 34 eyes of 34 young control subjects were tested two times each on two separate days with both forms of perimetry. Sensitivity was measured at 56 locations in the central visual field, based on maps for neuro-retinal rim and retinal nerve fibers, using Goldmann size III on a HFA II Model 750i and Contrast Sensitivity Perimetry (CSP) for Gabor sines with peak spatial frequencies from 0.14-0.50 cycle/deg, scaled for location and flickered at 5 Hz.

**Results:** Between-subject variability was similar for CSP and size III within 10° of fixation, averaging 1.29 dB for CSP and 1.44 dB for size III ( $t = 1.59$ ,  $p > 0.3$ ). SD increased with eccentricity for size III ( $t = 4.6$ ,  $p < 0.0005$ ) but not for CSP ( $t = 1.13$ ,  $p > 0.26$ ). Between-subject variability across all locations was more strongly correlated with eccentricity for size III ( $r^2 = 2\%$ ,  $p < 0.0001$ ) than for CSP ( $r^2 = 0.1\%$ ,  $p < 0.01$ ), and the difference in slopes was significant ( $z = 25.3$ ,  $p < 0.0001$ ). Test-retest variability was on average higher for size III than CSP ( $z = 5.4$ ,  $p < 0.0001$ ), and increased more dramatically with eccentricity ( $z = 7.0$ ,  $p < 0.0001$ ).

**Conclusions:** Normal variability was lower for CSP compared to size III, due to reduced effects of eccentricity for CSP.

## Relationship of the threshold values between the kinetic target and static target in normal subjects

Tomoyasu Kayazawa<sup>1</sup>, Chota Matsumoto<sup>1</sup>, Sachiko Okuyama<sup>1</sup>, Sonoko Takada<sup>1</sup>, Shigeki Hashimoto<sup>1</sup>, Eiko Arimura<sup>2</sup>, Hiroki Nomoto<sup>1</sup>, Fumi Tanabe<sup>1</sup>, Mariko Eura<sup>1</sup>, Yoshikazu Shimomura<sup>1</sup>

<sup>1</sup>Department of Ophthalmology, Kinki University Faculty of Medicine, Osaka-Sayama, Osaka, Japan, <sup>2</sup>Department of Ophthalmology, Kinki University Faculty of Medicine, Sakai, Osaka, Japan

**Purpose:** It is well known that divergence exists between threshold values of kinetic perimetry and those of static perimetry even under the same conditions. This statokinetic dissociation (SKD) cause problems when we decide visual disorder levels using both static and kinetic perimetry as well as when we decide the target luminance of the spot check using static perimetry, which is necessary for fully automated kinetic perimetry. Previous reports have examined physiologic SKD without consideration toward the reaction time (RT) of subjects. This study reports the relationship of static perimetric threshold and kinetic threshold with RT-corrected kinetic targets using the automated perimeter.

**Method:** The subjects were 5 eyes of 5 healthy youths (4 males and 1 female; age: 30.8±2.1 years). Perimetry was done using Octopus<sup>®</sup>900 with automated perimeter. Each of the 4 meridians (45°, 135°, 225°, 315°) was measured with Goldmann Kinetic Perimetry (GKP) using the target speed of 1-10 degrees/sec and the size and luminance of III4e, I4e, I3e, I2e, and I1e. When deciding threshold values, kinetic target was corrected with the RT. Static perimetry was performed using the custom test program with the normal strategy and stimulus size III on the meridians where the kinetic perimetry was carried out. The measuring points were arranged with distance of 2 degrees to one another, and threshold values were measured and compared with those of the points which corresponded to the points where response was obtained in GKP.

**Results:** Clinically the target speed of 3 degrees/sec is used and at this speed the threshold value of III4e obtained with kinetic targets corresponded to the static threshold value of 3.4±4.8 dB. The same applied for I4e value which corresponded to the static threshold value of 13.0±1.9; for I3e, to 17.9±2.1; for I2e, to 23.3±1.6; and for I1e, to 27.6±0.7. RT-corrected kinetic targets demonstrated divergence from the photometric harmony based on the theoretical spatial summation compared to the static targets.

**Conclusions:** When corrected by RT, the threshold values obtained using kinetic targets were lower than those with static targets, therefore, photometric harmony based on the simple spatial summation cannot be applied.

## The relative performance of visual field tests using subsets of the 24-2 test pattern at detecting glaucomatous field loss.

Yanfang Wang, David B Henson

University of Manchester, Manchester Academic Health Sciences Centre (MAHSC), NIHR Manchester Biomedical Research Centre, Manchester, UK

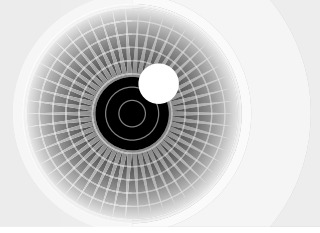
**Purpose:** To evaluate the performance of using subset of 24-2 SITA standard test patterns in detecting early glaucomatous eyes and the relative characteristics of detected visual field defects.

**Method:** The pointwise positive predictive value (PPV) was calculated from a database of the visual field test results (SITA standard 24-2 algorithm, Humphery Visual Field Analyzer, Carl Zeiss Meditec, USA) from 6696 eyes of 3586 suspicious/diagnosed glaucoma patients (age 66.0±13.0yrs). The sample was divided into three groups: normal: MD>-2.5dB, 3575 eyes; mild:-2.5 to -6dB, 2166 eyes and moderate -6 to -12 dB, 955 eyes. Calculation of the optimised test pattern started with a single test point at the maximum PPV location of the normal plus mild/moderate group. Eyes missing this location were removed from the sample and the PPV of the residual sample recalculated. This process was repeated until all eyes in the mild/moderate group had been detected. Receiver operating characteristic (ROC) curves were established for PPV-optimized and five randomized patterns, with a fail criteria of a single missed stimulus at p<0.01. Characteristics of visual field defects (MD, PSD) detected with subsets of optimized test pattern were established.

**Results:** In the mild and moderate groups the area under ROC curve was greater for the optimized pattern than the randomized. With the optimized pattern 88% and 96% of the moderate field defects were detected with 10 and 15 stimulus locations respectively. With each increment in the number of test locations, the MD of additionally detected eyes became more positive while PSD became less positive (for eyes detected with 1-10 locations in mild group: MD-4.17±0.97dB, PSD3.7±1.56; for 41-50 locations MD-3.57±0.95dB, PSD1.93±0.66, p<0.001).

**Conclusions:** High sensitivities can be obtained with optimized subsets of the current 24-2 stimulus pattern. Such patterns could be valuable for screening large populations where test times with the full 24-2 pattern are not cost effective.





## SE-03, Ageing and Quality of Life 2:15 pm – 3:30 pm

### Evaluation and comparison to functional performance of the California Central Visual Field Test (CCVFT)

Ronald Schuchard<sup>1,2</sup>, Donald Fletcher<sup>3</sup>, Gianfrancesco Villani<sup>4</sup>

<sup>1</sup>Stanford University, Stanford, CA, USA, <sup>2</sup>VA Palo Alto HCS, Palo Alto, CA, USA, <sup>3</sup>California Pacific Medical Center, San Francisco, CA, USA, <sup>4</sup>Unione Italiana Ciechi Ipovedenti, Verona, Italy

**Purpose:** Central Visual field characteristics (scotomas) are important for assessing dysfunctions and planning interventions for vision rehabilitation services. However, standard perimeters (e.g., HFA and Octopus) and specialized macular perimeters (e.g., SLO and MP1) are not widely used in most vision rehabilitation services. The CCVFT screening efficacy and the ability of results to relate to typical functional vision goals was evaluated for patients in vision rehabilitation services.

**Method:** Central visual fields were measured in 25 participants with the SLO and the CCVFT. The CCVFT uses a "tangent screen" form with a paper screen and laser pointers for stimuli. Three lasers with low, moderate, high light levels (factor of 10 between each level) determine three isopters of the central visual field. In a further study, 249 English reading participants and 38 Italian reading participants had binocular vision assessed by: visual acuity; dense/relative scotomas (CCVFT); contrast sensitivity testing (Peli-Robson); and reading performance (SKRead). Scotomas within 2.5 degrees of the fixation and right/left sided SKRead errors were noted.

**Results:** Comparison of scotoma screening showed a kappa of 0.89 in general detection (location relative to fixation) between SLO and CCVFT with further analysis showing that results that were not in agreement were all small scotomas ( $d < 3$  degrees). For the larger study: Visual acuity median (range) was 20/120 (20/20-20/962). 71% participants demonstrated a bordering scotoma of which 39% had a dense scotoma and 32% had only a relative scotoma. Binocular PRL scotoma borders were: Right – 40%; Left – 31%; Right and Left – 16%; Superior – 45%; Inferior – 24%; and 12% ring scotoma pattern. Total SK Read errors were significantly ( $p < 0.05$ ) related to visual acuity. SKRead errors on the right side of words were significantly higher with scotomas to the right, both sides of fixation and with ring scotomas while left errors were significantly ( $p < 0.05$ ) higher only in patients with left scotomas. Minor differences were found between languages.

**Conclusions:** CCVFT perimetry produces similar results as the SLO with added binocular testing. The location of scotomas and reading errors were significantly related. CCVFT scotoma prevalence and locations are remarkably similar to previous SLO macular perimetry.

### Flicker perimetry can be used to monitor progression in age-related macular degeneration

A. J. Vingrys<sup>1</sup>, P. Dimitrov<sup>1,2</sup>, C. D. Luu<sup>2</sup>, L. Robman<sup>2</sup>, M. Varasmidis<sup>2</sup>, K. Z. Aung<sup>2</sup>, R. H. Guymer<sup>2</sup>

<sup>1</sup>Department of Optometry & Vision Sciences, The university of Melbourne, Parkville, Vic, Australia, <sup>2</sup>Centre for Eye Research Australia, East Melbourne, Australia

**Purpose:** Given the report that flicker sensitivity loss can precede the development of wet AMD (Mayer et al. 2004) we consider whether luminance-pedestal flicker sensitivity can be used to predict progression of AMD patients to the dry end-stage (geographic atrophy) form of AMD.

**Method:** 226 patients were recruited and followed for at least 2 years (mean follow up = 4 years in AMD cases). Of these, 182 had early AMD (eAMD, drusen  $> 63$  micron  $\pm$  pigmentary changes) and 24 were age-similar normals with no evidence of AMD in either eye. Subjects were tested at 6-monthly intervals with luminance-pedestal flicker perimetry on 1°, 3°, 6° and 10° rings in their macula region using a Medmont M700 perimeter. Subjects were instructed to respond to "twinkle" or "flicker" and a static false positive monitor tolled for compliance to this instruction. Patients who gave false positive rates  $> 20\%$  were re-instructed and retested.

**Results:** No eye in the normal group developed AMD and returned an average flicker sensitivity of  $22.9 \pm 3.0$  dB (mean  $\pm$  SD). 166 eyes (91%) did not progress to end-stage and a subset of these eyes ( $n = 18$ ) matched to the conversion group had their flicker sensitivity evaluated: these had an average flicker sensitivity of  $17.3 \pm 3.6$  dB [95% CLs 15.6 to 19.0 dB] which was significantly reduced from normal ( $p < 0.01$ ). 16 eyes (of 16 subjects) converted to geographic atrophy over the follow up period: the average flicker sensitivity of this group was significantly depressed ( $9.6 \pm 2.8$  dB, [95% CLs 7.70 to 11.5 dB]) from both the control and eAMD groups. The eyes that progressed showed losses at multiple points 18 months prior to conversion and had a significantly greater rate of change in flicker sensitivity in the involved points over this same time period ( $-0.38 \pm 0.41$  dB/mnth, vs AMC  $-0.003 \pm 0.03$  vs eAMD  $-0.03 \pm 0.28$ ,  $p < 0.001$  each).

**Conclusions:** Flicker perimetry provides a useful biomarker for AMD progression and conversion to end-stage. Others show that it can predict the onset of wet AMD and we show that it does likewise for geographic atrophy some 18 months beforehand.

## Investigating perceptual learning effects in standard automated perimetry in ageing and in central and peripheral vision

Josephine Battista, Allison McKendrick

*The University of Melbourne, Melbourne, Victoria, Australia*

**Purpose:** It is generally agreed that repeated sessions lead to a learning effect in standard automated perimetry (SAP). In this study, we explore whether learning is altered by having the training paradigm involve different regions of the visual field. The study was motivated by reports of differences in perceptual learning between central and peripheral vision for a range of other non-perimetric perceptual tasks. We also compare this learning effect in different age groups as it is not fully understood whether learning effects in SAP change with age.

**Method:** Thirty-six people participated in this study: 18 older participants (aged 62-78 years; mean =  $69 \pm SD = 5.4$  years) and 18 younger participants (aged 20-34 years; mean =  $28 \pm SD = 3.6$  years). Each group was equally divided into three subgroups which were blocked by training paradigm: Full, Central and Peripheral. Each participant conducted SAP on a Medmont perimeter for a total of six sessions. The first five sessions were each separated by between 3 and 7 days. The final 'retention' session was conducted three months after the fifth session. The first session involved training to familiarize with the task to eliminate 'fast perceptual learning' or learning associated with the procedure. The same experimenter conducted all experiments. At all sessions, data was collected for one eye. At Sessions 1, 5 and 6, data was also collected on both eyes and in the non-trained field (for central and peripherally trained groups) to determine if learning transferred to the untrained location and untrained eye.

**Results:** Repeated sessions with SAP lead to learning. Age did not effect the amount of learning for either central [RM ANOVA:  $F_{(1, 20)} = 2.87, p = 0.11$ ] or peripheral tasks [RM ANOVA:  $F_{(1, 20)} = 0.21, p = 0.65$ ]. Analysis of the peripheral data demonstrates that the learning effect is significantly affected by the training paradigm [RM ANOVA:  $F_{(5, 100)} = 3.60, p = 0.005$ ].

**Conclusions:** By changing the training paradigm, the learning effect in SAP observed with repeated sessions will differ in the peripheral visual field; however this learning effect is not affected by age.

## Mobility limitations in patients with glaucoma

Sharon Bentley<sup>1,2</sup>, Raymond LeBlanc<sup>1</sup>, Marcelo Nicolela<sup>1</sup>, Paul Artes<sup>1</sup>, Balwantray Chauhan<sup>1</sup>

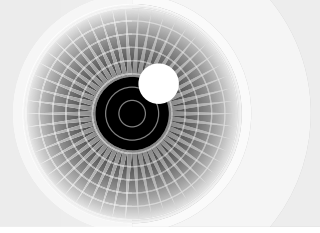
*<sup>1</sup>Department of Ophthalmology and Visual Sciences, Dalhousie University, Halifax, Nova Scotia, Canada, <sup>2</sup>Centre for Eye Research Australia, University of Melbourne, Royal Victorian Eye and Ear Hospital, East Melbourne, Victoria, Australia, <sup>3</sup>School of Medicine (Optometry), Faculty of Health, Deakin University, Waurin Ponds, Victoria, Australia*

**Purpose:** Glaucoma has major impact on mobility. It has been associated with involvement in motor vehicle collisions and decreased driving performance, increased risk of falls, and reduced walking speed. As yet, little is known about mobility limitations and adaptations. The purpose of this study was to investigate driving and walking limitations experienced by patients with glaucoma.

**Method:** We conducted a cross-sectional analysis of 48 patients with glaucoma aged over 50 years who were recruited from a university hospital-based eye care clinic (mean better eye MD -3.9 [SD 5.1] dB), and 47 age-matched healthy control participants. Driving limitations were evaluated using the Driving Habits Questionnaire (DHQ) and walking limitations using the Independent Mobility Questionnaire (IMQ). Clinical vision measures included visual acuity (VA), contrast sensitivity, standard automated perimetry and useful field of view (UFOV). Analyses were adjusted for age, sex, number of medical conditions and VA.

**Results:** Forty (83%) patients with glaucoma and 44 (94%) control participants were current drivers. Patients with glaucoma were more likely to not have driven to "distant towns" in the past year compared with control participants (OR = 6.4, 95% CI 1.4 to 29.1). Glaucoma was associated with self-reported difficulty walking at night, difficulty adjusting to lighting changes at night (going from indoor to street lighting), and difficulty walking in high glare areas due to vision ( $P < 0.05$ ). There was a significant difference in IMQ score (mean difficulty across 35 walking situations) between patients and control participants ( $P < 0.01$ ). Among patients with glaucoma, avoidance of challenging driving conditions (DHQ avoidance subscale) was correlated with UFOV divided attention processing speed ( $r = -0.50, P = 0.001$ ). Walking difficulty (IMQ score) was best correlated with mean better eye MD ( $r = -0.42, P < 0.01$ ).

**Conclusions:** Glaucoma is associated with driving limitations and walking difficulties, and corresponding lifestyle adaptations. UFOV and mean better eye MD are important predictors. These findings may inform clinical management, enhance efforts to provide access to local care, and be useful in the development of interventions that help patients with glaucoma maintain safe mobility and quality of life.



## Relationship between attentional visual fields and integrated visual field sensitivity among older adults with glaucoma

Alex Black, Joanne Wood

Queensland University of Technology, Kelvin Grove, Brisbane, Australia

**Purpose:** To examine how binocular integrated visual field (IVF) sensitivity relates to attentional visual field (AVF) performance among older adults with glaucoma, in order to better understand the functional impact of glaucomatous field loss.

**Method:** Participants included 59 older adults with primary open-angle glaucoma (aged 74±6 years, range 65-90). Binocular IVF were derived from monocular 24-2 SITA-Standard HFA plots, based on the more sensitive of the two eyes at each location. An overall mean deviation score was calculated, in addition to superior and inferior scores (locations above and below the horizontal midline). Binocular AVF performance was assessed using a custom-written program which measured the extent over which a person can simultaneously process visual information from both central and peripheral locations. The central task involved reporting whether a circle was present or absent; the peripheral task involved identification of the location of a triangle in one of 24 locations presented at three eccentricities (10, 20 and 28°). Two AVF tasks were examined for a stimulus duration of 90ms: [1] divided attention (no peripheral distractors present) and [2] selective attention (peripheral distractors present). The overall sum of incorrect responses was recorded, in addition to superior and inferior scores. Regression models examined the age-adjusted association between IVF sensitivity and AVF scores.

**Results:** Overall IVF sensitivity was predictive of AVF performance in this cohort, accounting for 63% of the variance in divided AVF scores. Only 26% of the variance in selective AVF scores was explained by IVF sensitivity, which may relate to the greater cognitive demands of this task. When the superior and inferior field locations were considered, no significant differences were found between divided AVF scores; however, in the selective AVF task, the inferior field performed significantly worse than the superior field, even after adjustment for IVF sensitivity.

**Conclusions:** Reduced visual field sensitivity among older adults with glaucoma impedes their visual search abilities, as demonstrated by poorer performance on the AVF. These findings assist in estimating the extent of attentional fields expected in older adults with glaucoma and is particularly relevant for functional activities such walking and driving.

## SE-04, Change 4:00 pm - 5:15 pm

### Peripapillary Retinal Nerve Fiber Layer (RNFL) - Thickness compared with RNFL retardance and electroretinographic changes at the onset of optic nerve head surface topography change in experimental glaucoma

Brad Fortune, Grant Cull, Juan Reynaud, Lin Wang, Claude Burgoyne

Discoveries in Sight Research Laboratories, Devers Eye Institute, Legacy Health, Portland, OR, USA

**Purpose:** To compare peripapillary RNFL thickness (RNFLT) with RNFL retardance and retinal functional changes at the onset of optic nerve head (ONH) surface topography change in a non-human primate experimental model of glaucoma.

**Method:** Thirty-three rhesus macaque monkeys had three or more weekly baseline measurements in both eyes of ONH surface topography (HRT2, Heidelberg Engineering, GmbH), RNFLT (Spectralis SD-OCT, Heidelberg), RNFL retardance (GDxVCC, Carl Zeiss Meditech, Inc) and three forms of electroretinography (ERG): multifocal ERG, transient pattern-reversal ERG and full-field photopic ERG. Laser photocoagulation was then applied to the trabecular meshwork of one eye each to induce chronic elevation of IOP. Testing continued approximately weekly thereafter, alternating between ONH surface topography and RNFLT in one week and RNFL retardance and ERG the next. Animals were sacrificed shortly after onset of ONH surface topography change, defined as the first HRT session when either the mean position of the disc (MPD) fell below the 95% confidence limit of each eye's individual baseline range or when the HRT Topographic Change Analysis map (subjectively) exhibited change, both requiring two confirmations. Longitudinal data were assessed by repeated-measures ANOVA with Bonferroni-corrected post-hoc testing of group or time point differences.

**Results:** There was no significant difference in RNFLT at the onset of ONH surface topography change in experimental eyes as compared with control eyes ( $p=0.70$ ) or baseline average ( $p=0.57$ ). RNFL retardance during the session immediately preceding ONH surface change ( $15 \pm 19$  days before onset, median=9 days) was reduced in treated eyes by an average of  $5 \pm 8\%$  (range +5% to -26%) relative to control eyes ( $p=0.002$ ) or to baseline average ( $p=0.001$ ). RNFL retardance during the session immediately subsequent to ONH surface change onset ( $7.5 \pm 5.4$  days after ONH onset) was reduced in treated eyes by an average of  $12 \pm 9\%$  (range 0 to 43% loss, median=10% loss,  $p<0.001$ ) relative to control eyes ( $p<0.0001$ ) or baseline average ( $p<0.0001$ ), representing progression of RNFL retardance ( $p<0.001$ ). High-frequency oscillations of the mfERG were also selectively reduced at this time point by  $16 \pm 20\%$  relative to control eyes ( $p<0.001$ ) and by  $23 \pm 18\%$  relative to baseline average ( $p<0.001$ ). At the next available SD-OCT session, an average of 9 days later, RNFLT exhibited its first significant decline as compared with



either control eyes ( $4\pm 7\%$  thinner, median = 2%,  $p=0.001$ ) or with baseline average ( $p=0.004$ ).

**Conclusions:** Decreased RNFL retardance and specific retinal ganglion cell functional loss in the absence of RNFLT changes represents evidence of dysfunction preceding axonal degeneration at the onset of ONH surface topography change in experimental glaucoma.

## Rates of matrix and standard automated perimetry change in glaucoma and high-risk ocular hypertension

Deborah Goren<sup>1</sup>, Stuart Gardiner<sup>1</sup>, Chris Johnson<sup>2</sup>, Shaban Demirel<sup>1</sup>

<sup>1</sup>Devers Eye Institute, Portland, OR, USA, <sup>2</sup>University of Iowa, Iowa City, IA, USA

**Purpose:** To compare rates of functional change in eyes with early glaucoma or high-risk ocular hypertension using Matrix FDT (MAT) and the Humphrey field analyzer (SAP) using each instrument's native units (MAT: 20 dB / log unit contrast and SAP: 10 dB / log). This study also compared rates of change for equivalent units.

**Method:** 207 eyes from 104 participants with early glaucoma or high-risk ocular hypertension were followed longitudinally using MAT (24-2 ZEST) and SAP (24-2 SITA) over 6 years, with a minimum of 7 exams. Rates of change were calculated using robust linear models with M-estimation (RLM). MAT and SAP were compared using Generalized estimating equations (GEE) to account for correlations between fellow eyes.

**Results:** On average, MAT MDs were worse than SAP MDs at the start of the sequence ( $-0.25\pm 3.26$  dB vs.  $0.44\pm 2.03$  dB,  $p=0.001$ ). Both techniques showed significant change in MD over time ( $p_{\text{MAT}}=0.01$ ,  $p_{\text{SAP}}<0.001$ ), but the rates of change were similar between the two techniques (MAT:  $-0.11\pm 0.41$  dB/yr vs. SAP:  $-0.13\pm 0.29$  dB/yr,  $p=0.6$ ) despite the different units. The difference in MD between techniques was consistent across visits (initial:  $-0.69\pm 2.34$  dB, recent:  $-0.35\pm 2.7$  dB,  $p=0.12$ ). Initial MAT PSDs were also worse than SAP PSDs ( $3.16\pm 1.35$  dB vs.  $2.12\pm 1.88$  dB,  $p<0.001$ ). MAT PSD rates of change were significantly slower than SAP ( $0.04\pm 0.14$  dB vs.  $0.07\pm 0.18$  dB,  $p=0.02$ ), reducing the difference between techniques ( $p=0.002$ ). Mean pointwise rates of change at each location were similar between techniques ( $0.03$  to  $-0.33$  dB/yr vs.  $-0.14$  to  $-0.37$  dB/yr). Rates of MAT and SAP change were significantly different at  $<20\%$  of locations. After applying a correction to make dB units equivalent, rates of MD ( $p<0.001$ ), PSD ( $p<0.001$ ) and pointwise ( $>90\%$  of locations) change were significantly slower for MAT than SAP.

**Conclusions:** When using instrument-specific dB units, MAT showed greater initial damage than SAP. However, neither pointwise nor global indices changed more rapidly using MAT. When using equivalent dB units, rates of change, for both pointwise and global indices, were more rapid for SAP.

## Relationship of central corneal thickness to visual field progression in eyes with Glaucoma

Deepa Viswanathan<sup>2</sup>, Stuart Graham<sup>1,2</sup>, Ivan Goldberg<sup>1,3</sup>

<sup>1</sup>Eye Associates, Sydney, New South Wales, Australia,

<sup>2</sup>Australian School of Advanced Medicine, Macquarie University, Sydney, New South Wales, Australia,

<sup>3</sup>University of Sydney, Sydney, New South Wales, Australia

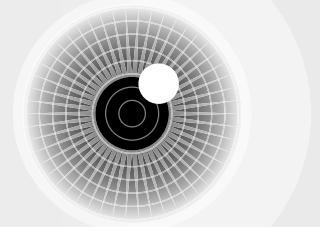
**Purpose:** To determine the relationship of central corneal thickness (CCT) at baseline to glaucomatous damage and whether CCT or change in CCT over time correlates with subsequent visual field progression.

**Method:** This was a prospective study of 392 eyes of 209 patients with medically treated glaucoma who were followed for a mean period of  $6.8\pm 1.8$  years. Patients with laser or surgery were excluded. All underwent ultrasonic corneal pachymetry, serial visual fields and confocal scanning laser tomography. There were 309 eyes with sufficient visual fields to determine progression using Glaucoma Progress Analysis (GPA).

**Results:** Baseline CCT correlated positively with both mean deviation (MD) ( $r=0.24$ ,  $p=0.001$ ) and neuroretinal rim area ( $r=0.21$ ,  $p=0.012$ ) such that thinner corneas were associated with more advanced presentation. Progression of visual field was detected in 50/309 eyes (16%) whereas 84% revealed no progression. Progressive eyes had significantly thinner ( $p=0.001$ ) baseline CCT at  $513.93\pm 31.36$   $\mu\text{m}$  and significantly worse ( $p<0.001$ ) MD at  $-5.41\pm 5.47$  dB compared to non progressive eyes with baseline CCT of  $537.50\pm 35.44$   $\mu\text{m}$  and MD of  $-1.99\pm 3.06$  dB.

The slope of visual field change was significantly greater ( $p=0.04$ ) for eyes with baseline CCT  $<540$   $\mu\text{m}$  compared to eyes with CCT  $>540$   $\mu\text{m}$ . Kaplan Meier analysis revealed higher survival ( $p=0.001$ ) in eyes with a baseline CCT  $>540$   $\mu\text{m}$  as compared to eyes with CCT  $<540$   $\mu\text{m}$ . A small but significant reduction (mean  $12.78\pm 13.35$  microns,  $p<0.001$ ) of CCT was noted in all treated eyes, however there was no difference in the amount of change between progressive and non progressive eyes. The amount of change in CCT did not correlate with the change in MD and rim area.

**Conclusions:** CCT correlates significantly with the amount of baseline glaucomatous damage and thinner corneas may be associated with increased risk of visual field progression. CCT reduced slightly over time in eyes with glaucoma however this did not relate to visual field progression.



## Sensitivity and specificity of a series of glaucoma change probability criteria

Gideon Zamba<sup>1</sup>, Carrie Doyle<sup>2</sup>, Chris Johnson<sup>2</sup>, Michael Wall<sup>2,3</sup>

<sup>1</sup>University of Iowa, Department of Biostatistics, Iowa City, IA, USA, <sup>2</sup>University of Iowa, Department of Ophthalmology and Visual Sciences, Iowa City, IA, USA, <sup>3</sup>University of Iowa, Department of Neurology, Iowa City, IA, USA

**Purpose:** Many combinations of abnormality have been proposed for defining progression using the glaucoma change probability (GCP) method. We tested a series of criteria varying the number of abnormal test locations from 2 to > 10 and the number of visits where the abnormality was confirmed to determine which combinations had optimum sensitivity and specificity.

**Method:** Sixty (60) normal subjects and 120 glaucoma patients were tested every six months for 4 years with SITA standard 24-2. We used the GCP method to compare 63 combinations of the presence of spatially repeated abnormal test locations at consecutive and semi-consecutive visits. Progression was confirmed at 2 consecutive, 3 consecutive, 2 of 3 visits, 3 of 4 and 2 of 4 each, at spatially repeated visual field test locations ranging in number from 2 to > 10.

**Results:** The optimal method emphasizing specificity was GCP with greater than 4 test locations that changed with confirmation at 3 of the 4 locations or GCP (>4, 3x4); this gave 47% sensitivity and 92% specificity. The optimal method emphasizing sensitivity was GCP (>5, 2) with sensitivity 65% and specificity 80%. The results of other methods will be presented.

**Conclusions:** Since specificity is critical for determining glaucoma progression, GCP (>4, 3x4) appears to be a clinically useful and efficient method of defining visual field change in glaucoma.

## Visual field progression in glaucoma: estimating the overall significance of deterioration with permutation analyses of point-wise linear regression

Neil O'Leary, Balwantray Chauhan, Paul Artes  
Dalhousie University, Halifax, Nova Scotia, Canada

**Purpose:** Point-wise linear regression (PLR) is a sensitive method to measure visual field change. We introduce a generic method for estimating the overall statistical significance of the observed pattern of change, and compare its sensitivity and specificity to other PLR criteria for progression.

**Method:** A statistic  $S$  was designed to summarise evidence for deterioration in series of visual fields, by combining the one-sided significance values from individual test locations using Fisher's method. To determine the overall statistical significance ( $p_s$ ) of the observed  $S$ , its null distribution was derived from repeated random reordering (permutation) of the visual field sequence. The technique was evaluated in a large clinical dataset from patients with glaucoma ( $n=1081$ , median mean deviation [MD] -3.0 dB, IQR: -6.3, -1.2 dB) followed for > 5 years (median 10 examinations). One subset ( $n=581$ ) was used to estimate the hit-rate (proportion of eyes with  $p_s < \alpha$ , the nominal significance levels between 0.001 and 0.10). To confirm that the specificity of the method was equivalent to the nominal significance level, the false-positive rate was estimated from the randomly reordered sequences of the other subset ( $n=500$ ). Hit-rate and specificity were estimated at the 5<sup>th</sup>, 8<sup>th</sup> and final examinations, at which corresponding median follow-up periods were 3.5, 6.1 and 8.3 years.

**Results:** Evidence for deterioration at  $p_s < 0.05$  was observed in 15%, 37% and 49% of series, at the 5<sup>th</sup>, 8<sup>th</sup> and final available examinations respectively. Corresponding false-positive rates of the analysis were 6%, 5% and 5%; not significantly different from  $\alpha$ . When compared to other PLR criteria (e.g., 1 point deteriorating at -1.0 dB/year at  $p < 0.01$ ), the hit-rate of this new method was higher at the 5<sup>th</sup> exam ( $p=0.002$ , McNemar's test) and similar at the 8<sup>th</sup> and final exam ( $p=0.96$ ,  $p=0.49$ ), at similar specificity. In series with  $p_s < 0.05$  the medians of MD change from baseline were -2.6, -3.3 and -3.9 dB at the 5<sup>th</sup>, 8<sup>th</sup> and final examinations.

**Conclusions:** Combining evidence from test locations provides a single, straightforward, and accurate estimate of statistical significance for localised visual field progression. Unlike previous methods, this approach is individualised to each patient's own data.



TUESDAY 24 JANUARY 2012	
8:00	<b>Registration opens</b>
8:30	<b>SE-05</b> <b>Structure-Function Maps</b> <b>Chairs: John Flanagan and Andrew Turpin</b>
	Development of patient-tailored structure/function maps <b>Julia Lamparter</b> Factors in the Retinal Nerve Fiber Layer (RNFL) bundle angles at the optic disc <b>Fumi Tanabe</b> Spatial correspondence between retinal nerve fiber layer thickness from OCT and perimetric sensitivity <b>Stuart Gardiner</b> The influence of ocular anatomical variables on individual structure-function maps <b>Jonathan Denniss</b>
9:30	<b>Mini Break</b>
9:35	<b>SE-06</b> <b>Perimetry II</b> <b>Chairs: Michael Wall and Andrew Anderson</b>
	Combining color with luminosity: green on red pupil perimetry in glaucoma <b>Corinne Carle</b> Comparison of the diagnostic capability of oculus-spark perimetry with respect to three procedures of morphological analysis (GDx, HRT and OCT) <b>Manuel Gonzalez de la Rosa</b> Influences of background complexity on monocular and binocular visual sensitivities <b>Akemi Wakayama</b> Response time measures relative to "probability of seeing" across the visual field <b>Allison McKendrick</b>
10:35	<b>MORNING TEA</b>
11:00	<b>SE-07</b> <b>Imaging and Electrophysiology</b> <b>Chairs: Stuart Graham and Ted Maddess</b>
	Does a simple stretch model account for retinal thinning seen in high myopia? <b>Michael Pianta</b> Imaging axonal transport in the rat visual pathway <b>Brad Fortune</b> Why do retinal nerve fiber layer measures differ across SD OCT Instruments? <b>Ronald Harwerth</b> Pattern electrophysiology and visual fields measured on the same day in between migraine attacks <b>Bao Nguyen</b>
12:00	The IPS Lecture <b>Chair: Michael Wall</b> <b>Prof Balwantray C. Chauhan</b> , Dalhousie University
13:00	<b>LUNCH</b>
13:00 - 18:00	<b>Field Trip</b> <b>Hanging Rock</b>

# Most Advanced Progression Analysis.

## Octopus EyeSuite Perimetry

**NEW**

### Overview at a Glance

- EyeSuite provides a complete overview of all examinations to analyse changes

### Progression Analysis

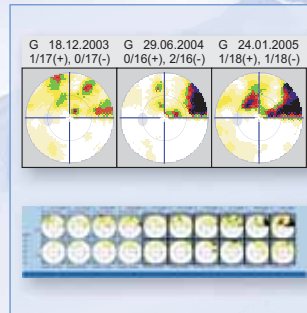
- Calculate the progression rate in dB per year as recommended by the International Glaucoma Societies

### Connectivity

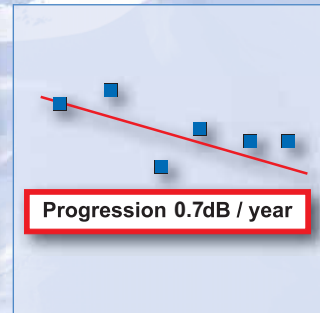
- Import existing visual fields and manage ongoing Octopus and HFA examinations in one solution



Octopus 900®



Overview at a Glance



Progression Analysis

For more information visit our website  
[www.haag-streit.com](http://www.haag-streit.com)

## Perimetry



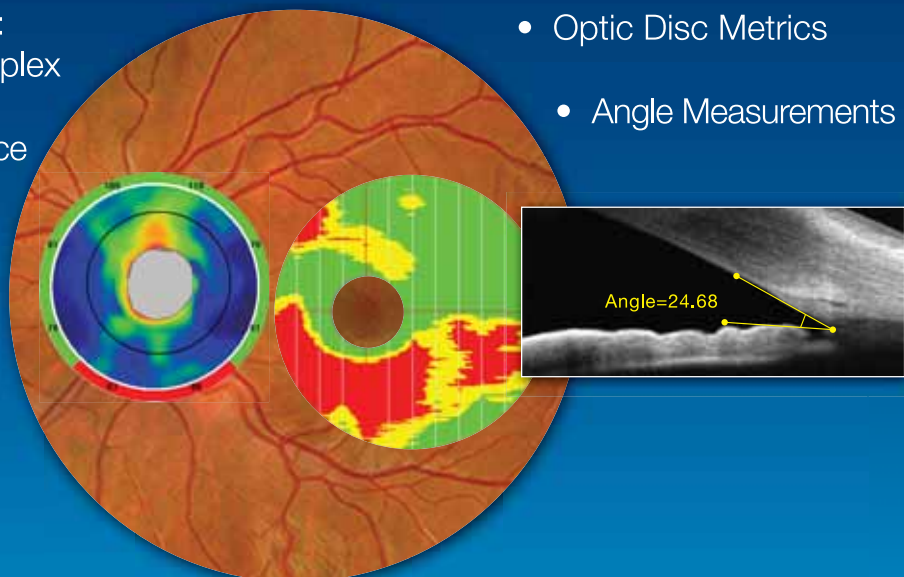
Tradition and Innovation

TUESDAY 24 JANUARY 2012

## Leading the Way in SD-OCT Glaucoma Diagnostics

- The Original GCC®: Ganglion Cell Complex Analysis with the exclusive Significance Mapping
- RNFL Thickness Analysis with comparison to Normative Database

- Optic Disc Metrics
- Angle Measurements



P/N 300-47328 Rev.A



GLAUCOMA • RETINA  
 ANTERIOR SEGMENT • CORNEA

\*Overlay of ONH and GCC maps on sample fundus image.  
 This image is for illustration purposes only and is not to scale.

optovue

DEFINING THE OCT REVOLUTION

OPTOVUE, INC. | FREMONT, CA | 1.510.623.8868 | WWW.OPTOVUE.COM



## SE-05, Structure-Function Maps 8:30 am – 9:30 am

### Development of patient-tailored structure/function maps

Julia Lamparter<sup>1,2</sup>, Haogang Zhu<sup>1,3</sup>, Richard A. Russell<sup>1,3</sup>, Takehiro Yamashita<sup>1,4</sup>, Ryo Asaoka<sup>1,3</sup>, David F. Garway-Heath<sup>1,3</sup>

<sup>1</sup>NIHR Biomedical Research Centre for Ophthalmology, Moorfields Eye Hospital NHS Foundation Trust and UCL Institute of Ophthalmology, London, UK, <sup>2</sup>Department of Ophthalmology, University of Mainz, Mainz, Germany, <sup>3</sup>Department of Optometry and Visual Science, City University London, London, UK, <sup>4</sup>Department of Ophthalmology, Kagoshima University Graduate School of Medical and Dental Sciences, Kagoshima, Japan

**Purpose:** To develop a model to predict the mapping between visual field (VF) test points and the optic nerve head (ONH) for individual eyes by taking into account ocular parameters.

**Method:** Forty-eight blue-filter retinal nerve fibre bundle photographs from 48 healthy subjects and glaucoma suspects were optimized digitally and single nerve fibre bundles were manually traced back to the ONH, using customised software. The ONH was divided into 5-degree sectors and the entry point of given nerve fibre bundles was noted. An appropriately scaled Humphrey Field Analyzer 24-2 visual field test grid pattern was superimposed onto the fundus images in order to relate visual field test points to retinal nerve fibre bundles and their entry points into the ONH. Axial length, spherical equivalent, the position of the ONH in relation to the fovea, size, rotation, tilt and shape of the ONH were assessed using partial coherence interferometry, spectral domain optical coherence tomography, and scanning laser ophthalmoscopy. A multilayer perceptron (MLP) neural network model was then generated to predict the entry point of retinal nerve fibre bundles into the ONH, taking into account the given ocular parameters. Bootstrapping was carried out (leave-one-out-method) in order to evaluate the accuracy of the model.

**Results:** The MLP neural network predictive model including ocular parameters was compared with the same model excluding these parameters. For the latter model, the mean ( $\pm$  standard deviation) absolute prediction error for the entry point into the ONH was 10.0 ( $\pm$  11.0) degrees. When taking into account the patient's ocular parameters, the absolute error was reduced to 5.6 ( $\pm$  5.0) degrees.

**Conclusions:** The entry point of retinal nerve fibre bundles into the ONH and, therefore, the structure/function relationship, varies between patients according to a given patient's ocular parameters. By taking into account these parameters (axial length, spherical equivalent, the position of the ONH in relation to the fovea, size, rotation, tilt and shape of the ONH), patient-tailored structure/function maps can be built. These maps are important for more accurately correlating structural measurements with functional measurements and should be useful to assist clinicians detecting glaucoma as well as monitoring glaucomatous progression.

### Factors in the Retinal Nerve Fiber Layer (RNFL) bundle angles at the optic disc

Fumi Tanabe<sup>1</sup>, Chota Matsumoto<sup>1</sup>, Sachiko Okuyama<sup>1</sup>, Sonoko Takada<sup>1</sup>, Shigeki Hashimoto<sup>1</sup>, Eiko Arimura<sup>2</sup>, Hiroki Nomoto<sup>1</sup>, Tomoyasu Kayazawa<sup>1</sup>, Mariko Eura<sup>1</sup>, Yoshikazu Shimomura<sup>1</sup>

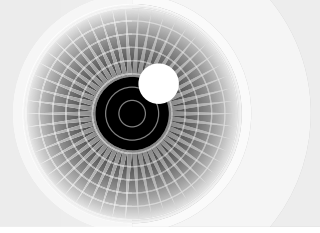
<sup>1</sup>Kinki University Faculty of Medicine, Osaka-Sayama City, Japan, <sup>2</sup>Kinki University Faculty of Medicine, Sakai Hospital, Sakai City, Japan

**Purpose:** The correspondence between the functional changes of the visual field and the structural changes of the optic disc is crucial for glaucoma diagnosis. Therefore, the retinal nerve fiber layer (RNFL) bundle angles at the optic disc can be useful for the diagnosis. We measured the RNFL bundle angles by scanning laser ophthalmoscopy (SLO, F-10) and further investigated the factors that could affect the bundle angles.

**Method:** Subjects were 45 eyes of 45 subjects ( $39.9 \pm 13.1$  years) including 12 glaucomatous eyes and 33 normal eyes. All the subjects had spherical equivalent (SE) of  $-8.88$  D to  $+0.25$  D. Their fundus images were taken by SLO and the SLO images were averaged using a software tracking method to construct a clear RNFL bundle image. Using the custom test of the Octopus 900 with 1° intervals, we detected the blind spot and inverted the G2 test program to match the found blind spot to the optic disc on the bundle image. The trajectories of the bundle were traced from each test location to the optic disc and the bundle angles at the optic disc were measured. SE, axial length (AL), the angle between the horizontal line passing through the fovea and the line connecting the fovea and the optic disc (the fovea-optic disc angle), and the angle formed by the central superior and inferior temporal retinal arteries (the retinal artery angle) were investigated for their correlations with the bundle angle.

**Results:** The standard deviation of the bundle angles was between 8.9° and 14.2°. The bundle angle correlated with SE and the retinal artery angle in the Bjerrum area, AL in the nasal visual field, and the fovea-optic disc angle within the central 15° visual field. Moreover, the trajectories of the bundle in the myopic eyes tended to approach the horizontal line passing through the fixation point.

**Conclusions:** An interindividual variation of 11 degrees in the bundle angle was observed. Depending on the test location, the bundle angle could be affected by SE, AL, the fovea-optic disc angle and the retinal artery angle.



## Spatial correspondence between retinal nerve fiber layer thickness from OCT and perimetric sensitivity

Stuart Gardiner, Brad Fortune, Shaban Demirel  
Devers Eye Institute, Portland, OR, USA

**Purpose:** To spatially characterize the retinal nerve fiber layer (RNFL) thinning that corresponds with loss of perimetric sensitivity at each visual field location.

**Method:** Data were taken from 1385 eligible visits of 213 participants enrolled in the ongoing Portland Progression Project study. Each visit comprised an Ocular Coherence Tomography scan together with a Standard Automated Perimetry visual field (using the SITA testing algorithm, with no more than 33% fixation losses or false negative errors). Linear mixed effects models were created to predict the sensitivity at each field location from the average RNFL thicknesses within each clock-hour sector of the optic nerve head, accounting for longitudinal and inter-eye correlations. Single backwards elimination was used to find the most predictive sectors. The correlations between these predictions and the observed sensitivities were calculated. First, a map was created using the entire dataset, repeating the process using different numbers of RNFL sectors in the final predictive model. To assess robustness, maps were then created using data from a randomly-chosen half of the participants, and used to predict the sensitivity at each location within data from the remaining half of the participants, repeating this process for different bootstrapped subsets of the dataset.

**Results:** Using the entire sample for both derivation and validation, the pointwise correlations averaged 0.40 using just one sector per field location; 0.44 using two sectors; 0.46 for three sectors; asymptoting to 0.47 using all twelve sectors. Henceforth three sectors were used per field location. Predictability was highest in the SupraNasal quadrant (mean correlation=0.53), followed by the SupraTemporal (mean=0.46), InferoNasal (mean=0.45) and InferoTemporal (mean=0.40) quadrants. RNFL sectors found to be predictive of sensitivity (for a right eye) were most commonly 6-8 o'clock for locations in the superior visual field, and 11 and 7 o'clock for the inferior visual field. Averaged over the bootstrapped subsamples, the correlations between the predicted and observed sensitivities at each field location had mean 0.48 in the SupraNasal quadrant, 0.41 SupraTemporal, 0.40 InferoNasal and 0.35 InferoTemporal.

**Conclusions:** RNFL thickness within three clock-hour sectors predicted observed pointwise sensitivity well enough to justify using it to help reduce test variability, but not well enough to justify using it as a surrogate for functional testing.

## The influence of ocular anatomical variables on individual structure-function maps

Jonathan Denniss<sup>1,2</sup>, Allison McKendrick<sup>1</sup>, Andrew Turpin<sup>1,2</sup>

<sup>1</sup>Dept. of Optometry & Vision Sciences, University of Melbourne, Melbourne, Australia, <sup>2</sup>Dept. of Computer Science & Software Engineering, University of Melbourne, Melbourne, Australia

**Purpose:** To present a computational model relating visual field (VF) locations to optic nerve head (ONH) sectors taking into account variations in ocular anatomy, and to use the model to assess whether anatomical variability is a potential cause of apparent structure-function discordance.

**Method:** A previously published model (Turpin et al IOVS 2009, 50(7); 3249-56) which related retinal locations to ONH sectors using a 'shortest path' algorithm was adapted to model eyes with varying axial length, ONH position and ONH dimensions. Individual structure-function maps (n=11550) were generated for a range of clinically plausible anatomical parameters in which VF locations (24-2 pattern, n=52 non blind-spot locations) were mapped to one-degree ONH sectors. To remove anatomically unlikely parameter combinations from the dataset, infrequently mapped ONH sectors (5%) were discarded for each VF location. The influence of anatomical variables on the mapping between individual VF locations and the ONH was explored by multiple linear regression.

**Results:** Across the total range of anatomical variants, for individual VF locations (24-2) the total angular subtense of mapped ONH sectors ranged from 12 to 90°. Twenty-five locations mapped to within 45° for the entire range of anatomical parameters. In 5 nasal-step locations, the distribution of mapped ONH sectors was bimodal, mapping to discrete, vertically opposite ONH sectors depending on vertical ONH position. ONH sector angle was significantly influenced (p<0.001) by axial length, ONH position and ONH dimensions for 39, 52 and 31 VF locations respectively. On average vertical ONH position explained the most variance in ONH sector angle, followed by horizontal ONH position, axial length, and ONH dimensions, although this varied between locations.

**Conclusions:** Approximately half of 24-2 VF locations can be mapped to the ONH within 45 degrees despite anatomical variability. Other locations, mainly in the nasal-step area are strongly anatomy-dependent, in some instances mapping to the opposite side of the ONH to that conventionally expected. Anatomical variability is one possible cause of apparent structure-function discordance. Our model may be useful for more accurately relating structural and functional measures in individual patients where some simple biometric parameters are known.

## SE-06, Perimetry II

9:35 am – 10:35 am

## Combining color with luminosity: green on red pupil perimetry in glaucoma

Corinne Carle<sup>1,2</sup>, Andrew James<sup>1,2</sup>, Maria Kolic<sup>1,2</sup>,  
Rohan Essex<sup>3,2</sup>, Ted Maddess<sup>1,2</sup>

<sup>1</sup>ARC Centre of Excellence in Vision Science, Canberra, Australia,

<sup>2</sup>The Australian National University, Canberra, Australia,

<sup>3</sup>The Canberra Hospital, Canberra, Australia

**Purpose:** This study investigated the diagnostic utility of multifocal pupillographic perimetry (mfPOP) stimuli with concurrent changes in luminance- and color-contrast. The intention of this method was to sample responses derived from a more extensive population of retinal ganglion cells than those involved in pupil responses to luminance changes alone. Yellow luminance-only stimuli targeted the M+L luminance pathway, as did the luminance component of the color plus luminance stimuli; however, the green/red component of these latter stimuli additionally targeted the M-L/L-M color-opponent pathway. The observation of reductions in responsiveness due to disease occurring in either pathway may lead to greater diagnostic sensitivity.

**Method:** Nineteen glaucoma subjects and 24 normal subjects were tested with three 4 minute mfPOP stimulus variants (protocols). Stimulus luminances were balanced in two of the three protocols to yield more uniform fields in normal subjects. The luminance-only protocol utilized 67-150 cd/m<sup>2</sup> yellow luminance-balanced stimuli on a 10 cd/m<sup>2</sup> yellow background. The color plus luminance protocols utilized either luminance-balanced 60-150 cd/m<sup>2</sup> or non-balanced 150 cd/m<sup>2</sup> green stimuli on a 10 cd/m<sup>2</sup> red background. These 33 ms duration stimuli were presented to each of 44 visual field regions per eye at mean intervals of 4 s.

**Results:** The luminance-balanced color plus luminance protocol produced the largest reductions in pupillary contraction amplitudes and the highest sensitivities and specificities (ROC AUC Severe: 100% ± 0% SE, n=3 eyes; Moderate: 88% ± 6% SE, n=10 eyes; Mild: 83% ± 6% SE, n=22 eyes). Combined amplitude and latency measures produced slightly better results in the non-balanced color plus luminance protocol (Severe: 100% ± 0% SE; Moderate: 89% ± 7% SE; Mild: 84% ± 7% SE). The luminance-only protocol, in contrast, produced best AUCs of: Severe: 87% ± 11% SE; Moderate: 77% ± 11% SE; Mild: 73% ± 7% SE.

**Conclusions:** Stimuli targeting both luminance- and color-contrast pupillary response components produced higher sensitivity and specificity for glaucoma than stimuli targeting luminance-contrast components alone.

## Comparison of the diagnostic capability of oculus-spark perimetry with respect to three procedures of morphological analysis (GDx, HRT and OCT)

Manuel Gonzalez de la Rosa, Marta Gonzalez-Hernandez,  
Mariel Sanchez-Garcia, Ricardo Rodriguez de la Vega,  
Tinguaro Diaz-Aleman

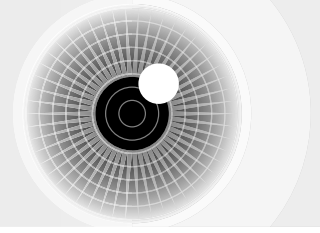
Hospital Universitario de Canarias. Univerfity of La Laguna,  
La Laguna, Islas Canarias, Spain

**Purpose:** To compare diagnostic capabilities and agreement between Oculus-Spark perimetry and three procedures of glaucoma morphological analysis.

**Method:** 102 normal eyes and 104 eyes with ocular hypertension, suspected or confirmed glaucoma (Group G) were examined using Spark perimetry (Oculus Easifield Perimeter), Laser Polarimetry (GDx), Heidelberg Retinal Tonograph (HRT III) and Cirrus OCT.

**Results:** Spark first phase lasted 37 seconds and all four phases lasted 2:34 minutes. Mean defect (MD) of normal subjects was 0.33dB (SD = 0.90) and of MD of patients was -9.2dB (sd = 9.16). Demanding high specificity, ROC analysis yielded the following specificities and sensitivities: phase 1 Spark-MD (97.1% and 71.2%), phase 1 Spark-PSD (98.0% and 70.2%), final Spark-MD (95.1% and 71.2%), final Spark-PSD (96.1% and 81.7%), GDx-NFI (95.1% and 57.4%), HRT-RB discriminant function (95.1% and 52.9%), HRT-GPS (95.1% and 71.2%), Cirrus OCT-Vertical C/D ratio (96.1% and 85.6%) and Cirrus OCT-NRFL thickness (95.1% and 68.0%). There was high diagnostic agreement between the Spark-MD of initial and final phases (kappa = 0.90); and good diagnostic agreement between phase 1 Spark-MD and Cirrus OCT-NRFL (kappa = 0.72) and the MD of the initial Spark phase and PSD final phase (kappa = 0.80). The remaining diagnostic agreements were good to moderate, even between the two Cirrus OCT indices (kappa = 0.69) or between the two HRT indices (kappa = 0.56).

**Conclusions:** Spark perimetry showed high sensitivity and specificity, even in the first phase lasting less than a minute and good diagnostic agreement with morphological studies.



## Influences of background complexity on monocular and binocular visual sensitivities

Akemi Wakayama<sup>1,2</sup>, Chota Matsumoto<sup>1</sup>, Masahiko Inase<sup>2</sup>, Yoshikazu Shimomura<sup>1</sup>

<sup>1</sup>Department of Ophthalmology, Kinki University Faculty of Medicine, Osaka-sayama city, Japan, <sup>2</sup>Department of Physiology, Kinki University Faculty of Medicine, Osaka-sayama city, Japan

**Purpose:** To assess how visual field background complexity influence monocular and binocular visual sensitivities.

**Method:** Monocular and binocular visual sensitivities measured using the noise and the noise-free backgrounds in six normal subjects. For the measurement of monocular visual sensitivity, the non-tested eye was occluded with an opaque cover so that the subject could only perceive the background luminance and the target. Either visual sensitivity for the right eye or visual sensitivity for the left eye, whichever was the higher, was used as the monocular visual sensitivity. To project a visual field background, the Octopus 900 perimeter combined with a micro-projector was used. The noise background was used the same 936 white -light dots with a dot size of 0.431° of visual angle that was the same dot size used for the white-spot test target in the visual sensitivity measurement. The noise-free background was used with same luminance of the noise background. The test locations were arranged at 25 points at the fovea and at 3° intervals on the 45°, 135°, 225° and 315° meridians in the central 30° visual field.

**Results:** The monocular threshold for the noise background was higher than that for the noise-free background ( $p < 0.01$ ). No significant difference in the binocular threshold was seen between the noise and the noise-free backgrounds ( $p < 0.01$ ). The binocular threshold was significantly lower than the monocular threshold for each background. The binocular summation ratio for the noise background was higher than the ratio for the noise-free background. The difference increased with eccentricity with significance seen at 15° and 18° eccentricities ( $p < 0.01$ ).

**Conclusions:** Only the monocular threshold increased with background complexity. The binocular summation increased significantly when the eyes detected the target projected to the peripheral area on the noise background. When the background has become more complex, binocular visual information process functions more effectively.

## Response time measures relative to probability of seeing across the visual field.

Allison McKendrick, Jonathan Denniss, Andrew Turpin

*The University of Melbourne, Parkville, Australia*

**Purpose:** To determine the relationship between a stimulus' probability of being seen and the observer's response time (RT) for perimetric stimuli. This work extends previous work of Wall et al (IOVS 1996; *Vis Res*, 2002), however measures frequency of seeing (FOS) curves across the central visual field via a series of repeated short (5 minute) tests to mimic the spatial attentional distribution and individual test duration of typical perimetric testing.

**Method:** Ten normal sighted adults participated. Response times were measured during the collection of FOS curves measured at 24 locations distributed across the central 29° of visual field for Size III SAP stimuli. Stimuli were presented on a CRT (Sony GDM500) using the Cambridge Research Systems ViSaGe system (Kent, UK). Each FOS curve consisted of 7 luminance intensities. A single test interleaved all 24 locations, presenting each FOS intensity once (i.e. a total of 7 x 24 stimuli within approximately 5 minutes). FOS curves were built via the repetition of the visual field test. Each observer repeated the test 20-30 times distributed across 4-8 sessions. FOS curves were fit with a cumulative Gaussian function (threshold is the mean ( $\mu$ ); spread/slope is the standard deviation ( $\sigma$ )). RTs were averaged across three "distance from threshold" bins: 1) easily seen (probability of seeing >93%); 2) near threshold (probability of seeing between 40-60%); and 3) rarely seen (probability of seeing <6%).

**Results:** Response times did not differ with eccentricity (repeated measures ANOVA:  $F(4,36) = 0.40$ ,  $p = 0.80$ ), but were significantly slower for stimuli with lower probability of being seen ( $F(2,18) = 4.14$ ,  $p < 0.0001$ ). The slowing of RT with stimulus difficulty did not differ in magnitude across eccentricity ( $F(8,72) = 0.05$ ,  $p = 0.99$ ). The average slowing for "near threshold" was 18% ( $\pm 6\%$ ) and for "rarely seen" was 42% ( $\pm 28\%$ ).

**Conclusions:** On average, response time increases as the probability of seeing a stimulus decreases. Understanding the relationship between response time and FOS across the visual field, and its variability, will allow further analysis of whether response time information can be used to improve stimulus placement in adaptive thresholding procedures (Turpin et al, IOVS 2011;52: E-Abstract 5511).

## SE-07, Imaging and Electrophysiology 11:00 am – 1:00 pm

### Does a simple stretch model account for retinal thinning seen in high myopia?

Michael Pianta, David Zhang, Carla Abbott, Neville McBrien  
*The University of Melbourne, Parkville, Victoria, Australia*

**Purpose:** It is well established from histological and clinical studies that the retina thins in eyes with axial myopia, but the mechanism producing this thinning is not well understood. The aims of this study are: 1) to characterize how total retinal thickness, and the thickness of retinal sub-laminae, varies with axial length, and 2) to test the prediction that thinning is a simple consequence of a fixed retinal volume being distributed across the increased surface area present in larger myopic eyes (the "simple stretch model").

**Method:** 53 subjects with high myopia (spherical equivalent refraction  $\leq -6.00$  D) and 52 age-matched controls (spherical equivalent refraction between  $\pm 1.50$  D) were included in the study after an extensive clinical examination. A-scan ultrasonography was performed to measure axial length in both eyes. Custom OCT scans (Zeiss StratusOCT) were performed along the horizontal and vertical midlines out to  $30^\circ$  in both eyes. Custom software was used to resample the OCT data into eccentricity bins, and mean longitudinal reflectivity profiles were calculated for each bin. Features of these profiles were then used to measure total retinal thickness and the thickness of retinal sub-laminae. 95% confidence intervals were calculated for the slope of the best-fit line relating log thickness to log eye radius. A slope of  $-2$  on these coordinates indicates thinning according to the "simple stretch model".

**Results:** Retinal thinning occurred at mid-peripheral and peripheral eccentricities ( $p < 0.05$ ); no thinning occurred at the fovea. More thinning was evident in the retinal plexiform layers compared to the nuclear layers. Only the retinal nerve fibre layer nasal to the optic nerve head thinned in accordance with the "simple stretch model" (95% CI for the slope contained  $-2$ ); all other locations and sub-laminae showed less thinning than predicted by the model (i.e. slopes were significantly more positive than  $-2$ ,  $p < 0.05$ ). The nerve fibre layer temporal to the optic nerve head thickened with increasing axial length ( $p < 0.05$ ).

**Conclusions:** Retinal thinning in axial myopia is a complex process that is not a simple consequence of a fixed retinal volume being stretched over a larger surface area.

### Imaging axonal transport in the rat visual pathway

Tiffany Choe<sup>1</sup>, Theresa Lusardi<sup>2</sup>, Carla Abbott<sup>1</sup>, Lin Wang<sup>1</sup>, Claude Burgoyne<sup>1</sup>, Brad Fortune<sup>1</sup>

<sup>1</sup>Discoveries in Sight Research Laboratories, Devers Eye Institute, Legacy Health, Portland, OR, USA, <sup>2</sup>R. S. Dow Neurobiology Laboratories, Legacy Health, Portland, OR, USA

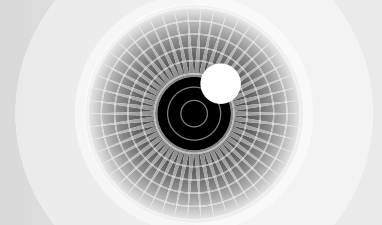
**Purpose:** To develop techniques for imaging and assaying axonal transport in vivo.

**Method:** Thirty-six adult male Brown-Norway rats were studied. All procedures were performed under anesthesia (ketamine, xylazine, acepromazine 55:5:1 mg/kg IM or 2% isoflurane inhalation). Anterograde transport was assessed by intravitreal injection of 2  $\mu$ l of 1% cholera toxin b-subunit conjugated to AlexaFluor488 (CTB). Retrograde transport was assessed by stereotactic injections of CTB into the superior colliculus (SC). Retinas were imaged in vivo by confocal scanning laser ophthalmoscopy (CSLO, Spectralis HRA, Heidelberg Engineering, GmbH) for up to 6 hrs after CTB injection and/or at longer post-injection time points (i.e. 16, 18, 20, 24, 48 hrs or several weeks later). Animals were sacrificed for post mortem microscopy of retinal, optic nerve and brain tissues. Subsets were pre-treated with unilateral intravitreal injections of colchicine (1 mM) or vehicle (deionized water) 1, 2 or 4 hours prior to CTB injections.

**Results:** Intravitreal injection of CTB resulted in rapid uptake and filling of retinal nerve fiber layer (RNFL) axon bundles in control eyes as visualized in vivo by CSLO and ex vivo by microscopy. In colchicine-injected eyes, RNFL bundles were only weakly fluorescent but brighter background represented intact CTB uptake into retinal ganglion cell (RGC) soma and dendrites, confirmed ex vivo by retinal flat-mount microscopy. CSLO imaging of the ventral and dorsal aspects of the midbrain revealed brightly fluorescent control optic nerves, contralateral chiasm and SC, but only weak or no fluorescence of those structures for colchicine-injected eyes. Retrograde transport of CTB was either delayed or disrupted by intravitreal colchicine as evidenced by patchy/weaker fluorescence of RGCs imaged by CSLO in vivo and by microscopy ex vivo compared with controls. In normal animals retrograde transport of CTB from the SC is detectable in the eye in vivo and by flat-mount retinal microscopy within 2.5 to 3 hrs of injection, representing a fast axonal transport rate of 160 to 200 mm per day. CTB appears at the SC above the background fluorescence 6 hrs after intravitreal injection, signal amplification by immunohistochemistry might result in faster anterograde transport rate estimates.

**Conclusions:** These results demonstrate that axonal transport of CTB in the rodent anterior visual pathway occurs by active transport mechanisms and can be monitored in vivo.





## Why do retinal nerve fiber layer measures differ across SD OCT Instruments?

Nimesh Patel, Ronald Harwerth

*University of Houston, Houston, Texas, USA*

**Purpose:** Measurement of peripapillary retinal nerve fiber layer (RNFL) thickness by SD OCT has become a clinical standard in the management of optic neuropathy, but significant differences in measurements across commercial SD OCT instruments have been reported. The purpose of this study was to investigate the underlying sources of disagreement in RNFL thickness measurements with different clinical SD OCT instruments.

**Method:** RNFL scans were acquired from 45 normal eyes (45 subjects, ages 21–68 years), using two commercially available systems—Spectralis HRA+OCT (Heidelberg Engineering, Heidelberg, Germany) and Cirrus HD-OCT (Carl Zeiss Meditec Inc, Dublin, CA). RNFL thickness measures were determined using both the instrument's internal algorithm for segmentation and a set of custom algorithms for segmentation that incorporated ocular biometry measures to compute the transverse scaling, image rotation to eliminate torsional eye movements, removal of major retinal blood vessels, and scaled placement of the 12 deg circular scan path. Bland-Altman analysis and intraclass correlation (ICC) were used to compare measurements with the two instruments.

**Results:** Instrument derived measures of global RNFL thicknesses from the two instruments well-correlated ( $R^2 = 0.70$ ,  $p < 0.01$ ), but with significant differences between instruments (mean of  $6.7 \mu\text{m}$ ,  $\text{ICC} = 0.62$ ). With custom RNFL segmentation, the mean difference was reduced to  $0.1 \mu\text{m}$  ( $\text{ICC} = 0.92$ ). Global RNFL thickness was related to axial length ( $R^2 = 0.24$ ,  $p < 0.01$ ), while global RNFL area measures were not ( $R^2 = 0.004$ ,  $p = 0.66$ ). Major retinal vasculature accounted for  $11.3 \pm 1.6\%$  (Cirrus) or  $11.8 \pm 1.4\%$  (Spectralis) of the RNFL thickness/area measures.

**Conclusions:** The disagreement in RNFL measures between SD-OCT instruments can be attributed to the location of the scan path and differences in retinal layer segmentation algorithms. With incorporation of methods to compensate for individual ocular biometry and differences in the optics of the instruments, RNFL thickness or area measures are comparable across the two instruments.

Support: NIH/NEI grants R01 EY001139 & P30 EY007551, Optometric Glaucoma Society Ezell Fellowship (NBP), John and Rebecca Moores Professorship (RSH).

## Pattern electrophysiology and visual fields measured on the same day in between migraine attacks

Bao Nguyen, Algis Vingrys, Allison McKendrick

*The University of Melbourne, Victoria, Australia*

**Purpose:** Separate visual field and electrophysiology studies have independently reported abnormally depressed visual function in between migraines. In this study, we consider whether the pattern electrophysiological response at the

retina (PERG) and visual cortex (PVER) correlate with poorer perimetric performance in the same individuals on the same day.

**Method:** Transient (1Hz, 250ms) and steady-state (8Hz, 480ms) full-field ( $31^\circ$ ) PERG and PVER were recorded simultaneously at least 7 days post-migraine in 24 patients without aura (20–41 years), 17 with aura (19–43 years) and 28 non-headache controls (19–45 years). Monocular checkerboard stimulation (mean luminance  $52 \text{ cd/m}^2$ , check size  $0.8^\circ$ , contrast 96%) yielded 200 artefact-free signals (1 kHz, bandpass filter 1.25–100 Hz). Groups were compared using peak-to-trough amplitudes and peak times of the transient PERG P50, N95 and PVER P100 components and steady-state amplitudes and phases at the second-harmonic (16Hz). On the same day, standard automated perimetry (SAP) and temporal modulation perimetry (TMP) were measured by the Medmont perimeter (model M700). Groups were compared using the global indices of the perimeter: Average Defect (AD) and Pattern Defect (PD), in addition to point-wise departures from age-matched control.

**Results:** The electrophysiological response did not differ between eyes or groups, except for lower steady-state PVER amplitudes in both migraine groups ( $F_{2,66} = 8.188$ ,  $p = 0.001$ ). Transient PVER amplitudes were also reduced in migraine with aura compared to migraine without aura ( $F_{2,66} = 3.429$ ,  $p = 0.038$ ) but did not differ from controls. PD of the worst eye in migraine without aura was significantly higher than controls for SAP ( $F_{2,66} = 3.649$ ,  $p = 0.031$ ). No group differences were evident for TMP PD or for AD of the worst eye. Pointwise comparisons found abnormality ( $p < 0.05$ ) in 38% SAP and 21% TMP visual fields of migraine participants. AD of the worst eye did not correlate with PVER amplitude (transient/SAP:  $r = 0.27$ ,  $p = 0.10$ ; steady-state/TMP:  $r = 0.059$ ,  $p = 0.72$ ). PD of the worst eye did not correlate with PVER amplitude (transient/SAP:  $r = -0.10$ ,  $p = 0.58$ ; steady-state/TMP:  $r = -0.08$ ,  $p = 0.64$ ).

**Conclusions:** We find an abnormally depressed electrophysiological response in people with migraine in between attacks that does not correlate with abnormal visual field results. This suggests that migraine produces a range of functional visual deficits, which cannot be readily attributed to a cortical or retinal origin.

## IPS Lecture: Modern imaging insights into the progression of glaucoma

Prof Balwantray Chuahan,

*Dalhousie University*

Over the last 20 years, modern imaging techniques have enabled clinicians and scientists to understand the nature of structural changes in glaucoma and incorporated into routine care. This Lecture will focus primarily on confocal scanning laser tomography (CSLT) of the optic nerve head, but a brief discussion of other techniques will be referenced.



WEDNESDAY 25 JANUARY 2012	
8:00	<b>Registration opens</b>
8:45	<b>SE-08</b> <b>Structure-Function</b> <b>Chairs: Uli Schiefer and Ron Harwerth</b>
	Comparing structure-function relationship in patients with early glaucoma: scanning laser tomography, flicker defined form and standard automated perimetry <b>Yuan-Hao Ho</b> Correlation between the concentration of hemoglobin in the optic nerve head and various morphological and functional indicators <b>Marta Gonzalez-Hernandez</b> Identifying eyes with glaucomatous visual field loss using the 'random forest' decision tree method applied to measurements from multiple imaging devices <b>Ryo Asaoka</b> Structure / function relations between SLP, OCT, Matrix and standard automated perimetry <b>Shaban Demirel</b> The structure-function relationship in patients with early glaucoma: spectral domain ocular coherence tomography, flicker defined form and standard automated perimetry <b>John Flanagan</b>
10:00	<b>Poster Session B</b> <b>Chair: Andrew Turpin</b>
11:00	<b>MORNING TEA</b>
11:30	<b>SE-09</b> <b>Invited Panel: Future Directions</b> <b>Chair: Allison McKendrick</b>
	<b>Prof Nathan Efron</b> , Queensland University of Technology <b>Clinical A/Prof Paul Healey</b> , University of Sydney <b>A/Prof Andrew Metha</b> , The University of Melbourne <b>Prof William Morgan</b> , University of Western Australia
13:00	<b>LUNCH</b>
	<b>Luncheon Presentation:</b> <b>Changing Stimulus Size in Automated Perimetry</b> Moderator: <b>John G. Flanagan</b> , PhD, MCOptom, FFAO. <b>Sponsored by Carl Zeiss</b> The relationship between target size and visual field defect in experimental glaucoma. <b>Ronald S. Harwerth</b> , O.D., Ph.D., FFAO, <b>John and Rebecca Moores</b> Professor, University of Houston. When is bigger better? - Criteria for stimulus scaling in perimetry. <b>Paul Artes</b> , PhD, FCOptom, Foundation Scholar in Glaucoma Research, Dalhousie University Changing stimulus size in automated perimetry - Clinical perspectives. <b>Michael Wall</b> , MD, Professor of Neurology and Ophthalmology, University of Iowa
	 We make it visible.
14:00	<b>IPS General Business Meeting</b> <b>Chair: Chris Johnson</b> , President IPS
14:45	<b>AFTERNOON TEA</b>
15:15	<b>SE-10</b> <b>Perimetry III</b> <b>Chairs: Fritz Dannheim and Shaban Demirel</b>
	Compensatory eye movements allow for successful collision avoidance under virtual reality conditions in a subgroup of patients with homonymous visual field defects <b>Ulrich Schiefer</b> Standard automated perimetry using variable stimulus size improves test-retest characteristics <b>John Flanagan</b> The index FD, a new measure of functional damage of the visual field <b>Joerg Weber</b> The repeatability of mean deviation with size III and size V standard automated perimetry <b>Michael Wall</b>
16:15	<b>The Aulhorn Lecture</b> <b>Chair: Chris Johnson</b> <b>Prof Joanne Wood</b> , Queensland University of Technology
17:15	<b>Sessions Finish</b>
19:00 - 23:00	<b>Symposium Dinner</b> <b>Ormond College</b>

// CIRRUS HD-OCT  
MADE BY CARL ZEISS

The moment your course  
of action is made clear.

**This is the moment we work for.**

#### Introducing Cirrus software Ver 6.0.

- Advanced RPE Analysis used for quantifying drusen and geographic atrophy
- Choroid Enhanced Depth Imaging
- Ganglion Cell Analysis
- Guided Progression Analysis (GPA) now with Optic Nerve Head parameters

**Certainty in Seconds. Certainty for Years.™**

[www.meditec.zeiss.com/cirrus](http://www.meditec.zeiss.com/cirrus)



We make it visible.

WEDNESDAY 25 JANUARY 2012

## SE-08, Structure-Function

8:45 am - 10:00 am

### Comparing structure-function relationship in patients with early glaucoma: scanning laser tomography, flicker defined form and standard automated perimetry

Yuan-Hao Ho<sup>1</sup>, Ziad Butty<sup>2</sup>, Ayako Anraku<sup>2</sup>, Yvonne M. Buys<sup>2</sup>, Graham E. Trope<sup>2</sup>, John G. Flanagan<sup>1,2</sup>

<sup>1</sup>School of Optometry, University of Waterloo, Waterloo, Ontario, Canada, <sup>2</sup>Department of Ophthalmology and Vision Sciences, University of Toronto, Toronto, Ontario, Canada

**Purpose:** To investigate the correlation between structure and function using scanning laser tomography, flicker defined form (FDF) perimetry and standard automated perimetry (SAP).

**Method:** The sample consisted of 119 participants ranging from 40-83 years with early to moderate glaucoma (mean age  $63.45 \pm 9.12$  years, Female=61). One eye of each participant was randomly assigned if both eyes were eligible for the study (57 OD). The Heidelberg Edge Perimeter (HEP; Heidelberg Engineering (HE)) was used to present both the FDF and SAP stimuli, data was analyzed using the same normative database. Patients participated in 3 test visits over a 6 week period, Tests performed are: SAP (24-2 ASTA-Std; visits 2 and 3), FDF (24-2 ASTAStd; all visits) and scanning laser tomography (HRTII; visits 2 and 3). Unreliable visual fields and poor quality images were excluded from the study. The SAP/FDF visual fields were divided into sectors corresponding to the six HRT Moorfields regression analysis sectors. The relationship between global and sectoral HRT parameters and the mean sensitivity (MS) of FDF and SAP were analyzed using correlation coefficients and linear regression. Kappa analysis was used to score the agreement between global and sectoral classifications.

**Results:** The mean MS of FDF and SAP were  $16.78 \pm 10.27$  cd and  $32.42 \pm 63.11$  cd. There was significant correlation between the FDF and SAP MS and HRT rim area, cup shape, rim volume, cup to disc ratio and FSM discriminant function measured by the HRT ( $P < 0.001$ ), with FDF generally giving higher correlations. For example, the correlation between HRT rim area and FDF/SAP MS were (r-value): Global: -0.42/-0.12, sup tmp: -0.34/-0.10, tmp: -0.28/-0.24, inf tmp: -0.52/-0.16, sup nsl: -0.23/-0.26, nsl: -0.26/0.02, inf nsl: -0.27/-0.16. Kappa analysis showed fair agreement between FDF and HRT classifications. The Kappa score was similar between FDF and SAP. However, FDF showed more agreement in patients classified as "outside normal limits" and SAP in those "within normal limits".

**Conclusions:** FDF perimetry correlated better with scanning laser tomography than SAP in this sample of patients with early to moderate glaucoma. There was a noticeable difference in the distributions of the structure/function relationship between FDF and SAP.

### Correlation between the concentration of hemoglobin in the optic nerve head and various morphological and functional indicators

Marta Gonzalez-Hernandez<sup>1</sup>, Francisco Fumero<sup>2</sup>, Nathan Radcliffe<sup>3</sup>, Julian Garcia-Feijoo<sup>4</sup>, Isabel Fuertes-Lazaro<sup>5</sup>

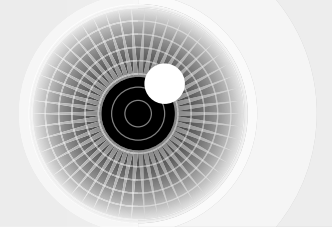
<sup>1</sup>Hospital Universitario de Canarias. University of La Laguna., La Laguna, Canary Islands, Spain, <sup>2</sup>Dept. of Systems Engineering, University of La Laguna., La Laguna, Canary Islands, Spain, <sup>3</sup>Weill Cornell Medical College, New York, USA, <sup>4</sup>Hospital Clínico San Carlos. University Complutense, Madrid, Spain, <sup>5</sup>Hospital Miguel Servet. University of Zaragoza, Zaragoza, Spain

**Purpose:** To analyze the relationship between the concentration of hemoglobin [Hb] in the optic nerve head (ONH) and various indices of glaucoma, as well as the reproducibility of this indicator of perfusion.

**Method:** 102 normal eyes and 101 eyes with ocular hypertension, suspected or confirmed glaucoma (Group G) were examined using the [Hb] method, Spark perimetry (Oculus Easifield Perimeter), Laser Polarimetry (GDx), Heidelberg Retinal Tomography (HRT) and Cirrus OCT. Normal eyes were tested on two separate days.

**Results:** The 65th percentile of [Hb] in intermediate regions above and below the ONH vertical diameter showed high correlation with functional and morphological indices, namely 0.79 with mean defect (MD) of Spark initial phase (37 seconds) and final phase (2:52 minutes), and -0.59 and -0.61 with the respective values of PSD. With HRT the correlation was 0.56 for RB Discriminant Function and -0.68 for GPS. For GDx NFI it was -0.64 and for OCT it was 0.67 for average RNFL thickness and -0.71 for vertical C/D ratio. Although linear regression analysis was performed, the relationship was linear between morphological indices and [Hb] and curvilinear between them and perimetry. For other percentiles, the correlation showed specific variation. Test-retest correlation in normal subjects was the same ( $r = 0.96$ ) for [Hb], OCT vertical C/D ratio and GDx NFI, but the coefficients of variation for these three indices were 3.0%, 5.5% and 9.0% respectively.

**Conclusions:** ONH concentrations of hemoglobin correlated well with most morphological and functional indices of glaucoma. Hemoglobin determination showed high reproducibility.



## Identifying eyes with glaucomatous visual field loss using the 'random forest' decision tree method applied to measurements from multiple imaging devices

Ryo Asaoka<sup>1,2</sup>, Richard Russell<sup>1,2</sup>, Rizwan Malik<sup>1</sup>, Gay Verdon-Roe<sup>1</sup>, David Garway-Heath<sup>1,2</sup>

<sup>1</sup>NIHR Biomedical Research Centre for Ophthalmology, Moorfields Eye Hospital NHS Foundation Trust and UCL Institute of Ophthalmology, London, UK, <sup>2</sup>Department of Optometry and Visual Science, City University London, London, UK

**Purpose:** To generate a 'Random forest' decision tree classifier to identify eyes with glaucomatous visual field (VF) loss using measurements from multiple imaging instruments.

**Method:** Subjects consisted of 37 open-angle glaucoma (OAG) patients (mean±SD age: 69±9 years) and 36 healthy volunteers (mean±SD age: 64±9 years).

Scanning Laser Polarimetry (GDxVCC), Optical Coherence Tomography (OCT; Stratus), Confocal Scanning Laser Tomography (CSLT; Heidelberg Retina Tomograph 3) and VF (Humphrey Field Analyzer, SITA standard, 24-2) measurements were carried out in one eye of all subjects at one visit.

Glaucoma was defined as baseline IOP > 20mmHg plus an abnormal MD ( $p < 0.05$ ), PSD ( $p < 0.05$ ) or GHT (outside normal limits). Among the 37 OAG patients, MD was abnormal in 23 patients, PSD was abnormal in 36 patients and GHT was abnormal in 25 patients.

For the 'Random forest' classifier, first, 60% of each dataset was randomly chosen as a learning dataset and a decision tree was generated to identify glaucomatous VF loss using measurements (average RNFL thickness for GDxVCC and OCT, and rim area for CSLT) from (1) all the imaging devices, (2) only GDxVCC, (3) only OCT and (4) only CLST. Next, the diagnostic accuracy of each decision tree was analyzed in the test data (40% remaining). This procedure (random data sampling followed by evaluation of diagnostic accuracy) was repeated 10,000 times.

**Results:** With the MD definition ( $n=59$ ), diagnostic accuracy of method (1) was 82.5±5.4%. The accuracies of methods (2)-(4) were 2.0 to 11.5% lower than method (1). With the PSD definition ( $n=72$ ), diagnostic accuracy with method (1) was 80.1±5.7%, which was better than methods (2)-(4) by 5.0 to 9.9%. With the GHT definition ( $n=61$ ), diagnostic accuracy of method (1) was 85.4±6.1%, which was 5.0 to 9.5% better than methods (2)-(4). Across all definitions, diagnostic accuracy was significantly improved by combining all three imaging methods ( $p < 0.01$ , Friedman test).

**Conclusions:** The Random forest decision tree is an effective method to combine structural measurements from different devices and significantly improve the identification of eyes with glaucomatous VF loss. The method could be used as a gold-standard structural classifier for glaucoma when evaluating functional tests in research studies.

## Structure/function relations between SLP, OCT, matrix and standard automated perimetry

Shaban Demirel, Brad Fortune, Stuart Gardiner  
Devers Eye Institute, Portland, OR, USA

**Purpose:** To compare structure / function relations when comparing RNFLT and perimetry and seek non-linearity.

**Method:** 391 eyes from 202 participants with early glaucoma or high-risk ocular hypertension underwent two forms of perimetry (Matrix 24-2 [MAT]; SAP 24-2 SITA [SAP]) and two forms of RNFL thickness (RNFLt) assessment (GDxPro Scanning Laser Polarimetry [SLP]; Spectralis Spectral Domain Optical Coherence [OCT]). All four tests for a participant were done on the same day. Perimetric indices (Mean Deviation [MD]; Pattern Standard Deviation [PSD]) in dB were regressed against TSNIT average RNFLt measure by SLP and OCT. Segmented regression was used to determine whether data were significantly better fit by a 'broken line', indicating non-linearity.

**Results:** In all comparisons between a perimetric index and RNFLT, a broken line with at least two and as many as three segments provided a significantly better fit than a continuous line. When regressed against SLP, neither SAP nor MAT MD was significantly related to RNFLT above 45 microns. Below 45 microns, both SAP and MAT MD declined with RNFLT. However SAP MD required two segments to fit this declining portion and MAT required one. Similarly, when regressed against OCT, neither SAP nor MAT MD was significantly related to RNFLT above 85 microns, but once again, SAP MD required two segments to fit the declining portion and MAT required one. When PSD was regressed against RNFLT, two line segments were needed in all four cases. There was no significant relation between SAP or MAT PSD and RNFLT above 45 microns for SLP or above 85 microns for OCT.

**Conclusions:** All structure function relations were significantly better fit using segmented linear regression compared to simple linear regression. For all comparisons there was a criterion RNFLT, above which there was no significant association between structure and function. Below this criterion value, a significant relation existed that could be fit with a single line segment in all cases except when SAP MD was compared to RNFLT. This association required two line segments, suggesting that the relation between SAP MD and RNFLt (SLP or OCT) is more non-linear.



.....

### The structure-function relationship in patients with early glaucoma: Spectral domain ocular coherence tomography, flicker defined form and standard automated perimetry

John Flanagan<sup>1,2</sup>, Ziad Butty<sup>1</sup>, Ayako Anraku<sup>1</sup>, Yvonne Buys<sup>1</sup>, Graham Trope<sup>1</sup>

<sup>1</sup>University of Toronto, Toronto, Canada,

<sup>2</sup>University of Waterloo, Waterloo, Canada

**Purpose:** To investigate the correlation between structure and function using spectral domain optical coherence tomography, flicker defined form (FDF) perimetry and standard automated perimetry (SAP).

**Method:** The sample consisted of 110 participants, mean age of 63.28 years ( $\pm$  8.84; 45 to 83) (59 women), from the glaucoma clinics at the Toronto Western Hospital. All participants had a diagnosis of early (82.2% ) to moderate (11.8%) glaucoma (MD: 2.8 to -10.37). One eye of each participant was randomly assigned if both eyes were eligible for the study (56 OD). The study consisted of 3 visits over a 6 week period and included SAP (24-2 ASTA-Std; visits 2 and 3) and FDF perimetry (FDF 24-2 ASTAStd; all visits) using the Heidelberg Edge Perimeter (HEP; Heidelberg Engineering (HE)). Digital stereo disc photography and spectral domain optical coherence tomography (SD-OCT; Spectralis HRA+OCT; HE) were acquired at the third visit. The relationship between global and sectoral retinal nerve fibre layer (RNFL) thickness with FDF and SAP were analyzed using correlation coefficients and linear regression analysis.

**Results:** All sectors and global measures gave a significant correlation between RNFL thickness with mean deviation (MD) and mean sensitivity (MS) of the visual function measures ( $p < 0.002$ ; Bonferroni corrected) other than the temporal sector. The Global measures gave a correlation for MD of  $r = 0.53$  (FDF) and  $r = 0.48$  (SAP). The highest correlations were found for FDF in the Superior and Inferior Temporal sectors using MD (FDF:  $r = 0.70$  &  $0.68$ ; SAP:  $r = 0.60$  &  $0.58$  respectively). Although the  $r$ -values were similar between FDF and SAP the structure-function relationships were quite distinct. The FDF showed a steep linear relationship over the entire range of RNFL thickness while SAP had a flat distribution (most SAPs within normal limits).

**Conclusions:** FDF demonstrated better correlation with SD-OCT than SAP in all sectors of the ONH, in particular in the superior temporal and inferior temporal sectors. SAP showed relatively little abnormality whereas FDF gave a linear reduction over the entire range of RNFL thickness in the superior and inferior temporal sectors.

.....

### SE-09, Invited Panel: Future Directions 11:30 am - 1:00 pm

.....

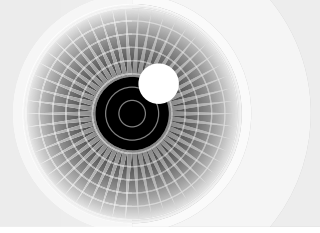
#### Assessment of diabetic neuropathy using novel corneal markers

Professor Nathan Efron

Queensland University of Technology, QLD

Diabetic peripheral neuropathy is a debilitating condition that affects about 50% of diabetic patients. The symptoms of neuropathy include numbness, tingling or pain in the arms and legs. If left untreated, patients with numbness may develop foot ulcers which may ultimately require foot amputation. Currently the only method of directly examining peripheral nerves is to conduct skin punch biopsies, which are uncomfortable and invasive. Indirect methods include quantitative sensory testing (assessing responses to heat, cold and vibration) and nerve electrophysiology. Recent research has investigated the possibility of using novel corneal markers to assess diabetic neuropathy. Specifically, corneal nerve structure and function can be assessed using corneal confocal microscopy and non-contact corneal aesthesiometry. Using these techniques, we have demonstrated that diabetic neuropathy—assessed using conventional techniques—is associated with altered morphology of corneal nerves and reduced corneal sensitivity. A nerve mapping technique is described; this enables accurate plotting of a wide (4 mm diameter) field of the subbasal nerve plexus, revealing interesting nerve features that are not readily apparent when capturing single frames. Our initial findings establish these ophthalmic markers as rapid, painless, non-invasive, sensitive, reiterative and cost-effective means of screening for early detection and diagnosis of diabetic peripheral neuropathy, and for monitoring the progression and quantifying the severity of this debilitating condition. Looking to the future, this research may pave the way for an expanded role of optometry in diabetes management.

.....



## Future directions in retinal imaging: pushing the spatial, temporal and functional boundaries.

A/Prof Andrew Metha

*The University of Melbourne, VIC*

The past decade has seen impressive improvements to the spatial resolution achievable in retinal imaging due to incorporation of deformable mirrors and adaptive optics (AO) technology. The list of interesting retinal features that have been imaged in living human and other animal eyes grows steadily, with retinal pigment epithelial cells and rod photoreceptors recently adding to the collection of important microscopic retinal structures now observable. To be able to see these structures in living eyes has profound implications on the way we are to understand the structure-function relationships existing in health, what happens as disease strikes and progresses, and how our attempts for therapeutics may or may not help. Spatial resolution in retinal imaging is fundamentally limited by the fidelity of ocular wavefront aberration measurement and how these can be corrected in real-time for large pupils without damaging the eye using short wavelength lights. Photon detector technologies (e.g. cameras) place limits on how much light is required, and how quickly images can be obtained in quick succession to capture information about dynamic processes such as capillary blood flow. The nature of the light source too imposes essential limits on imaging utility: spatial and temporal coherence plays a role as does wavelength especially when it comes to anatomical and functional inferences based on interference effects and differential spectral absorption. This talk will describe these considerations in the context of the supercontinuum laser-based, multispectral AO flood ophthalmoscope developed in my laboratory, and how this is being used to make discoveries about the bleaching kinetics of individual cone photoreceptors and functional oximetry in the peri-foveal microvasculature. Future directions in retinal imaging are certainly limited by the technologies at hand, but properly understanding these limits allow great scope for interesting enquiry and useful discovery.

## Imaging meets epidemiology: Results from the Blue Mountains Eye Study

Clinical Associate Professor Paul Healey

*Centre for Vision Research, Westmead Millennium Institute, University of Sydney*

**Objective:** To evaluate the diagnostic accuracy of scanning laser ophthalmoscopy for glaucoma detection in an elderly population.

**Methods:** Heidelberg Retinal Tomograph (HRT) 2 optic nerve head scans were classified using HRT2 and HRT3 software. Open angle glaucoma (OAG) was diagnosed independently from optic disc photographs and Humphrey 24-2 visual fields. Raw HRT 3 GPS data was used to identify improved screening cut-points. The diagnostic accuracy of combined classification of MRA and the new GPS cut-points was then evaluated.

**Results:** Mean age was 73.7 years. HRT scans could be acquired in 1644 participants, 95.9% of those fully examined. The great majority (87.4%) of scans had a topography standard deviation (TSD)  $\leq 40$ mm. Larger TSD was associated with older age and OAG. For HRT2, MRA sensitivity as 64.1%, specificity 85.7%, positive predictive value 21% and negative predictive value 97.6% for detecting OAG. Including borderline results improved sensitivity (87.0%) but lowered specificity to 70.6%. OAG, older age, greater TSD and larger disc size were significant predictors of abnormal MRA. Single eye analyses overestimated specificity and underestimated sensitivity compared to using data from both eyes. Compared with HRT2, HRT3 MRA showed improved sensitivity but lower specificity. HRT 3 GPS analyses using standard cut-points were more sensitive but even less specific. Older age was associated with lower MRA and GPS sensitivity. The combined MRA and GPS classification gave the best balance of sensitivity and specificity.

**Conclusions:** Diagnostic test evaluation studies of using single eye analyses or restrictive selection overestimate test accuracy compared with this population-based study. Although the specificity of the current diagnostic algorithms was inadequate for use as a glaucoma screening test, the HRT performed relatively well in an unselected older population with acceptable quality scans in most eyes.

Professor William Morgan

*Lions Eye Institute, University of Western Australia*

No abstract provided

## SE-10, Perimetry III

3:15 pm – 5:15 pm

### Compensatory eye movements allow for successful collision avoidance under virtual reality conditions in a subgroup of patients with homonymous visual field defects

Ulrich Schiefer<sup>1</sup>, Gregor Hardiess<sup>2</sup>, Hanspeter A. Mallot<sup>2</sup>, Eleni Papageorgiou<sup>1</sup>

<sup>1</sup>Centre for Ophthalmology, Tuebingen, Germany,

<sup>2</sup>Lab of Cognitive Neuroscience, Tuebingen, Germany

**Purpose:** The aim of this study was to identify the subgroup of patients with HVFD, applying efficient compensatory gaze patterns in a cross traffic scenario under standardized, reproducible virtual reality (VR) conditions.

**Method:** Thirty patients (age range: 19-71 yrs) with HVFD due to vascular brain lesions and 30 group-age-matched normal subjects performed a collision avoidance task at a VR intersection with cross traffic under two difficulty levels. Eye and head movements were measured with eye and head tracking systems. Visual performance was assessed as the number of collisions. Based on their performance, patients were assigned to either an "adequate" (HVFDA) or an "inadequate" (HVFDI) subgroup by means of the median split method. Fourteen patients and 19 normal subjects were finally evaluable, after excluding participants with insufficient eye and head tracking data. Saccades, fixations, mean number of gaze shifts, scanpath length and the mean gaze eccentricity in the horizontal plane, were compared between HVFDA, HVFDI patients and normal subjects. Analysis of variance and post-hoc Tukey's HSD test were applied for normally distributed data. The Kruskal-Wallis and the Mann-Whitney U tests were used for non-normally distributed data. In order to identify the anatomic structures that might be specifically affected in HVFDI patients but spared in HVFDA patients, overlap and subtraction lesion analyses were performed using the MRIcro software.

**Results:** The following gaze-related parameters differed significantly between evaluable HVFDA patients (N1=5) and HVFDI patients (N2=9): (mean) number of gaze shifts (13.5 vs. 9.4, Tukey's HSD,  $p < .0001$ ), saccadic amplitude towards the affected side (19 vs. 15.6 deg, Tukey's HSD,  $p < .0001$ ), saccadic amplitude towards the intact side (23.2 vs. 17.3 deg, Tukey's HSD,  $p < .0001$ ), percentage of fixations on vehicles (80.2% vs. 69.7%, Tukey's HSD,  $p < .0001$ ), percentage of fixations on the intersection (12.2% vs. 18.5%, Tukey's HSD,  $p < .0001$ ), scanpath length (1126 vs. 793 deg, Tukey's HSD,  $p < .0001$ ) and mean gaze eccentricity (25.60 vs. 18.90, Tukey's HSD,  $p < .0001$ ). Both patient groups displayed more fixations ( $p < .0001$ , unpaired t-test) and longer saccades ( $p < .01$ , unpaired t-test) in the affected compared to the intact hemifield. HVFDA patients (N1=5) and normal subjects (N=19) demonstrated similar scanpath length (1126 vs. 1146 deg, Tukey's HSD,  $p = 0.17$ ) and number of gaze shifts (13.5 vs. 12.7, Tukey's HSD,  $p = 12.86$ ). Lesion analysis revealed that the cortical structures associated with impaired collision

avoidance in HVFDI patients were the parieto-occipital region and posterior cingulate gyrus in the right hemisphere, and the inferior occipital cortex and parts of the fusiform (occipito-temporal) gyrus in the left hemisphere.

**Conclusions:** A subgroup of patients with HVFD sufficiently compensates for their visual deficit by exploratory gaze (eye and head) movements, becoming manifest by a higher number of gaze shifts, larger saccades, longer scanpaths and greater mean gaze eccentricity, compared to the subgroup of HVFD subjects with impaired compensation. The above-mentioned subgroups also differ with regard to the location of cerebral lesions.

Outlook: Standardized tests should be developed to correctly identify patients with adequate "exploratory compensation" of homonymous visual field defects in a clinical setting. The results should be corroborated by experiments, based on real-life scenarios, i.e. activities of daily living, such as car driving or shopping.

Support: EU MEST-CT-2004-504321, DFG SFB 550-A4 and GRK 778

### Standard automated perimetry using variable stimulus size improves test-retest characteristics

John Flanagan<sup>1,2</sup>, Derek Ho<sup>1</sup>, Deborah Goren<sup>1</sup>

<sup>1</sup>University of Waterloo, Waterloo, Canada,

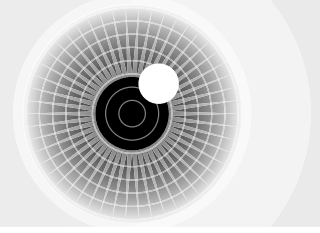
<sup>2</sup>University of Toronto, Toronto, Canada

**Purpose:** To validate a monitor based system for Standard Automated Perimetry (SAP) using variable stimulus size to give a Goldmann Size III equivalent test.

**Method:** A novel system for SAP was developed for use on the Heidelberg Edge Perimeter (HEP). It was designed to be equivalent to the Humphrey Field Analyzer (HFA), when using a Goldmann III target. A 0.43° diameter stimulus and a 10cdm<sup>2</sup> background luminance was used for the 40dB to 16dB range for both tests. For the brighter 15dB to 0dB stimuli an increasingly larger target was used by the HEP-SAP to give equivalence to the HFA-SAP test. Size equivalence was based on a modified version of Ricco's law. To validate the approach 89 normal participants (age range 19-81 years) were tested 3 times using the HEP-SAP and HFA-SAP, 24-2 program. The 2<sup>nd</sup> and 3<sup>rd</sup> tests were analysed for test-retest characteristics. A second study, using the same protocol, recruited 81 patients with early to moderate glaucoma (age range 50 to 80 years).

**Results:** The normal test group showed similar test-retest characteristics (CoR: HFA-SAP: 4.79dB vs. HEP-SAP: 4.55dB). Similar results were found within the normal range for the glaucoma test group (MoD: HFA-SAP 0.2dB, HEP-SAP 0.35dB; CoR: HFA-SAP 5.65dB, HEP-SAP 5.79dB). However, stimuli locations within the abnormal range were found to be more repeatable for HEP-SAP when compared to HFA-SAP (<16dB; CoR: 16.29 vs. 19.04dB).

**Conclusions:** HEP-SAP gave similar accuracy and repeatability to HFA-SAP within the normal to near normal range, and across age and eccentricity. HEP-SAP demonstrated similar accuracy but better repeatability than the HFA-SAP in the abnormal range (0 to 16dB).



---

## The index FD, a new measure of functional damage of the visual field

Joerg Weber

*Eye Center Koeln North-East, Koeln, Germany*

**Purpose:** There is strong evidence that the decibel scale is not a suitable scale to represent the visual field. Several studies with independent approach have shown that there is an exponential relation between the decibel scale and other functional measures. A recalculation of the decibel values appears to be necessary to generate visual field values that give better equivalence to genuine linear functional measures like visual acuity. Damage indices based on such recalculations are expected to give also better equivalence with structural changes of damaging diseases like glaucoma. And they are expected to give a more linear temporal behaviour.

**Method:** Based on an equivalence study between acuity perimetry and standard perimetry (Bartz-Schmidt KU, Weber J: Comparison of spatial thresholds and intensity thresholds in glaucoma, *Int Ophthalmol* 1993, 17:171-178), decibel values are recalculated. The deviation from normal is averaged across the visual field, creating the new index FD (functional defect). Using a new version of the field analysis program PeriData, FD and traditional MD are compared to several HRT indices of the optic disc in cases of glaucoma. Furthermore, FD and MD are compared in their temporal behaviour in cases of progressing glaucoma.

**Results:** The relation of FD and HRT indices shows more linearity than the relation of MD and HRT indices. The temporal course of MD and FD show more linearity for FD in some cases, but not in all. These are mainly cases with an observation time over 10 years.

**Conclusions:** The index FD proves to be a useful new tool for the evaluation of visual fields. Especially in glaucoma, the comparison of disc changes and visual field changes becomes easier. For follow-up, the advantages show only over long follow-up periods.

---

## The repeatability of mean deviation with size III and size V standard automated perimetry

Michael Wall<sup>1,2</sup>, Carrie Doyle<sup>1</sup>, Gideon Zamba<sup>3</sup>, Paul Artes<sup>4</sup>, Chris Johnson<sup>1</sup>

<sup>1</sup>University of Iowa, Department of Ophthalmology and Visual Sciences, Iowa City, IA 52242, USA, <sup>2</sup>Veterans Affairs Hospital, Iowa City, IA 52242, USA, <sup>3</sup>University of Iowa, Department of Biostatistics, Iowa City, IA 52242, USA, <sup>4</sup>Dalhousie University, Department of Ophthalmology and Visual Sciences, Halifax, Canada

**Purpose:** The mean deviation (MD) of the visual field is a statistical index used to determine the average difference in visual field sensitivity compared to the mean sensitivity of a normal observer of the same age. MD has also been used to

monitor overall visual field change over time. Our goal was to investigate the relationship of MD and its variability for two clinically used strategies (SITA standard, size III and full threshold size V in glaucoma patients and controls who were tested 5 times.

**Method:** We tested 46 glaucoma subjects with Humphrey program 24-2 SITA Standard for size III and full threshold for size V each 5 times over a 5 week period along with 28 ocular healthy subjects. Mean Deviation (our age-adjusted MD was calculated from our set of 60 normals tested twice) for size III was  $-10.19 \pm 6.9$ ; for size V  $-7.85 \pm 6.0$ . The standard deviation of MD was regressed against the MD for the five repeated tests. A paired t-test was used to compare the standard deviations of the two testing methods.

**Results:** We confirmed the well known relationship of increasing variability with increasing visual field damage with both test strategies. The  $R^2$  of SITA III was 0.19 and size V was 0.29. The SD of size V was less than size III ( $p = 0.024$ ).

**Conclusions:** The repeatability of size V MD appears slightly better than size III SITA testing. When using MD to determine visual field progression, a change of 1.5 – 4 dB is needed to be outside the normal 95% confidence limits, depending on the size of the stimulus and the amount of visual field damage.

---

## The Alhorn Lecture

---

### Visual Function and Driving

Professor Joanne Wood BSc PhD

*School of Optometry and Institute of Health and Biomedical Innovation, Queensland University of Technology, Brisbane, AUSTRALIA*

It has been suggested that over 90% of the sensory information for driving is visual. However, despite this widely held belief, there is still much debate regarding which specific visual functions are important for safe driving, the level of visual function at which driving performance and safety are impaired and how different visual impairments impact upon driving performance.

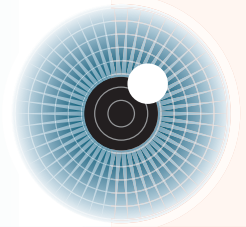
The aim of ongoing research studies has been to address these research questions using a range of experimental approaches including measures of real-world driving performance on a closed circuit driving course and under on-road in-traffic conditions. Specific areas of research have included understanding how different types of visual impairment impact on driving performance, identifying visual predictors of driving performance and quantifying the effect of different types of distracters on driving. Studies have also assessed driving performance under night-time driving conditions to determine how the age and visual status of the driver can impact on night-time driving ability and to identify ways in which to improve the visibility and hence safety of vulnerable road users including pedestrians and cyclists. An overview of a range of these studies will be presented.



## POSTER SESSION A - MONDAY 23RD JANUARY 2012

No.	Title/Presenter
P01	Changes in ocular fundus images with progression of myopia in a 12-year follow-up: a case of primary open-angle glaucoma developed in childhood <b>Sachiko Okuyama</b>
P02	The rate of visual field progression after trabeculectomy in glaucoma patients <b>Yoshio Yamazaki</b>
P03	Dichoptic versus monocular mfVEP in the detection of early glaucoma <b>John Leaney</b>
P04	2-segment analysis for perimetric long term follow-up in glaucoma <b>Fritz Dannheim</b>
P05	Multifocal pupillographic responses of patients with age-related macular degeneration in photopic and scotopic conditions <b>Yanti Rosli</b>
P06	Detection of early visual field defects with macular multifocal pupillographic objective perimetry in type 2 diabetes mellitus <b>Faran Sabeti</b>
P07	Motion perimetry in pre-perimetric glaucoma <b>Marco Zeppieri</b>
P08	The relationship between the peak retinal nerve fibre layer position and the papillo-macular position in Japanese normal eyes <b>Minoru Tanaka</b>
P09	The influence of the conus on the retinal nerve fibre layer thickness in Japanese normal eyes <b>Yuya Kii</b>
P10	Characterization of the effect of acute intraocular pressure increase on the in vivo human optic nerve head <b>John Flanagan</b>
P11	Correlation between Oculus-Spark perimetry and three procedures of morphological analysis (GDX, HRT and OCT) <b>Marta Gonzalez-Hernandez</b>
P12	Quantification of retinal venous pulsatility using non-invasive infrared imaging <b>Mojtaba Golzan</b>
P13	Relative effects of sampling errors and eye movements upon SAP test-retest variability <b>Ted Maddess</b>
P14	Relationships between NFLT analyzed by normal database with Cirrus OCT and visual field testing results <b>Hiroki Nomoto</b>
P15	Flicker, speed and motion sensitivity in glaucoma: central temporal processing is altered in intact central visual field <b>Fleur O'Hare</b>
P16	Eye movement perimetry in young and aged adults <b>Joy Carroll</b>





## POSTER SESSION B - WEDNESDAY 25TH JANUARY 2012

No.	Title/Presenter
P17	Structural and functional anomalies of Autosomal Recessive Spastic Ataxia of Charlevoix-Saguenay (ARSACS) <b>Marie-Josée Fredette</b>
P18	Optimal pointwise linear regression criteria for detecting glaucoma progression <b>Colleen Kummert</b>
P19	Method for calculating the concentration of hemoglobin in the optic nerve head: diagnostic capability with respect to morphological and functional indices <b>Manuel Gonzalez de la Rosa</b>
P20	Effect of intra-ocular lenses on diagnostic performance of multifocal pulsiographic objective perimetry in glaucoma <b>Maria Kolic</b>
P21	The variability of the peak retinal nerve fibre layer position in Japanese normal eyes <b>Takehiro Yamashita</b>
P22	Optic nerve evaluation by ultrasonography in glaucoma as a predictive index <b>Rajiv Garg</b>
P23	Death versus dysfunction in glaucoma: the relationship between threshold and miss rate for tiny perimetric stimuli <b>Andrew Anderson</b>
P24	Comparison between the GDX Staging System (GDS SS) and the Nerve Fiber Indicator (NFI) in the detection of early glaucomatous structural damage <b>Marco Zeppieri</b>
P25	Applications of noise-corrected progression analysis of automated visual fields <b>David W Richards</b>
P26	Combining an expert glaucoma staging and evaluating system with SPARK perimetry on the OCULUS Easyfield perimeter <b>Zoltan Gagy-Palfy</b>
P27	Relationship between Frequency-Doubling Technology perimetry and angle width of retinal nerve fiber defects in preperimetric glaucoma <b>Shinji Ohkubo</b>
P28	Glaucoma patients with large optic disc size have reduced retrobulbar optic nerve diameter <b>Heather Connor</b>
P29	Disc area and neuroretinal rim measurements by optical coherence tomography in highly myopia <b>Sheng-Yao Hsu</b>

---

 POSTER SESSION A  
 MONDAY 23RD JANUARY 2012
 

---

## P01

---

 Changes in ocular fundus images with progression of myopia in a 12-year follow-up: a case of primary open-angle glaucoma developed in childhood
 

---

Sachiko Okuyama, Yasuko Tamura, Chota Matsumoto, Yoshikazu Shimomura

Department of Ophthalmology, Kinki University Faculty of Medicine, Osaka-Sayama, Japan

**Purpose:** To report the changes in the ocular fundus images of a young patient who developed primary open-angle glaucoma with myopia progression in childhood and was followed up for twelve years.

**Method:** A 10-year-old girl, whose father had glaucoma, was referred to our glaucoma clinic with ocular hypertension in both eyes. During a 12-year follow-up, her visual field was assessed with Goldmann perimeter until the age of 14 and with the Octopus 101 perimeter program G2 subsequently. Since the age of 17, her ocular fundus has been evaluated by optical coherence tomography (OCT) in addition to fundus photography.

**Results:** At the age of 13, her spherical equivalent (SE) had decreased from +0.5 diopters (D) to 0 D OD and from -2.75 D to -4.25 D OS. The left optic disc had reduced in size and the margin of the disc appeared elevated and indistinct in this period. At 17, SE had further decreased to -3.0 D OD and -5.75 D OS. Between the ages of 13 and 17, the right optic disc also had reduced in size and changed in shape. Both discs had inclined inferotemporally in association with inferotemporal peripapillary crescents. In the left eye, the margin of the disc had flattened and the retinal nerve fiber layer (RNFL) defects had developed and caused glaucomatous visual field defects. At 17, the average thickness of the peripapillary RNFL evaluated with Stratus OCT was thinner in the left eye than in the right eye. The roots of retinal vessels had shifted temporally due to the myopia progression during the follow-up. By the end of the follow-up, the thickest portions of the peripapillary RNFL had shifted temporally in both eyes as compared with the normative data provided by Cirrus OCT.

**Conclusions:** The features of the optic disc and RNFL can dramatically change with myopia progression in childhood. When analyzing the optic disc and RNFL imaging data, we should therefore carefully consider the effect of myopic changes.

---

## P02

---

 The rate of visual field progression after trabeculectomy in glaucoma patients
 

---

Yoshio Yamazaki<sup>1</sup>, Fukuko Hayamizu<sup>2</sup>

<sup>1</sup>Nerima Hikarigaoka Hospital, Nihon University, Nerima, Tokyo, Japan, <sup>2</sup>Itabashi Hospital, Nihon University, Itabashi, Tokyo, Japan

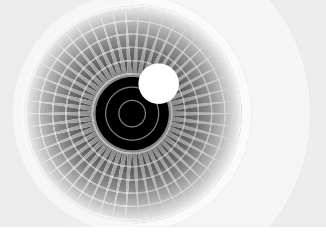
**Purpose:** To investigate the relationship between the rate of visual field progression and the IOP reduction after trabeculectomy in patients with POAG.

**Method:** Twenty-nine eyes with 29 POAG patients with 10 or more reproducible SITA standard VF examinations with the 30-2 program of HFA were enrolled into the study. Patients who underwent successful trabeculectomy were followed up for at least more than 2 years preoperatively and more than 5 years postoperatively. We retrospectively reviewed the clinical records and the results of HFA examination, and evaluate the relationship of the mode of visual field change based on mean deviation (MD) slope and the change of IOP.

**Results:** The mean numbers  $\pm$  SD of analyzed VFs was  $15.6 \pm 4.6$  times, spanning a mean of  $10.0 \pm 3.2$  years. Mean IOP decrease from  $22.7 \pm 5.2$  mmHg before surgery to  $14.1 \pm 1.7$  mmHg after surgery (Paired t-test;  $p < 0.001$ ). Mean MD slope decreased from  $-0.86 \pm 0.86$  dB/year to  $-0.28 \pm 0.38$  dB/year ( $p < 0.01$ ). 14 eyes with IOP reduction ratio  $\geq 40\%$  showed significant increase of MD slope from  $-0.83 \pm 1.15$  dB/year to  $-0.12 \pm 0.44$  dB/year ( $p < 0.05$ ), but 15 eyes with IOP reduction ratio  $< 40\%$  showed no significant change ( $p$ ; n.s.). 13 eyes with preoperative MD slope  $\leq -1.0$  dB/year revealed significant increase of MD slope from  $-1.63 \pm 0.49$  dB/year to  $-0.24 \pm 0.28$  dB/year ( $p < 0.001$ ), but 16 eyes with preoperative MD slope  $> -1.0$  dB/year had no significant change ( $p$ ; n.s.).

**Conclusions:** Successful IOP reduction after trabeculectomy delays the rate of visual field progression, but the effect to the rate of visual field progression is different according to the clinical background in each patients.

---



## P03

### Dichoptic versus monocular mfVEP in the detection of early glaucoma

John Leaney<sup>1</sup>, Prema Sriram<sup>1</sup>, Hemamalini Arvind<sup>1</sup>, Alexander Klistorner<sup>1,2</sup>, Stuart Graham<sup>1</sup>

<sup>1</sup>Australian School of Advanced Medicine, Macquarie University, NSW, Australia, <sup>2</sup>University of Sydney, NSW, Australia

**Purpose:** Dichoptic-recorded multifocal visually evoked potentials (mfVEP) have previously been demonstrated (with VR goggles) to provide some advantages monocular recording conditions. In this study we assess the efficacy of different stimuli in a novel dichoptic mfVEP setup using split LCD screens for the detection of glaucomatous damage.

**Method:** Initially 8 subjects with early glaucoma (MD < -6, Humphrey visual field) were recruited for a pilot study comparing different types of mfVEP stimuli to assess the relative sensitivity and variability of each stimulus. 4 different types of stimuli were used – blue on yellow (BonY) fast, BonY slow, low luminance contrast (LLC) fast and LLC slow. A further 15 glaucoma patients were subsequently tested using BonY fast stimulation comparing monocular with dichoptic recordings to investigate whether there were potential benefits to be gained from dichoptic versus monocular recording conditions.

**Results:** In the initial study fast (minimal separation between binocularly corresponding segments) BonY stimulation was found to be the most sensitive stimulus with the least variability when compared to slow BonY stimulation, fast LLC and slow LLC. In the second study, dichoptic BonY fast stimulation appeared to generate a more sensitive asymmetry profile at points of glaucomatous damage corresponding to Humphrey visual field changes. Mean relative asymmetry coefficients (RAC) for the whole field (calculated as: difference in amplitudes between eyes/sum of amplitudes of both eyes at each segment) were significantly ( $p = 0.02$ ) greater for dichoptic ( $0.161 \pm 0.14$ ) versus monocular ( $0.111 \pm 0.09$ ) recording conditions. Qualitative assessment of topography of defects showed good correlation with both stimulus conditions.

**Conclusions:** The dichoptic setup is effective in the detection of glaucomatous defects and provides advantages over monocular testing by reducing testing time, testing the both eyes under the same psycho-physical conditions and may have the advantage of utilising interocular suppression to enhance asymmetry profiles.

## P04

### 2-segment analysis for perimetric long term follow-up in glaucoma

Fritz Dannheim<sup>1</sup>, Matthias Monhart<sup>2</sup>, Nicole Mewes<sup>3</sup>

<sup>1</sup>Asklepios Clinic, Hamburg-Harburg, Germany, <sup>2</sup>Haag-Streit, Koeniz-Berne, Switzerland, <sup>3</sup>Asklepios Clinic, Hamburg-Heidelberg, Germany

**Purpose:** To investigate the frequency of the 2-segment approximation of a time series of visual fields to be superior to the linear regression, and to discuss its dependence on the follow-up period.

**Method:** The visual field series of 217 eyes of 109 patients with ocular hypertension, suspicious optic discs, or with manifest chronic glaucoma of different severity were analysed retrospectively (SAP, program G, Octopus 1-2-3). Trend analysis was carried out with the Octopus Field Analysis experimental software V 2.67. The time series can be fitted by means of a linear regression or by a 2-segment approximation, and the superiority of the two segment approximation was tested at a level of significance of 5%. The follow-up, after removing initial exams, covered 8 to 12 examinations within 4 to 14.5 years (mean 6.9 years).

**Results:** Thirty of 217 eyes (14%) exhibited a significantly better fit with the 2-segment regression of MD within 30°, visible as a kink in the regression line. Of all 109 patients, 32 (64 eyes) could be analysed for a longer follow-up of 8 to 18 years (mean 11.7 years). Of this subgroup, 7 eyes (11%) showed a significantly better fit for the 2-segment regression over the original period and 18 over the extended time range (28%). Four of the 46 series without a significant kink in MD within 30° had this kink within at least one relevant cluster. The rate of progression increased in 14 of the 18 series with this feature for MD within 30°. The current trend in these eyes reflected the clinical findings better than the all time linear regression, mostly due to a relevant increase in progression of pathology. The occurrence, amount and significance of the kinks did not correlate with the initial field damage or the continuous linear trend of MD.

**Conclusions:** The frequency of significantly discontinuous rates of progression in glaucoma doubled when extending the period of observation from an average of 7 to 12 years. Identifying these changes in trend adds valuable extra information on the functional prognosis.

P05

### Multifocal pupillographic responses of patients with age-related macular degeneration in photopic and scotopic conditions

Yanti Rosli<sup>1,2</sup>, Ted Maddess<sup>1</sup>, Sue Bedford<sup>1</sup>, Andrew James<sup>1</sup>

<sup>1</sup>The ARC Centre of Excellence in Vision Science, John Curtin School of Medical Research, Australian National University, Canberra, ACT, Australia, <sup>2</sup>Programme of Biomedical Science, School of Diagnostic and Applied Health Sciences, Faculty of Health Sciences, Universiti Kebangsaan Malaysia, Kuala Lumpur, Malaysia

**Purpose:** To compare the power of photopic and scotopic multifocal pupillography to diagnose age-related macular degeneration (AMD).

**Method:** Both eyes of 18 normal and 14 AMD subjects were tested with 8 stimulus variants, comprising 4 basic stimulus types presented at time-average luminances of either 0.23 or 28.0 cd/m<sup>2</sup>. Both eyes were tested concurrently with independent stimuli. All stimuli had 24 test regions/eye within the central 60°. The 4 basic stimulus variants had 2 different check sizes, and when presented either flickered (15 Hz) for 266 ms, or were steady for 133 ms. The duration of each test was 4 min divided into 8 segments of 30s.

**Results:** When mean regional effects were considered differences from normal of 5 to 7 dB were observed in the central visual field for both photopic and scotopic stimuli (all  $p < 0.00002$ ). The best areas under curve (AUC) for receiver operating characteristic (ROC) plots for exudative AMD in the photopic and scotopic conditions were  $92.9 \pm 8.0$  and  $90.3 \pm 5.7\%$ . In less severely affected AMD eyes the results were  $83.8 \pm 9.7\%$  for the best photopic test, and  $76.9 \pm 8.2\%$  for the best scotopic test.

**Conclusions:** Central response amplitudes in AMD patients were reduced in both photopic and scotopic viewing conditions. Photopic damage was possibly more diffusely distributed across the visual field. The best overall sensitivity and specificity was found for photopic stimuli.

P06

### Detection of early visual field defects with macular multifocal pupillographic objective perimetry in type 2 diabetes mellitus

Faran Sabeti<sup>1</sup>, Chris Nolan<sup>2</sup>, Maria Kolic<sup>1</sup>, Andrew James<sup>1</sup>, Ted Maddess<sup>1</sup>, Rohan Essex<sup>3</sup>, Andrew Bell<sup>1</sup>

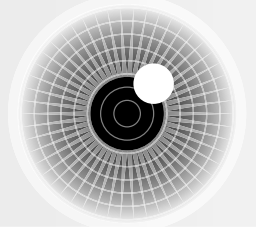
<sup>1</sup>ARC Centre of Excellence in Vision Science, Australian National University, Canberra, Australia, <sup>2</sup>Department of Endocrinology and Diabetes, The Canberra Hospital, Australian National University Medical School, Canberra, Australia, <sup>3</sup>Department of Ophthalmology, The Canberra Hospital, Australian National University Medical School, Canberra, Australia

**Purpose:** To evaluate the efficacy of macular compared with wide field multifocal pupillary objective perimetry (mfPOP) stimuli in patients with mild non-proliferative diabetic retinopathy (NPDR).

**Method:** Sixteen patients diagnosed with early type 2 diabetes ( $51.7 \pm 13.5$  years, 9 females) and 24 normal ( $55.8 \pm 7.2$  years, 13 females) subjects were recruited. Pupillary contraction amplitudes and time to peak responses to 3 multifocal stimulus protocols comprising of 44 stimulus regions per eye extending to either  $\pm 15^\circ$  or  $\pm 30^\circ$  were measured dichoptically. Variations in stimulus luminance were achieved by employing a balancing strategy. All protocols had a mean presentation interval of 4 s/region and a duration of 33 ms on each presentation. Cameras under infrared illumination monitored pupil responses. Multiple linear models were fitted to contraction amplitudes and times to peak responses to determine the independent effects of disease. Area under receiver operator characteristic curves (AUCs) compared the diagnostic accuracy of macular and wide field mfPOP.

**Results:** Stimuli presented in the central  $\pm 15^\circ$  with luminance balancing achieved the largest amplitude deviations ( $-2.0 \pm 0.14$  dB,  $p < .0005$ ) and highest diagnostic accuracy in eyes with mild NPDR. ROC area under the curve (AUC) of 100% was achieved from the 8 worst performing regions of the visual field. Stimuli extending to  $\pm 30^\circ$  were more informative when response delays were considered.

**Conclusions:** MfPOP responses from the macular region appears to achieve higher sensitivity and specificity than stimuli directed to a wider field. This pilot study suggests that visual field defects can be detected in mild NPDR and identifies the utility of mfPOP as a screening test for visual dysfunction in patients with early stage type 2 diabetes. Longitudinal studies evaluating changes in macular and wide field mfPOP responses in noninsulin and insulin-dependent patients are warranted.



P07

## Motion perimetry in pre-perimetric glaucoma

Paolo Brusini, Marco Zeppieri, Claudia Tosoni, Lucia Parisi, Maria Letizia Salvetat

*Santa Maria della Misericordia Hospital, Udine, Italy*

**Purpose:** To test the diagnostic accuracy of Motion Perimetry, a non-conventional testing method that selectively assesses the magnocellular pathway, in patients with pre-perimetric glaucoma and in normal subjects.

**Method:** The study included 45 pre-perimetric glaucoma patients, defined as having glaucomatous optic disc early damage and/or retinal nerve fiber layer (RNFL) defects shown by HRT and/or GDx VCC, with normal automated static perimetry (30-2 SITA standard test), and 32 healthy subjects. All participants underwent the Motion-30 test (MonPack3 perimeter), which involves the horizontal movement of thin vertical lines in different areas within the central 30° of visual field. A test was defined as abnormal based on the presence of at least one of the following criteria: Mean Deficit (MD) >1.1 dB; Defect Variance (DV) >18 dB; and, a cluster of at least 3 points not adjacent to the blind spot with a p<5%, with at least one point with a p<1%.

**Results:** The MD and DV values were significantly different between normal and pre-perimetric patients (Mann-Whitney test, p<0.01). The specificity for Motion Perimetry test was 90%. The test was abnormal in 24 pre-perimetric patients, showing a sensitivity of 53.3%.

**Conclusions:** Motion Perimetry is a quick and easy non-conventional visual field testing method. The sensitivity of this technique was quite good in our relatively small cohort of pre-perimetric patients with structural damage and normal SAP results.

P08

## The relationship between the peak retinal nerve fibre layer position and the papillo-macular position in Japanese normal eyes

Minoru Tanaka<sup>1</sup>, Takehiro Yamashita<sup>1</sup>, Ryo Asaoka<sup>2,3</sup>, Yuya Kii<sup>1</sup>, Kumiko Nakao<sup>1</sup>, Taiji Sakamoto<sup>1</sup>

<sup>1</sup>*Department of Ophthalmology, Kagoshima University Graduate School of Medical and Dental Sciences, Kagoshima, Japan,* <sup>2</sup>*NIHR Biomedical Research Centre for Ophthalmology, Moorfields Eye Hospital NHS Foundation Trust and UCL Institute of Ophthalmology, London, UK,* <sup>3</sup>*Department of Optometry and Visual Science, City University London, London, UK*

**Purpose:** To investigate the relationship between the peak retinal nerve fibre layer (RNFL) position and the papillo-macular position (PMP) in Japanese young normal eyes.

**Method:** Prospective observational cross-sectional study comprised 50 right eyes. All patients (mean age 25.8 ± 3.7) underwent comprehensive ophthalmologic examination, including RNFL imaging and fundus photograph. RNFL thickness was assessed using TOPCON 3D OCT-1000 MARK II RNFL 3.4 mm circle scan. The RNFL TSNIT curves were used to measure the angle between the horizontal meridian and the supra-temporal peak RNFL position (supra-peak RNFL angle), infra-temporal peak RNFL position (infra-peak RNFL angle). The PMP is the angle made between the horizontal meridian and a line connecting the optic disc centre and the fovea (from horizontal meridian to papilla-macular line, positive value if anticlockwise direction) (Garway-Heath DF et al. *Ophthalmology* 2000). The relationship between the supra, infra-peak RNFL angle and PMP were investigated using the linear regression analysis.

**Results:** The mean supra-peak RNFL angle was 64.5 ± 10.8 degrees, the mean infra-peak RNFL angle was 60.8 ± 13.3 degrees and the mean PMP was 5.7 ± 3.8 degrees. The infra-peak RNFL angle was significantly associated with PMP (r=0.40, p<0.0039); however the supra-peak RNFL angle was not significantly associated with PMP (r=-0.27, p<0.56).

**Conclusions:** The infra-temporal peak RNFL position tended to be shifted inferiorly with increasing PMP.



P09

### The influence of the conus on the retinal nerve fibre layer thickness in Japanese normal eyes

Yuya Kii<sup>1</sup>, Takehiro Yamashita<sup>1</sup>, Ryo Asaoka<sup>2,3</sup>, Minoru Tanaka<sup>1</sup>, Kumiko Nakao<sup>1</sup>, Taiji Sakamoto<sup>1</sup>

<sup>1</sup>Department of Ophthalmology, Kagoshima University Graduate School of Medical and Dental Sciences, Kagoshima, Japan, <sup>2</sup>NIHR Biomedical Research Centre for Ophthalmology, Moorfields Eye Hospital NHS Foundation Trust and UCL Institute of Ophthalmology, London, UK, <sup>3</sup>Department of Optometry and Visual Science, City University London, London, UK

**Purpose:** To investigate the influence of the conus on the retinal nerve fibre layer (RNFL) thickness and TSNIT curve in Japanese young normal eyes.

**Method:** Prospective observational cross-sectional study comprised 15 right eyes with obvious conus. All patients (mean age 25.7 ± 4.2) underwent RNFL measurement with the TOPCON 3D OCT-1000 MARK II optic disc 3D scan and fundus photograph. The centres of the optic disc including or excluding the conus were decided using the fundus photograph. Then, the disc centered peripapillary RNFL thickness (DC-R, did not include conus) and conus plus disc centered peripapillary RNFL thickness (CC-R) were calculated. The angles of less and more than 95 percentile of the normative database and sectorial (12 clock hours) RNFL thickness were compared between the DC-R and the CC-R.

**Results:** The degree of the angle of less than 95 percentile of the CC-R (19.1 ± 28.5 degrees) was equal to or narrower than that of the DC-R (28.3 ± 34.7 degrees) in 93.3 % (14/15) of the subjects. The degree of angle of more than 95 percentile of the CC-R (31.5 ± 34.2 degrees) was equal to or narrower than that of the DC-R (46.4 ± 36.6 degrees) in 86.7 % (13/15) of the subjects. The temporal sectorial RNFL thicknesses of the CC-R (7, 8, 9, and 10 o'clock) (145.9 ± 21.4, 89.9 ± 21.9, 72.3 ± 11.7, 101.4 ± 21.6 µm) were significantly thinner than that of the DC-R (156.0 ± 21.5, 105.5 ± 28.6, 85.1 ± 17.5, 116.9 ± 24.2 µm). In contrast, the nasal sectorial RNFL thicknesses of the CC-R (1, 2, 5, and 12 o'clock) (115.7 ± 16.9, 94.0 ± 17.1, 106.5 ± 16.8, 125.1 ± 23.7 µm) were significantly thicker than that of the DC-R (105.9 ± 15.2, 85.9 ± 18.5, 100.5 ± 15.6, 115.7 ± 21.5 µm).

**Conclusions:** The CC-R corresponded more closely to the existing normative database of the TOPCON 3D OCT-1000 than the DC-R. There was a significant difference between the CC-R and the DC-R in temporal and nasal sectors.

P10

### Characterization of the effect of acute intraocular pressure increase on the *in vivo* human optic nerve head

John Flanagan<sup>1,2</sup>, Richard Norman<sup>1</sup>, Catrina Constanz<sup>2</sup>, Graham Trope<sup>1</sup>

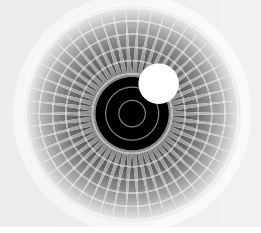
<sup>1</sup>University of Toronto, Toronto, Canada, <sup>2</sup>University of Waterloo, Waterloo, Canada

**Purpose:** The eye is subject to many acute intraocular pressure (IOP) spikes during day-to-day life (e.g. eye rubbing). This study investigated the biomechanical response of the choroid, optic nerve (ON) and retina to an acute IOP change *in vivo* in normal human volunteers.

**Method:** The right eye of 10 healthy adult volunteers (age: 29 ± 9 years; 5 female) was imaged using spectral domain optical coherence tomography (SD-OCT; Spectralis HRA-OCT, Heidelberg Engineering, Heidelberg, Germany) at normal IOP (15 ± 3 mmHg) and following acute elevation of IOP (54 ± 5 mmHg). Scans were centered on the optic nerve head (ONH). The resulting image sets were segmented and measured. IOP was raised using pressure ophthalmodynamometry. To characterize the time course of the observed changes, a second cohort of participants (31 ± 8 years; 3 women) was imaged continuously during a step increase of 20 mmHg induced via ophthalmodynamometry. OCT images through the ONH were recorded at approximately 32 frames per second for 8 seconds as the pressure was applied and removed. The resulting image sequences were processed, segmented and measured using custom software.

**Results:** In the first cohort, choroidal thickness was significantly thinner following IOP elevation (mean thickness decrease of 21 ± 12 µm or 12.9% ± 7.3%; p = 0.05). There was no change in retinal thickness (p = 0.75), Bruch's membrane opening (BMO) area (p = 0.97) and the position of the anterior lamina cribrosa. However the pre-laminar neural tissue within the ON was displaced. In the second cohort, the choroid was observed to thin by an average of 10% ± 6% during a step 20 mmHg IOP increase, and returned to its original thickness within approximately 150 ms when pressure was removed. The ON flattened and rebounded during the same pressure pulse.

**Conclusions:** In normal human eyes retinal thickness was relatively unchanged following acute IOP elevation to approximately 54 mmHg, whereas the choroid thinned significantly. The biomechanical environment of the ON is dynamic, with obvious structural changes evident within 200msecs. Pressure-induced thinning of the choroid may act as a second-to-second modulator of acute changes in IOP.



## P11

### Correlation between Oculus-Spark perimetry and three procedures of morphological analysis (GDx, HRT and OCT)

Marta Gonzalez-Hernandez, Manuel Gonzalez de la Rosa, Mariel Sanchez-Garcia, Ricardo Rodriguez de la Vega, Tinguaro Diaz-Aleman

*Hospital Universitario de Canarias. University of La Laguna, La Laguna, Canary Islands, Spain*

**Purpose:** To compare the relationship between anatomical and functional indices using Spark perimetry.

**Method:** We examined 102 normal eyes and 104 eyes with ocular hypertension, suspected or confirmed glaucoma using Spark perimetry (Oculus Easifield Perimeter), Laser Polarimetry (GDx), Heidelberg Retinal Tonograph (HRT) and Cirrus OCT.

**Results:** The correlation coefficient between mean sensitivity (MS) of Spark initial phase 1 (37 seconds) and final phase 4 (2:34 minutes) was 0.99. A correlation of 0.97 was found between the respective values of PSD, and 0.99 between the percentage of scomatotomous points of both phases (average 52.9% and 54.8% in the group G,  $p > 0.05$ ). There was high concordance in scotoma position in both phases ( $\kappa = 0.86$ ). The correlation coefficients between the morphological indices were 0.48 to 0.78, with similar results comparing morphological and functional indices, ranging from 0.47 to 0.70 ( $p > 0.05$ ). The best correlation between morphological procedures was 0.78 (HRT-GPS versus Cirrus OCT Vertical C/D Ratio). Between morphological and functional procedures, the best linear correlation was 0.71 (inferior fiber layer thickness versus Spark final phase superior MS), increasing to 0.77 using curvilinear regression [thickness =  $56.8 + (0.0019 \times MS^3)$ ]. There was no significant difference between correlation coefficients on comparing morphological and functional indices obtained in the first or the last phase of Spark ( $p > 0.05$  in all cases).

**Conclusions:** Scotoma detection is accurate from the first phase of Spark, presenting high correlation with morphological indices, equivalent to that obtained when the latter are compared.

## P12

### Quantification of retinal venous pulsatility using non-invasive infrared imaging

Mojtaba Golzan, Alberto Avolio, Stuart Graham

*Macquarie University, Sydney, Australia*

**Purpose:** Retinal venous pulsatility (RVP) can provide an index of the relationship between retinal venous pressure, intraocular pressure (IOP) and intracranial pressure, and may be of particular relevance to glaucoma. Although a variety of devices are available to monitor the presence and amplitude of venous pulsations, relatively few techniques record pulsations dynamically. In this study we propose a novel and dynamic approach to characterize RVP using infrared imaging available on most optical coherence tomography (OCT) or retinal angiography devices.

**Method:** A 30 second continuous recording of the optic disc (central retinal vein) using the Heidelberg Spectralis HRA (Heidelberg, Germany) was acquired from five healthy subjects ( $27 \pm 5$  yrs, 3 male 2 female). Measurements were obtained at a rate of 8.8 frames per second with a  $15^\circ$  field of view and a centre wavelength of 840nm. Amplitude of RVP was extracted using an image processing algorithm programmed in Matlab<sup>®</sup>. Following the Spectralis recording RVP pulsatility was recorded for 30 sec using the Dynamic Vessel Analyser device (DVA, Imedos, Germany) with the pupil dilated by application of tropicamide. IOP was monitored throughout the test (Goldman).

**Results:** Mean RVP amplitude was  $7.8 \pm 2.2 \mu\text{m}$  and  $8.6 \pm 4.1 \mu\text{m}$  using DVA and Spectralis respectively, with no significant difference between the two techniques. Number of pulsations for a given specific time frame was similar for both recordings. A slight time difference was detected to occur at some peaks due to variation in heart rate during the tests. IOP did not vary throughout the test.

**Conclusions:** This study shows that the degree of RVP can be quantified by analysis of retinal images acquired by infrared techniques available in ophthalmic devices using OCT (Spectralis), with amplitude values being similar to those obtained using dynamic analysers requiring pupil dilation and bright light illumination (DVA). In addition, the image analysis algorithms developed for this purpose in this study can be made readily available as plug-in software for HRA/OCT devices conventionally used in ophthalmology clinics.

P13

### Relative effects of sampling errors and eye movements upon SAP test-retest variability

Ted Maddess

*ARC Vision Centre, Australian National University, Canberra, Australia*

**Purpose:** To determine the relative contributions of eye movements and visual field undersampling to test-retest variability (TRV). Undersampling occurs in standard automated perimetry (SAP) if sensitivity varies across a visual field faster than the Nyquist rate: 1/12 cycles/degree (Nq), a very gentle rate of change of sensitivity across the field. The present study sought to quantify the relative contributions of eye movements and undersampling to TRV.

**Method:** High resolution model visual fields were spatially smoothed in 9 gradations from nil to  $< Nq/4$ . For each of the 9 levels of smoothing inter-quartile ranges (IQR = 25th to 75th percentiles) of box plots of TRV were determined for 11 bands of scotoma depth from -28.5 to -1.5 dB. This was repeated for 500 sampled fields for each smoothness. Sampling included eye movements equal to that of good fixation ( $\sigma = 0.6^\circ$ ).

**Results:** As observed for SAP fields TRV for the unsmoothed fields grew with scotoma depth, being larger than smooth fields at the 9 largest scotoma depths (all  $p < 0.003$ ). At the 5 test scotoma depths larger than -28.5 dB the IQRs of smoothed fields were only  $2.3 \pm 0.33$  dB and so were smaller by  $6.0 \pm 0.5$  dB than normal unsmoothed fields,  $p < 0.0005$ .

**Conclusions:** Only about 2.3 dB of the IQR of TRV can be attributed to eye movements, the remainder appears to be due to undersampling of the field which is exacerbated by the small Type III stimulus size. Large, blurry, perimeter stimuli, which smooth the visual field as it is sampled, should therefore reduce TRV. This agrees with recent findings on using larger SAP stimuli by Wall et al IOVS 2009; 50: 974-9.

P14

### Relationships between NFLT analyzed by normal database with Cirrus OCT and visual field testing results

Hiroki Nomoto<sup>1</sup>, Chota Matsumoto<sup>1</sup>, Sachiko Okuyama<sup>1</sup>, Sonoko Takada<sup>1</sup>, Shigeki Hashimoto<sup>1</sup>, Eiko Arimura<sup>2</sup>, Fumi Tanabe<sup>1</sup>, Tomoyasu Kayasawa<sup>1</sup>, Mariko Eura<sup>1</sup>, Yoshikazu Shimomura<sup>1</sup>

<sup>1</sup>*Kinki university faculty of medicine, Osaka-sayama, Japan,*

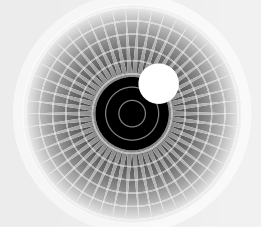
<sup>2</sup>*Sakai hospital kinki university faculty of medicine, Sakai, Japan*

**Purpose:** NFLT results of Cirrus OCT is analyzed by built-in normal database and classified into 3 grades (normal, 5 percentile(%tile) limit and 1%tile limit). This instrument can measure total average NFLT, quadrant NFLT and 12 clock-hour NFLT. Our interest is that NFLT classification of cirrus OCT has how much detecting ability with glaucoma.

**Method:** Subjects were 103 eyes of 103 glaucoma patients and 45 eyes of 45 glaucoma suspects. Glaucoma patients were divided into early, moderate and advanced stages by mean deviation (MD) of SAP result. All subjects underwent SAP, FDT, Flicker perimetry, SWAP and cirrus OCT. Visual field testing results were evaluated by the number of abnormal test points. Outcome measurements of NFLT were total average NFLT, quadrant NFLT and 12 clock-hour NFLT. 12 clock-hour NFLT sectors were divided into 2 groups, superior sectors(10, 11, 12, 1, 2 clock hour sector) and inferior sectors(4, 5, 6, 7, 8 clock hour sector). These parameters were classified into 3 grades. In each glaucoma stage, the ratio of these 3 grades was calculated. Additionally, relationships between upper hemi-visual field and inferior sectors, lower hemi-visual field and superior sectors were investigated.

**Results:** In glaucoma suspect, 56% subjects were within normal limit with total average NFLT. More than 80% subjects were within 5% tile limit and 33% subjects were within 1% tile limit with quadrant NFLT. In patients with early stage, 40% subjects were within normal limit with total average NFLT and more than 80% subjects were within 5% tile limit. FDT, Flicker perimetry and SWAP have more abnormal points than SAP with upper and lower hemi-visual field with 5% tile limit of inferior and superior NFLT sectors.

**Conclusions:** Abnormal criteria of cirrus OCT is useful to detect glaucoma changes. In 5%tile NFLT sectors, FDT, Flicker perimetry and SWAP detect more abnormal points than SAP.



P15

## Flicker, speed and motion sensitivity in glaucoma: central temporal processing is altered in intact central visual field

Fleur O'Hare<sup>1</sup>, Allison McKendrick<sup>2</sup>, Gary Rance<sup>2</sup>, Jonathan Crowston<sup>1,2</sup>

<sup>1</sup>Centre for Eye Research Australia, East Melbourne, VIC, Australia, <sup>2</sup>University of Melbourne, Parkville, VIC, Australia

**Purpose:** Glaucoma is associated with neural processing deficits within the visual pathways that are believed to result from direct insult to retinal ganglion cells. Little is reported about the impact of glaucoma on higher order visual processing mechanisms. That which is reported mainly focuses on the disruption of second order perception of motion which requires more complex and integrated neural processing of both spatial and temporal signals (Karwatsky et al., 2006; McKendrick et al., 2005). Therefore this study aimed to explore the impact of glaucoma upon a range of temporal processing tasks measured in central vision (as defined by intact visual field sensitivity within the central 10 degrees of field). We investigated whether individuals with OAG display specific signs of temporal processing dysfunction in the presence of intact central visual field.

**Methods:** A hierarchical sequence of temporal processing tasks was conducted in 25 OAG individuals and 25 age and gender-matched controls. Tests of central vision included baseline visual field assessment, temporal contrast detection at two flicker rates, speed discrimination at two reference velocities and coherent global motion detection.

**Results:** Irrespective of stage of disease, OAG individuals overall showed a tendency toward poorer performance at each temporal processing level on tasks that required a high degree of temporal resolution. Specifically, impaired temporal contrast detection at 10Hz was identified along with poorer visual speed discrimination for slow velocities in a significant proportion of OAG individuals compared to controls (19.4% and 42.8% respectively, were outside the 90th percentile of control performance;  $p < 0.05$ ). Similarly, a significant proportion displayed impaired global coherent motion detection (23.9% below 90th percentile of control performance,  $p = 0.025$ ).

**Conclusions:** A significant proportion of OAG individuals display evidence of central temporal processing dysfunction but this was not found to correlate with stage of disease as measured by standard visual field assessment.

**Clinical Significance:** This is the first study to explore speed discrimination ability in individuals with OAG. OAG individuals with impaired speed and motion discrimination may require interventional strategies to improve driving/pedestrian safety and navigation, an area for future research.

P16

## Eye movement perimetry in young and aged adults

Joy Carroll<sup>1,2</sup>, David Warren<sup>1,2</sup>

<sup>1</sup>Veterans Administration Hospital, Iowa City, IA, USA,

<sup>2</sup>Departments of Neurology and Ophthalmology, University of Iowa, Iowa City, IA, USA

**Purpose:** We aim to use a new automated perimetry technique to test the hypothesis that adults sixty years and older will have a reduction in visual threshold along with an increased latency and decreased accuracy of eye movements when compared to adults in their twenties.

**Method:** We tested 20 subjects aged 18-30 years old, and 21 subjects at least 60 years old for detection of stimuli in eight locations along the horizontal meridian. Eye movements were recorded with an EyeLink1000 infrared camera. System accuracy measuring the horizontal visual field is  $< 0.5^\circ$ , with temporal resolution of 1000 Hz. We analyzed saccadic eye movement latency, accuracy, visual threshold, and frequency of seeing curve data with repeated-measures ANOVA on ranks.

**Results:** Latency, accuracy, and visual threshold between groups are compared at  $-4^\circ$ ,  $-12^\circ$ ,  $-20^\circ$ , and  $-28^\circ$ . Younger subjects had lower thresholds, increased accuracy, and decreased latency. Latency increased as stimulus size approached visual threshold. Repeated-measures ANOVA on ranks showed statistically significant differences ( $P = < 0.01$ ) between the groups in threshold ( $-4^\circ$ ,  $-12^\circ$ ,  $-20^\circ$ ,  $-28^\circ$ ), latency ( $-4^\circ$ ,  $-12^\circ$ ,  $-20^\circ$ ,  $-28^\circ$ ), and accuracy ( $-4^\circ$ ,  $-12^\circ$ ,  $-20^\circ$ ).

**Conclusions:** Eye movement perimetry shows significant differences in visual threshold, saccadic latency, and saccadic accuracy between young and older adults. It has much promise for clinical visual testing.

---

POSTER SESSION B  
WEDNESDAY 25TH JANUARY 2012

---

P17

---

**Structural and functional anomalies of Autosomal Recessive Spastic Ataxia of Charlevoix-Saguenay (ARSACS)**

Marie-Josée Fredette<sup>1,2</sup>, Mathieu Mercier<sup>1</sup>, Jean-Pierre Bouchard<sup>1,3</sup>, Alain Gourdeau<sup>1,3</sup>, Lalatiana Razafindrabe<sup>4</sup>

<sup>1</sup>University Laval, Quebec, QC, Canada, <sup>2</sup>CHA-CUO(Centre Universitaire d'Ophtalmologie), CEVQ, Centre de Recherche FRSQ, Quebec, QC, Canada, <sup>3</sup>CHA-Hopital Enfant-Jesus, Quebec, QC, Canada, <sup>4</sup>CHA-Centre d'Excellence sur le Vieillessement, Quebec, QC, Canada

**Purpose:** To characterize and correlate structural and functional anomalies of Autosomal Recessive Spastic Ataxia of Charlevoix-Saguenay (ARSACS), a rare neurodegenerative autosomal recessive disease.

**Method:** 27 eyes of 14 ARSACS patients had both Frequency-Doubling perimetry with the FDT-Matrix and Retinal Nerve Fiber Layer measurement with the Stratus-OCT done on the same day. Mean RNFL, quadrants and clock hours of the OCT as well as the FDT-Matrix parameters were evaluated.

**Results:** All patients had a generalized decrease in sensitivity on the FDT, with MD ranging from -4.01 dB to -26.31 dB in their right eye and from -4.69 dB to -22.27 dB in their left eye. Mean MD in these patients were  $-11.83 \pm 5.42$  dB OD and  $-10.87 \pm 4.86$  dB OS. All FDT tests were reliable except for one eye of a patient who was also unable to take the test for the second eye. On the OCT, the RNFL curve and the mean RNFL thickness was above normal values in all patients ( $p < 0.05$ ), and was  $158 \pm 31$  microns on average. 25 eyes had signal strength of 6 or above. Even though these patients had abnormal FDT visual fields and above normal RNFL thickness, a good correlation was found between their mean RNFL thickness and their MD on the FDT (Pearson correlation coefficient = 0.78); patients with thicker RNFL had less FDT visual field defects.

**Conclusions:** Autosomal Recessive Spastic Ataxia patients of Charlevoix-Saguenay seem to have a generalized decrease in sensitivity on FDT visual fields even though they have a RNFL thickness above normal values. Nonetheless, a good correlation coefficient was found between the 2 tests. This could suggest that, even though their structural test does not seem to be a good predictor of their functional result, a change in either one might predict a change in the other.

---

P18

---

**Optimal pointwise linear regression criteria for detecting glaucoma progression**

Colleen Kummet, Gideon Zamba, Carrie Doyle, Chris Johnson, Michael Wall

University of Iowa, Iowa City, USA

**Purpose:** The goal of this study was to evaluate a range of pointwise linear regression (PLR) slope and significance criteria to determine an optimal decision rule for the visual field exam to predict a clinical determination of glaucomatous visual field progression.

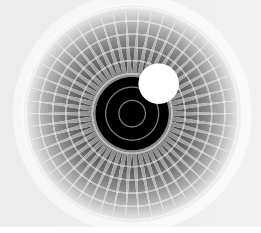
**Method:** Visual field data for 54 locations in each of 140 eyes, one per subject (96 glaucomatous and 44 ocular healthy), were collected using the Humphrey Field Analyzer II program 24-2. The Goldmann size III (0.43° diameter, 4 mm<sup>2</sup>) stimuli were used with 24-2 SITA Standard test strategy. The PLRA2 method was used to analyze the data containing visual field exams at 9 separate time points taken every six months for 4 years.

**Results:** Many slope criteria produced a specificity of 0.90 or higher, particularly slope criteria  $< -1.2$  dB/y and more restrictive. The highest sensitivity for a criterion maintaining a specificity of 0.90 or more was found in the slope criterion  $< -1.8$  dB/y and a significance level of 0.10 which yielded a sensitivity of 0.48 and a specificity of 0.93. Use of the slope criterion  $< -1.4$  dB/y and significance level  $< 0.05$  for classification resulted in sensitivity and specificity values of 0.38 and 0.91, respectively. At the standard criterion of slope  $< -1.0$  dB/y and significance level of  $< 0.01$ , the sensitivity was found to be very low at 0.10. However, at this criterion, all healthy individuals were classified as not progressing by PLRA2 (specificity = 1.0).

**Conclusions:** Our results show that PLR can be optimized by adjusting the standard criteria of slope and significance level. Maintaining a high specificity and increasing the sensitivity of PLR in the detection of visual field decay may contribute to the early detection and treatment of glaucoma.

---





## P19

### Method for calculating the concentration of hemoglobin in the optic nerve head: diagnostic capability with respect to morphological and functional indices

Manuel Gonzalez de la Rosa<sup>1</sup>, Silvia Alayon<sup>2</sup>, Carmen Mendez-Hernandez<sup>3</sup>, Ricardo Rodriguez de la Vega<sup>1</sup>, Susana Perez-Olivan<sup>4</sup>

<sup>1</sup>Hospital Universitario de Canarias. University of La Laguna, La Laguna. Canary Islands, Spain, <sup>2</sup>Dept. of Systems Engineering, University of La Laguna, La Laguna. Canary Islands, Spain, <sup>3</sup>Hospital Clínico San Carlos. University Complutense, Madrid, Spain, <sup>4</sup>Hospital Miguel Servet. University of Zaragoza., Zaragoza, Spain

**Purpose:** To describe and evaluate a method for topographical calculation of optic nerve head (ONH) hemoglobin concentration [Hb].

**Method:** 102 normal eyes and 101 eyes with ocular hypertension, suspected or confirmed glaucoma (Group G) were examined using the [Hb] method, Spark perimetry (Oculus Easifield Perimeter), Laser Polarimetry (GDx), Heidelberg Retinal Tomograph (HRT) and Cirrus OCT.

**Results:** A glaucoma discriminant function (GDF) based on the [Hb] in the ONH vertical diameter presented an area under the ROC curve of 0.97, with 95% specificity and 89% sensitivity ( $p < 10^{-44}$  between the two groups), superior than those obtained with the other procedures, but without statistical significance for some of them as the OCT Vertical C/D ratio (ROC area = 0.95, specificity = 96%, sensitivity = 85%). Diagnostic agreement (kappa) between [Hb] and the morphological and functional indices ranged between 0.461 for HRT RB discriminant function, 0.678 for mean defect (MD) of initial phase Spark perimetry (duration 37 seconds), 0.680 for final PSD and 0.762 for OCT Vertical C/D ratio. The worst agreement between morphological indices was found with OCT thickness and HRT RB discriminant function (kappa=0.553) and the best was with OCT Vertical C/D ratio and HRT GPS (kappa=0.747). The agreement between initial MD and Spark final phase PSD was 0.813.

**Conclusions:** This measure of hemoglobin concentration showed good diagnostic capability and diagnostic agreement with other morphological procedures, similar to that found when such procedures are mutually compared.

## P20

### Effect of intra-ocular lenses on diagnostic performance of multifocal pupillographic objective perimetry in glaucoma

Maria Kolic<sup>1</sup>, Andrew James<sup>1</sup>, Rohan Essex<sup>2</sup>, Ted Maddess<sup>1</sup>

<sup>1</sup>ARC Vision Centre, Australian National University, Canberra, Australia, <sup>2</sup>The Canberra Hospital, Australian National University Medical School, Canberra, Australia

**Purpose:** To investigate the effect of intra ocular lens implants (IOLs) on the diagnostic performance of 4 stimulus variants of multifocal pupil objective perimetry in glaucoma.

**Method:** Of the 76 healthy subjects, 31 eyes had IOLs, and of the 86 glaucoma subjects, 39 eyes had IOLs. All subjects were tested with HFA achromatic, SWAP and Matrix 24-2 perimetry, Stratus OCT and a prototype of the Truefield Analyzer (TFA). The 4 variants of multifocal stimuli presented by the TFA varied in mean presentation rates interval 2 or 4 presentations/s/region and stimulus durations on of 33 or 66 ms, designated R2\_D33, R4\_D33, R2\_D66, R4\_D66. The measure of diagnostic performance was the area under the curve (AUC) of receiver operator characteristics plots, and the method used to determine the effect of IOLs on pupil responses for both subject groups was multiple regression analysis.

**Results:** Mean pupil response amplitudes in normal and glaucoma groups with IOLs, across all 4 variants of multifocal stimuli were only (slightly) smaller for the two stimuli with longer pulse durations: R4\_D66, -0.29 dB  $p=0.003$ ; R2\_D66, -0.25 dB  $p=0.01$ . The best diagnostic power, however, was achieved with one of the shorter duration stimuli: R4\_D33 which provided %AUC values of 94.2% for subjects without IOLs, and 94.0% for subjects with IOLs.

**Conclusions:** This study of 324 eyes demonstrates that IOLs had either a tiny or no effect on mean pupillary response amplitudes. The diagnostic performance of multifocal objective perimetry in glaucoma was not affected by intraocular lens implants.

P21

### The variability of the peak retinal nerve fibre layer position in Japanese normal eyes

Takehiro Yamashita<sup>1</sup>, Ryo Asaoka<sup>2,3</sup>, Yuya Kii<sup>1</sup>, Minoru Tanaka<sup>1</sup>, Kumiko Nakao<sup>1</sup>, Taiji Sakamoto<sup>1</sup>

<sup>1</sup>Department of Ophthalmology, Kagoshima University Graduate School of Medical and Dental Sciences, Kagoshima, Japan, <sup>2</sup>NIHR Biomedical Research Centre for Ophthalmology, Moorfields Eye Hospital NHS Foundation Trust and UCL Institute of Ophthalmology, London, UK, <sup>3</sup>Department of Optometry and Visual Science, City University London, London, UK

**Purpose:** To investigate the relationship between the peak retinal nerve fibre layer (RNFL) position and axial length / spherical equivalent (SE) in Japanese young normal eyes.

**Method:** Prospective observational cross-sectional study comprised 50 right eyes. All participants (mean age  $25.8 \pm 3.7$ ) underwent comprehensive ophthalmologic examination, including RNFL thickness imaging, axial length and SE. RNFL thickness was assessed using TOPCON 3D OCT-1000 MARK II RNFL 3.4 mm circle scan. Axial length was measured with AL-2000 ultrasound device (TOMEY, Japan). SE was measured with KR8800 auto-kerato-refractometer (TOPCON, Japan). The RNFL TSNIT curves were used to measure the angle between supra-temporal and infra-temporal peak RNFL position (peak angle). The relationship between the peak angle and axial length, spherical equivalent (SE) were investigated using linear regression analysis.

**Results:** The mean axial length was  $25.5 \pm 1.3$  mm, the mean SE was  $-4.3 \pm 3.1$  diopter and the mean peak angle was  $125.3 \pm 20.9$  degrees. The peak angle was significantly negatively associated with axial length ( $r = -0.49$ ,  $p < 0.001$ ) and positively associated with SE ( $r = 0.55$ ,  $p < 0.001$ ).

**Conclusions:** The supra-temporal and infra-temporal peak RNFL position tended to be displaced toward the fovea with increasing axial length or decreasing SE.

P22

### Optic nerve evaluation by ultrasonography in glaucoma as a predictive index

Rajiv Garg, Shweta Rani, Sarita Beri, Pamela D'Souza  
Lady Hardinge Med. College, New Delhi, India

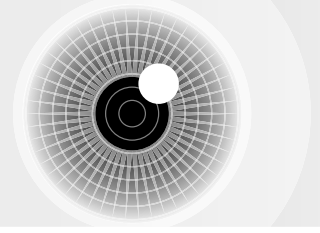
**Purpose:** Study sonographic measurements of vertical cup diameter (SVCD) and compare and correlate it with the photographic parameters of the optic discs in glaucoma and normal eyes.

**Method:** 50 glaucoma and 45 control patients with appropriate inclusion criteria were subjected to complete ophthalmic examination including A scan biometry (for axial length), fundus photography and B scan USG. Optic discs were photographed and examined in a masked fashion by one experienced observer. Photographic vertical cup diameter (PVCD) of cases and controls were measured using image editing software and recordings were made after magnification correction using Bengtsson formula. High resolution ultrasound of the optic disc was performed in vertical transverse position and onscreen measurements of the vertical cup diameters were obtained.

**Results:** Mean SVCD is  $1.06 \pm 0.29$  mm in glaucoma and  $0.75 \pm 0.3$  mm in control.

Mean PVCD is  $0.965 \pm 0.248$  mm in glaucoma and  $0.650 \pm 0.29$  mm in control. A significant correlation between PVCD and SVCD both in glaucoma and control groups was found in our study. The ultrasonic cup values (SVCD) had a strong positive correlation with vertical CDR, cup area, cup area / disc area; strong negative correlation with vertical NRR, NRR area / disc area and a weak negative correlation with NRR area.

**Conclusions:** Optic cup diameter can be reliably measured by ultrasound. A significant increase in B-scan estimate of optic cup diameter over time may be considered as objective evidence of glaucomatous damage. This may solve the problem of evaluation of glaucoma patients with opaque ocular media where fundus evaluation, fields charting and other modalities like HRT, OCT fail. Also in glaucoma patients, follow up and monitoring of glaucoma can be done by ultrasound analysis of optic cup diameter and calculation of CDR values despite development of media haze using photographic disc diameter values from previous records.



## P23

### Death versus dysfunction in glaucoma: the relationship between threshold and miss rate for tiny perimetric stimuli

Andrew Anderson, Deborah Hackett, Michael Pianta  
*The University of Melbourne, Parkville, Victoria, Australia*

**Purpose:** Rarebit Perimetry (RBP) uses small, intense stimuli to sample the visual field, with the proportion of missed targets (the miss rate) believed to represent the proportion of non-functioning visual elements; for example, dead retinal ganglion cells in glaucoma. Luminous thresholds for detecting RBP targets are also increased in glaucoma, indicating visual dysfunction in addition to ganglion cell death. Whether such dysfunction precedes retinal ganglion cell death or is a contemporaneous accompaniment to cell death in surrounding areas is unknown. We therefore examined cross-sectional estimates of miss rate and luminous threshold to see if threshold changes preceded miss rate changes.

**Method:** 14 observers with primary open angle glaucoma and 14 age-matched normal controls were tested with a customised RBP test that presented targets on average 30 times over each of 8 mid-peripheral (~10-15°) regions. The test was repeated for 13 stimulus luminances (10-150 cd/m<sup>2</sup>, in 0.14 log unit intervals), and a four-parameter (threshold, spread, miss rate and false positive rate) cumulative normal fitted to the data. All test zones were analysed for each observer, save the two closest to the blindspot.

**Results:** When expressed on logarithmic scales, the difference between the median parameter values for the normal and glaucoma groups was 0.59 and 0.30 log units for the miss rate and threshold, respectively. 41 miss rate values from glaucomatous observers fell outside the non-parametrically determined 95% normal limits, in contrast to 28 threshold values (Fisher's exact test,  $p = 0.04$ ). There was a significant correlation between log miss rate and threshold (Spearman rank  $r = 0.55$ ,  $p < 0.001$ ; 95% confidence interval: 0.42 to 0.66) and a Deming regression showed that the data did not depart significantly from linearity (Runs test,  $p = 0.18$ ).

**Conclusions:** We find no evidence of changes in threshold preceding changes in miss rate, consistent with the idea that visual dysfunction is a contemporaneous accompaniment, rather than a precursor, to retinal ganglion cell loss.

## P24

### Comparison between the GDx Staging System (GDS SS) and the Nerve Fiber Indicator (NFI) in the detection of early glaucomatous structural damage

Paolo Brusini, Maria Letizia Salvetat, Claudia Tosoni, Lucia Parisi, Marco Zeppieri  
*Santa Maria della Misericordia Hospital, Udine, Italy*

**Purpose:** To assess the sensitivity and specificity of a new staging system designed for the classification of structural damage with GDx VCC in comparison to the Nerve Fiber Indicator (NFI) in patients with early glaucoma.

**Method:** 78 patients with early glaucoma (IOP > 21 mmHg, early visual field defects classified as stage 2 or less with the Glaucoma Staging System, and early optic disc alterations), and 76 normal subjects were considered. All subjects underwent testing with GDx VCC. Test results were assessed with both the built-in NFI parameter and the new GDx Staging System (GDx SS), that differentiates the retinal nerve fiber layer (RNFL) damage severity in 6 different categories using the Superior and Inferior Average values. This system also provides information on the location of the RNFL defect. Tests with evident atypical birefringence patterns were excluded from the study. Sensitivity, specificity, and area under ROC curve for discriminating between healthy and early glaucomatous eyes were determined for NFI and GDx SS.

**Results:** The area under the ROC curve was  $0.89 \pm 0.03$  (CI 95%: 0.840 – 0.949) for the NFI and  $0.86 \pm 0.03$  (CI 95%: 0.786 – 0.921) for the GDx Staging System, respectively. Sensitivity and specificity at the best cut-off were respectively 71.0% and 97.4% for NFI (cut-off set at >26) and 71.0% and 98.7% for GDx SS (best cut-off >Stage 0). When the cut-off of NFI was set at >30 and at >50 (as suggested by the manufacturer), sensitivity and specificity were 64.0% and 97.4%, and 33% and 100%, respectively. Using the GDx VCC, when the cut-off of was set at  $\geq$ Stage 1, the sensitivity and specificity were 50% and 100%, respectively.

**Conclusions:** The GDx Staging System was as sensitive and slightly more specific than the GDx VCC NFI in separating normal subjects from patients with early glaucoma. Moreover, it provides an easy and standardized classification of both the severity of RNFL and the location of the damage.

P25

### Applications of noise-corrected progression analysis of automated visual fields

David W Richards<sup>1</sup>, Arthur D Snider<sup>1</sup>, Arunava Mukherjea<sup>2</sup>

<sup>1</sup>University of South Florida, Tampa, Florida, USA,

<sup>2</sup>University of Texas, Edinburg, Texas, USA

**Purpose:** To account for all mathematically quantifiable systematic and random errors that degrade the quality of global and pointwise progression analysis of automated visual fields, using "Noise-Corrected Maximum Likelihood" (NCML) analysis.

**Method:** We retrospectively analyzed 92 Zeiss-Humphrey (ZH) 24-2 Sita-Standard visual fields (VFs) of 10 eyes of 10 glaucoma patients. There were 7 to 11 serial VFs per eye extending over 4 to 8 years. All eyes had acuities of 20/40 or better and combined false positive + false negative rates of < 20%. Mean Defect (MD) was -19 to 0, and Pattern Standard Deviation (PSD), 2.17 to 15.63. Raw sensitivity and Total Deviation (TD) were used. A histogram of TD revealed a bimodal distribution, whose low-end secondary peak was determined to be due to non-thresholded (NT) points. A source of random error was fluctuation over time at individual TD locations. Using transformation of variable, elimination of NT points, and calculation of pointwise time-variability of transformed TD, we calculated the Maximum-Likelihood (ML) pointwise slope (in db/y), the ML global slope of TD for each eye, and the slope of the standard deviation (SDPD) of the ZH parameter PD (Pattern Deviation).

**Results:** With NCML, significant pointwise slopes of as little as -0.15 db/y were detectable. The error bar of global VF global slope was reduced ( $p < 0.001$ , Mann-Whitney U Test) to a mean of 0.222 db/year (by NCML), compared to a 1.33 db/year (using MD and PSD as inputs). Slopes of SDPD and negative global slope of TD (by NCML) were well correlated (Pearson  $r = 0.861$ ). By Mann-Whitney U Test, the two sets of slopes were not statistically different ( $p = 0.322$ ). By T-Test, none of the 10 pairs of slopes differed at the  $p = 0.05$  level.

**Conclusions:** NCML analysis reduces the errors of TD progression analysis and increases the accuracy of pointwise slopes and of global slope of the VF's. NCML demonstrates that global slope based on local fluctuations (PD) is, surprisingly, equivalent to that calculated based on TD.

P26

### Combining an expert glaucoma staging and evaluating system with SPARK perimetry on the OCULUS Easyfield perimeter

Zoltan Gagyi-Palffy, Rainer Kirchhübel

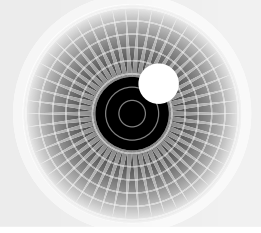
OCULUS Optikgeraete GmbH, Wetzlar, Germany

**Purpose:** Purpose of this study is to evaluate the performance of an expert glaucoma staging and evaluating system based on pattern recognition by using visual field data obtained using SPARK perimetry with the OCULUS Easyfield perimeter. We also pursue a comparison of the results of the Glaucoma Staging Program (GSP) with other classification systems, like the Glaucoma Staging System 2 (GSS2) of Brusini.

**Method:** Visual field results obtained by SPARK perimetry of 112 eyes of patients with confirmed or suspected glaucoma were reviewed; all the data were analysed with the GSP classifier. Classifications into visual field classes and risk classes were noted, and the Glaucoma Likelihood Index (GLI) calculated for each examination. Classification into the class "Neuro" by GSP was recorded as an error and taken into account accordingly. Correlation of the GLI with MD, PSD and GSS2 score were also evaluated.

**Results:** 85% of the fields were classified by GSP into visual field classes "Normal" or "Glaucomatous". GLI shows strong correlation with MD and GSS2 score. Correlation with PSD is weaker due to the fields with extended absolute defects.

**Conclusions:** The results of combining GSP with SPARK perimetry on the OCULUS Easyfield do not differ significantly from the case when other threshold strategies are used. The speed of SPARK in this case represents a practical advantage. Optimizing parameters in the evaluation of GLI can improve the usability in progression monitoring.



P27

## Relationship between Frequency-Doubling Technology perimetry and angle width of retinal nerve fiber defects in preperimetric glaucoma

Shinji Ohkubo<sup>1</sup>, Tomomi Higashide<sup>1</sup>, Chiaki Kawaguchi<sup>1</sup>, Hisashi Takeda<sup>1</sup>, Sachiko Udagawa<sup>1</sup>, Aiko Iwase<sup>2</sup>, Kazuhisa Sugiyama<sup>1</sup>

<sup>1</sup>Ophthalmology and Visual Science, Kanazawa University Graduate School of Medical Science, Kanazawa, Ishikawa, Japan, <sup>2</sup>Tajimi Iwase Eye Clinic, Tajimi, Gifu, Japan

**Purpose:** To evaluate the structure-function relationship using frequency-doubling technology (FDT) perimetry and fundus photographs in patients with localized retinal nerve fiber layer defects (RNFLD) and normal standard automated perimetry (SAP) results (preperimetric glaucoma).

**Method:** Twenty-four eyes of 24 preperimetric glaucoma subjects who had glaucomatous optic disc abnormalities with localized RNFLDs were included in this study (53.0±10.6 years). None of reliable SAP results showed glaucomatous visual field defects, which were determined according to Anderson's criteria. Reliable SAP results were defined as a false-positive error < 15%, a false-negative error < 15%, and a fixation loss < 20%. All subjects had complete ophthalmic examinations and had to meet the following criteria: best corrected visual acuity ≥ 1.0, with a spherical error within ±6.0D and a cylinder error within ±3.0D. All subjects also underwent FDT perimetry using the C-20-5 program and fundus photographs. The angular widths of RNFLDs were determined by red-free fundus photographs at two circles which centered on the optic disc. One had a 3.4mm diameter (NFLD@3.4mm) and the other had a radius of half the distance between the disc center and fovea (NFLD@DM/2).

**Results:** From 24 eyes, there were 9 and 19 localized RNFLDs in the superotemporal and inferotemporal quadrants, respectively (28 RNFLDs in total). When there was RNFLD in both side, we analyzed larger angle width RNFLD for later analysis. Thirteen eyes (54.2%) showed abnormal FDT results with at least 1 abnormal test point (p<5%). There were no significance differences in age between the subjects with normal and abnormal FDT results. Angle width of RNFLD was significantly larger for eyes with abnormal FDT results (NFLD@3.4mm: 25.2±8.5 degree, NFLD@DM/2: 26.3±9.8 degree) than for eyes with normal FDT results (NFLD@3.4mm: 10.8±3.7 degree, NFLD@DM/2: 10.1±3.7 degree) (p < 0.01).

**Conclusions:** The ability to detect visual field abnormality of FDT in preperimetric glaucoma is influenced by the angle width of RNFLD.

P28

## Glaucoma patients with large optic disc size have reduced retrobulbar optic nerve diameter

Heather Connor<sup>1,3</sup>, David Abbott<sup>2,1</sup>, Sarah Hosking<sup>3</sup>

<sup>1</sup>University of Melbourne, Melbourne, VIC, Australia,

<sup>2</sup>Brain Research Institute, Melbourne, VIC, Australia,

<sup>3</sup>National Vision Research Institute, Melbourne, VIC, Australia

**Purpose:** Reduced retrobulbar optic nerve diameter (ROND) in primary open angle glaucoma (POAG) may be a consequence of retinal nerve cell loss, or a greater susceptibility of these patients to damage. This study will determine if severity of functional loss is related to retrobulbar nerve anatomy.

**Method:** 84 eyes of 42 normal controls (NC; mean age 59±11y range 41–82y) and 46 eyes of 23 POAG patients (POAG mean age 64±11y range 44–87y) were recruited. POAG patients had a confirmed diagnosis of glaucoma and repeatable Humphrey 24-2 visual field results. AGIS grading system was used to group POAG patients as mild (n=10) or moderate/severe (n=13). HRT II imaging was used to measure optic disc area (DA) and rim volume (RV); 3T MRI T2 orbital scans were acquired and used to measure ROND 10mm behind the disc (Siemens DICOM software). ANOVA was used to determine differences between the three groups with age as a covariate and Bonferroni Post Hoc Analysis used to compare groups.

**Results:** Pattern standard deviation (PSD) in the NC group was 1.51 ± 0.2 compared to 1.87 ± 0.38 for the mild POAG group (p>0.05) and 10.21 ± 0.38 for the moderate/severe group (p<0.01). DA in the NC group (1.96 ± 0.05mm<sup>2</sup>) was similar to the mild POAG group (1.95 ± 0.11mm<sup>2</sup>; p>0.05) but significantly larger in the moderate/severe group (2.37 ± 0.41mm<sup>2</sup>; p < 0.01). RV in the NC group (0.36± 0.02 mm<sup>3</sup>) was similar to the mild POAG group (0.29 ± 0.03mm<sup>3</sup>; p=NS) but significantly reduced in the moderate/severe POAG group (0.21 ± 0.04mm<sup>3</sup>; p<0.01). ROND was 2.42 ± 0.3mm in the NC group, and was significantly smaller in both the mild POAG group (2.18 ± 0.11mm; p<0.01) and moderate/severe POAG group (1.95 ± 0.12mm; p<0.01). There was no significant difference in ROND between the two glaucoma groups.

**Conclusions:** In this study POAG patients with moderate/severe visual field loss exhibited larger optic disc area with reduced rim volume compared to those with mild POAG. POAG is associated with thinner ROND for both mild and moderate/severe groups as defined by visual field loss.

P29

---

### Disc Area and Neuroretinal Rim Measurements by Optical Coherence Tomography in Highly Myopia

Sheng-Yao Hsu, Rong-Kung Tsai

*Tzu Chi General Hospital and Tzu Chi University, Hualien, Taiwan*

**Purpose:** To measure the disc area and neuroretinal rim in high myopia and analyze the correlations between the measurements with magnification correction and confounders.

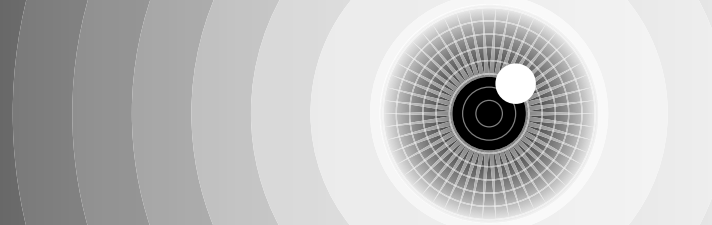
**Method:** This cross-sectional study measured the disc area and neuroretinal rim (rim area and horizontal integrated rim width) in one randomly chosen eye in each of 52 subjects with high myopia using optical coherence tomography (OCT) with magnification correction, and 61 subjects without high myopia as controls. Confounders, such as subject age, spherical equivalent, or axial length, were investigated in highly myopic eyes; and comparisons of the OCT measurements between highly myopic and non-highly myopic eyes were performed.

**Results:** In high myopia, the disc area ( $p=0.954$ ), rim area ( $p=0.901$ ), and horizontal integrated rim width ( $p=0.325$ ) did not correlate with subject age. The disc area, rim area, and horizontal integrated rim width negatively correlated with spherical equivalent and positively correlated with axial length in highly myopic eyes ( $p<0.05$ ). The rim area ( $p<0.001$ ) and horizontal integrated rim width ( $p<0.001$ ) both correlated positively with the disc area in high myopia. The disc area ( $p<0.001$ ), rim area ( $p<0.001$ ), and horizontal integrated rim width ( $p<0.001$ ) were significantly larger in highly myopic eyes than in non-highly myopic eyes.

**Conclusions:** In highly myopic eyes, neuroretinal rim increases as disc area increases, disc area and neuroretinal rim enlarge as myopia progresses, and disc area or neuroretinal rim are larger than in non-highly myopic eyes.

---





## INDEX

<b>Presenter Name</b>	<b>Page No.</b>	<b>Presenter Name</b>	<b>Page No.</b>
Anderson, Andrew.....	52	Kummet, Colleen.....	49
Artes, Paul.....	22	Lamparter, Julia.....	25
Asaoka, Ryo.....	34	Leaney, John.....	42
Battista, Josephine.....	19	Maddess, Ted.....	47
Bentley, Sharon.....	19	Matsumoto, Chota.....	15
Black, Alex.....	20	McKendrick, Allison.....	28
Carle, Corinne.....	27	Metha, Andrew.....	36
Carroll, Joy.....	48	Morgan, William.....	36
Chauhan, Balwantray.....	30	Nguyen, Bao.....	30
Connor, Heather.....	54	Nomoto, Hiroki.....	47
Dannheim, Fritz.....	42	O'Hare, Fleur.....	48
Demirel, Shaban.....	34	Ohkubo, Shinji.....	54
Denniss, Jonathan.....	26	Okuyama, Sachiko.....	41
Dul, Mitchell.....	16	Parwal, Sandeep.....	13
Efron, Nathan.....	35	Pianta, Michael.....	29
Eura, Mariko.....	14	Richards, David W.....	53
Flanagan, John.....	35, 37, 45	Rosli, Yanti.....	43
Fortune, Brad.....	20, 29	Sabeti, Faran.....	43
Fredette, Marie-Josée.....	49	Schiefer, Ulrich.....	37
Gagyi-Palfy, Zoltan.....	53	Schuchard, Ronald.....	18
Gardiner, Stuart.....	26	Tanabe, Fumi.....	25
Garg, Rajiv.....	51	Tanaka, Minoru.....	44
Golzan, Mojtaba.....	46	Turpin, Andrew.....	15
Gonzalez de la Rosa, Manuel.....	27, 50	Tuten, William.....	13
Gonzalez-Hernandez, Marta.....	33, 46	Vingrys, Algis.....	18
Goren, Deborah.....	21	Viswanathan, Deepa.....	21
Harwerth, Ronald.....	30	Wakayama, Akemi.....	28
Hashimoto, Shigeki.....	16	Wall, Michael.....	38
Healy, Paul.....	36	Wang, Yanfang.....	17
Ho, Yuan-Hao.....	33	Weber, Joerg.....	38
Hsu, Sheng-Yao.....	55	Wood, Joanne.....	38
Johnson, Chris.....	14	Yamashita, Takehiro.....	51
Kayazawa, Tomoyasu.....	17	Yamazaki, Yoshio.....	41
Kii, Yuya.....	45	Zamba, Gideon.....	22
Kolic, Maria.....	50	Zeppieri, Marco.....	44, 52

Booth No.	Organisation
1	
2	
3	
4	 We make it visible.
5	



**VISION SCIENCE**  
ARC CENTRE OF EXCELLENCE

The Vision Centre conducts world leading vision research and sponsors a number of national and international vision meetings. It is a collaborative effort of the Australian National University, University of Melbourne, University of Queensland, University of Western Australia, and Sydney University.

<http://vision.edu.au/>



**OCULUS Twinfield®, Centerfield® and Easyfield®**  
**Relying on Threshold Noiseless Trend (TNT)**  
**for efficient progression analysis**

Fast and reproducible tests with the SPARK strategy, sensitive progression evaluation with Threshold Noiseless Trend (TNT) – the latest highlights for all OCULUS perimeters. Booth no 5



[www.ocus.de](http://www.ocus.de) 



[www.ivfis.com](http://www.ivfis.com)

GOLD SPONSORS



We make it visible.

SILVER SPONSORS



BRONZE SPONSORS

